Study of mass and thermal transport in non-equilibrium environment

A Thesis Submitted for the Degree of Doctor of Philosophy

By

Archana G R



School of Chemistry

University of Hyderabad

(P.O) Central University, Gachibowli

Hyderabad-500046

Telangana

India

March, 2023

Dedicated to

My Parents

DECLARATION

I, Archana G R, hereby declare that this thesis entitled "study of mass and thermal

transport in non-equilibrium environment" submitted by me under the guidance and

supervision of **Dr. Debashis Barik** is a bonafide research work. I also declare that it

has not been submitted previously in part or in full to this University or any other

University or Institution for the award of any degree or diploma.

In keeping with the general practice of reporting scientific investigations, due

acknowledgments have been made whenever the work described is based on the finding

of other investigations. Any omission or error that might have crept is regretted. This

research work is free from plagiarism. I hereby agree that my thesis can be deposited in

Shodhganga/INFLIBNET. A report on plagiarism statistics from the University library

is enclosed.

University of Hyderabad

March, 2023

Archana G R

Reg No. 17CHPH27



CERTIFICATE

This is to certify that the thesis entitled 'study of mass and thermal transport in non-equilibrium environment' submitted by Archana G R bearing the registration number 17CHPH27 in partial fulfilment of the requirements for the award of Doctor of Philosophy in Chemistry is a bonafide work carried out by her under my supervision and guidance.

This thesis is free from plagiarism and has not been submitted previously in part or in full to this University or any other University or Institution for award of any degree or diploma.

Parts of this thesis have been published in the following publications:

- G.R. Archana and D. Barik, Roughness in the periodic potential induces absolute negative mobility in a driven Brownian ratchet, *Phys. Rev. E.* 106, 044129 (2022). (Chapter 3)
- 2. G.R. Archana and D. Barik, Roughness in the periodic potential enhances transport in a driven inertial ratchet, *Phys. Rev. E.* **104**, 024103 (2021). (Chapter 2)
- 3. G.R. Archana and D. Barik, Temperature dependent divergence of thermal conductivity in momentum-conserving one-dimensional lattices with asymmetric potential, *Phys. Rev. E.* **99**, 022103 (2019). (Chapter 5)
- G.R. Archana and D. Barik, Roughness in the periodic potential induces multiple current reversal in a driven coupled inertial ratchet (manuscript under preparation). (Chapter 4)

She also participated in oral/poster presentations in the following conferences:

- 12th India-Japan Science -Technology Conclave: International Conference on Frontier Areas of Science and Technology (ICFAST-2022), Poster: 'Study of Transport Properties of a Driven Brownian Ratchet in a Rough Periodic Potential', 09-10 September 2022, University of Hyderabad, India. Received Best Poster Prize.
- 2. 19th Annual In-House Symposium CHEMFEST-2022, Oral: 'Study of Mass and Thermal transport in non equilibrium environment', 22-23 April 2022, School of Chemistry, University of Hyderabad, India. Received Best Oral Presentation Prize.
- 3. 17th Theoretical Chemistry Symposium (TCS-2021), Poster: 'Roughness in the periodic potential enhances transport in a driven inertial ratchet', 11-14 December 2021, IISER Kolkata, India. Received Best Poster Prize.
- 4. 16th Annual In-House Symposium CHEMFEST-2019, Poster: 'Temperature dependent divergence of thermal conductivity in momentum-conserving one-dimensional lattices with asymmetric potential', 22-23 February, 2019, School of Chemistry, University of Hyderabad, India.
- 5. 16th Theoretical Chemistry Symposium (TCS), Poster: 'Temperature dependent divergence of thermal conductivity in momentum-conserving one-dimensional lattices with asymmetric potential', 13-16 February, 2019, BITS Pilani, Rajasthan, India.

Further the student has passed the following courses towards the fulfilment of course work requirement for PhD:

Sl. No.	Course No.	Title of the Course	No. of Credits	Grade
1	CY801	Research Proposal	4	Pass
2	CY805	Instrumental Methods-A	4	Pass
3	CY806	Instrumental Methods-B	4	Pass

Dr. Debashis Barik Supervisor

Dr. Debashis Barik
Associate Professor
School of Chemistry
University of Hyderabad
Hyderabad-500 046, India.

School of Chemistry

Dean
SCHOOL OF CHEMISTRY
University of Hyderabad
Hyderabad-500 046

ACKNOWLDEGEMT

This thesis, which is entitled as "Study of mass and thermal transport in non-equilibrium environment," is an outcome of research work that I've been doing since August 2017 under the direction of Dr. Debashis Barik in the School of Chemistry at University of Hyderabad.

First of all, I would like to express my deep and sincere gratitude to my supervisor Dr. Debashis Barik for his invaluable guidance, continuous motivation and enthusiasm throughout my work. I am genuinely grateful for his patience and the wealth of knowledge he has imparted to me. His guidance has led me to where I am today, overcoming obstacles and doubts along the way. Without you, Sir, I would not have made it this far.

I would like to express my sincere regards to present and former deans of School of Chemistry. I would like to thank my DRC members, Prof. Susanta Mahapatra and Dr. Manju Sharma for their suggestions throughout my research. Also, I acknowledge teaching and non-teaching staff of our school for their help during my doctoral work. I am extending my heartfelt thanks to my fellow lab mates Dr. Anupam Dey, Soutrick Das and Hafijur Rahman for their immense help, stimulating discussions and for all the fun we have had in the last six years. I would like to extend my gratitude to Dr. Durba Roy for her constant and sincere encouragement, as well as for warmly welcoming me every time we had a conversation. Additionally, I would like to thank Trinab Barik for cultivating a light and enjoyable lab environment.

I am extremely grateful to my parents Gopakumar M and Remanidevi P for their enduring support and trust in me during my PhD journey. They never failed to say that they were proud of me for doing what I wanted to do in my life, no matter how worried they were about me. My brother, Achyuthan G R, gave quiet encouragement and positive belief in my every success from my childhood that kept me going regardless of the challenge that I faced.

As I reflect on my educational journey, I cannot help but feel immense gratitude for the teachers who have shaped me into the person I am today. They have not only imparted knowledge, but also instilled in me a love for learning, a sense of curiosity, and a passion for excellence. To my M.Sc project supervisor, Dr. Jayasree E.G , thank you for introducing me to the world of theoretical research. Your passion for your subject was contagious, and your intellectual curiosity and insights have stayed with me long after I graduated. I would also like to remember

and thank Dr. Suresh C H and Dr. Vijayalakshmi for inspiring me to pursue a research carrier from my childhood itself.

I would like to express my sincere appreciation to Dr. Akhil S Nair, Anu Bovas, Dr. Jeladhara, Anju Joseph, for their friendship and support during my entire PhD journey. While this academic pursuit has been a significant part of my life, their unwavering presence and encouragement have been equally important. Their support has gone beyond academic assistance, and they have been there for me through the ups and downs of life. Their willingness to lend an ear, offer a shoulder to cry on, and celebrate my accomplishments has meant the world to me.

Also, special shout out to Ramessa P M, Ishfaq, Rithesh, Shyam S, Ligesh, Salman, Subhu, Pooja, Abin, Athira, Anjana P O, Lakshmi. I wanted to take a moment to express my sincere gratitude for their friendship and support outside of my PhD journey. As much as I value and appreciate the academic community and my fellow scholars, having you all as my close friends has been an invaluable source of joy and comfort. Your kind words, listening ears, and laughter have been a source of encouragement during the times when my research and academic demands have become overwhelming. The unwavering support has helped me to keep a balanced perspective on what truly matters.

I would also like to express my thanks to Prachi, Arun, Daradi, Ajay Rawat, Ajay Yerram, Alamgir, Jaya Krushna, Jhansi, Rani, Shampitha, Sathyam, Sreenivas, Praveen, Sridatri, Gunjan and many others for helping me in many different ways.

Last but not the least I would like to express my heartfelt gratitude to myself for my hard work, perseverance and dedication for completing this journey.

I acknowledge funding agencies for my fellowship.

Archana G R

Content

-	oter 1. Introduction Part1 tudy of transport properties of an inertially driven Brownian particle in a rough periodic potential	1-26
1.1	Historical Background	1
1.2	Langevin Dynamics: Brownian motion	2
1.2	Introduction to Brownian ratchets	6
1.3	Anomalous diffusion and research scenario	14
1.7	Scope of our chosen problems in the current research background	15
1.8	References	17
Chap	oter 1. Introduction Part2	2 20
	Thermal transport in low-dimensional lattices	27-39
1.2.1	Introduction	27
1.2.2	Basic definitions	28
1.2.4	Origin of the research problem	32
1.2.5	References	35
_	pter 2. Effect of roughness in the periodic potential in the sport of a driven inertial ratchet aided by Gaussian noise.	40-59
2.1	Introduction	40
2.2	Model	41
2.3	Results and Discussions	44
2.4	Conclusion	54
2.5	References	56
_	pter 3. Effect of roughness in the periodic potential in the sport of a driven Brownian ratchet in the presence of external	60-78
load	post of a siriou brownian rationed in the proponed of external	00 10
3.1	Introduction	60
3.2	Model	61
3.3	Results and Discussions	63

3.4	Conclusion	73
3.5	References	75
_	r 4. Effect of roughness in the periodic potential in the ort of driven coupled inertial Brownian particles.	79-94
4.1	Introduction	79
4.2	Model	80
4.3	Results and Discussions	82
4.4	Conclusion	88
4.5	References	89
Chapte	r 5. Investigation of divergence of thermal conductivity in a	
momen	r 5. Investigation of divergence of thermal conductivity in a tum-conserving one-dimensional lattice with asymmetric well potential	95-112
momen	tum-conserving one-dimensional lattice with asymmetric	95-112 95
momen double-	tum-conserving one-dimensional lattice with asymmetric well potential	
momen double- 5.1	tum-conserving one-dimensional lattice with asymmetric well potential Introduction	95
momen double- 5.1 5.2	tum-conserving one-dimensional lattice with asymmetric well potential Introduction Model	95 96
momen double- 5.1 5.2 5.3	tum-conserving one-dimensional lattice with asymmetric well potential Introduction Model Results and Discussions	95 96 98
momen double- 5.1 5.2 5.3 5.4 5.5	tum-conserving one-dimensional lattice with asymmetric well potential Introduction Model Results and Discussions Conclusion	95 96 98 107

CHAPTER:1

INTRODUCTION: Part1

Study of transport properties of an inertially driven Brownian particle in a rough periodic potential

1.1 Historical background

Diffusion is a universal process that can be seen in many diverse systems. It is essential not only on all the scientific disciplines but also in socioeconomic background, when processes like the diffusion of ideas or innovations are taking place¹. Diffusion, derived from the Latin word 'diffundere' meaning spreading out, involves movement of particles in a directional way. Macroscopically, diffusion leads to the transport of particles from regions of higher to lower concentrations. Whereas microscopically, diffusion is a result of random walk of particles. Random motion of tiny particles was first observed on pollen grains and was investigated by botanist Robert Brown in 1828 and these random motions of microscopically large but macroscopically small particles were termed as Brownian motion². Later Albert Einstein in his annus mirabilis 1905, provided a probabilistic explanation of Brownian motion by modelling the motion of pollen particles in a liquid based on the molecular kinetic theory of heat³. In his theoretical explanation for Brownian motion, he pointed out that the erratic motion indicates the molecular nature of fluid and, randomness is due to the thermal fluctuations in the liquid itself. He formulated the diffusion equation for Brownian particles⁴ which relates the diffusion coefficient, D, of the particles and coefficient of viscosity, η , of the liquid as given by

$$D = \frac{k_B T}{6\pi \eta r} \tag{1.1}$$

where r is the radius of the spherical particle, k_B , and T, are the Boltzmann constant and temperature of the system respectively. The Einstein's relation represents the balance between the energy gained by the Brownian particle from the thermal fluctuations and the energy lost by it due to the dissipation in a thermodynamically closed system. According to the Stokes' law the dissipation constant, γ , is related to coefficient of viscosity as, $\gamma = 6\pi\eta r$. The well-known fluctuation-dissipation relation is an outgrowth of this energy balance mechanism in a closed system. The probability density, $\rho(x,t)$, of the Brownian particles at position, x, at time, t, which satisfies the diffusion equation:

$$\frac{\partial \rho(x,t)}{\partial t} = D \frac{\partial^2 \rho(x,t)}{\partial x^2} \tag{1.2}$$

Assuming that N particles start from the origin at the initial time, t = 0, the solution of diffusion equation is given by

$$\rho(x,t) = \frac{N}{\sqrt{4\pi Dt}} e^{-\frac{x^2}{4Dt}}.$$
(1.3)

The solution indicate gaussian spread of particle over spread space and the width of the distribution increases with time indicating the spread of particle over time. The solution allows one to calculate the moments and the first moment (or mean) is $\langle x \rangle = 0$ and the second moment or variance is given as

$$\langle \Delta x^2(t) \rangle = 2Dt \tag{1.4}$$

The linear increase of variance of x is known as normal diffusion of particle. Marian Smoluchowski carried out independent research on the kinetic theory of Brownian motion. and derived the same result as of Einstein⁵. Smoluchowski also proposed a device called "Brownian Ratchet" that can extract energy from random motion of molecules. In 1908, Jean Baptiste Perrin⁶ experimentally verified Einstein's predictions and confirmed the atomic nature of matter and determined the value of Avogadro-Loschmidt number N_A .

Major drawback of the diffusion model proposed by the Einstein^{3,4}, which he himself noticed later is that the inertia of the Brownian particle is completely discarded. This brought to light the fact that such an infinite force is required to change the particle's velocity and thereby achieving the random walk at all the steps. Then, Paul Langevin⁷ established a further pillar in 1908 for the development of the theories of the Brownian motion.

1.2 Langevin Dynamics: Brownian motion

In Langevin's model based on the Brownian motion, the inertial force of the Brownian particle is explicitly considered. This model describes the random motion of a particle in a fluid due to the collisions with the fluid molecules. In this formulation, the equation of motion for the particle is modeled using the Newton's second law of motion.

1.2.1 Model

In this model, we are considering the one-dimensional motion of the spherical particles having the mass, m, position, x, velocity, v, and radius, a, moving in a dense fluid having the coefficient of viscosity, η . Assume that the individual masses of those spherical particles are

much greater than that of the mass of fluid particles. Radius of the spherical particle is chosen in the range of $10^{-9}m < a < 5 \times 10^{-7}m$. And these bigger particles, undergo Brownian motion in this fluid due to the random collisions with the surrounding fluid molecules. For instance, we can think this scene as pumpkins being bombarded with mustard seeds. We assume that the concentrations of bigger particles are sufficiently small in the fluid, so that they do not interfere with each other. So essentially, we can treat each one of them as an isolated system. Due to the collisions of lighter particles with the heavy ones, heavier ones will feel drag force as well as the random kicks with all the possible directions. The nature of the force exerted by the fluid molecules on the Brownian particle is found to be random over the time. In order to write the equation of motion, we are assuming that Brownian particle is in thermal equilibrium with the heat bath provided by the fluid molecules.

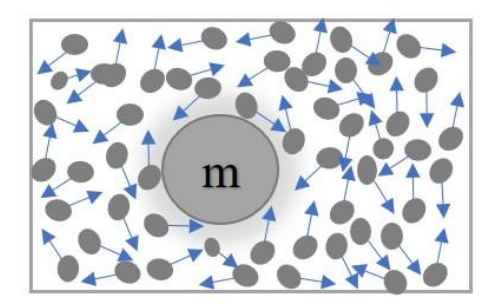


Fig.1.1: Big Brownian particle of mass, m, submerged in a fluid of very small particles

Corresponding equation of motion in one dimension can be written as:

$$\frac{dx}{dt} = v(t) \tag{1.5}$$

$$m\frac{dv}{dt} = -\zeta v + \eta(t) \tag{1.6}$$

where $\eta(t)$ represents the random force or fluctuating force (noise) which has the physical dimensions of force. This force-balanced equation (Eq. (1.6)) is called Langevin equation for a Brownian particle, where the first term defines the inertial force experienced by the particle of mass, m. Drag force $(-\zeta v)$ of the Brownian particle with a frictional coefficient, ζ is represented by the second term in the Eq. (1.6). The frictional coefficient is given by Stokes' law, $\zeta = 6\pi\eta a$. Both friction and noise arises due to the interaction between the Brownian particle and the heat bath. The statistical properties of the random force can be sum up using its first and second moment.

$$\langle \eta(t) \rangle = 0 \tag{1.7}$$

 $\langle ... \rangle$ represents the ensemble average with respect to the distribution of realizations of $\eta(t)$. The first moment of random force is zero Eq. (1.7), because the average random force exerted on this Brownian particle by all other fluid molecules is on average is zero. The second moment of the random force is

$$\langle \eta(t)\eta(t')\rangle = 2B\delta(t-t') \tag{1.8}$$

The term B measures the strength of the random force. Here, we can see that the individual random kicks hitting the Brownian particle is completely uncorrelated. In other words, what hits at one time say t is very different from what hits at t'. The memory between random forces at different times gets lost because of the continuous random collisions,. The autocorrelation function depends only on the time difference between the two times and its future is defined from the present value without considering the past information. It has no memory which indicates that it is a Markovian force. Fourier transform of the autocorrelation of this noise will give white noise, which is independent of the frequency. In other words, white noise has flat power spectrum. The auto correlation function of white noise is delta function.

Eq. (1.6) is a first order linear, inhomogeneous differential equation and have the solution:

$$v(t) = v(0)e^{-\zeta t/m} + \frac{1}{m} \int_0^t dt' e^{-\zeta(t-t')/m} \eta(t')$$
 (1.9)

The first and second term gives the exponential decay of the initial velocity and the extra velocity produced by the random noise respectively. We can use this solution Eq. (1.9), in order to get the mean squared velocity $\langle v(t)^2 \rangle$. There are three contributions to $\langle v(t)^2 \rangle$. The first one corresponds to:

$$e^{-2\zeta t/m}v(0)^2$$
 (1.10)

and at longer times it decays to zero. The second one is the cross term which is a first order in noise $\eta(t)$, Eq. (1.11) which becomes zero on averaging over noise.

$$2v(0)e^{-\zeta t/m}\frac{1}{m}\int_{0}^{t}dt'\,e^{-\zeta(t-t')/m}\eta(t')$$
(1.11)

The third contribution is second order in the noise $\eta(t)$:

$$\int_{0}^{t} dt' e^{-\zeta(t-t')/m} \eta(t') \frac{1}{m^{2}} \int_{0}^{t} dt'' e^{-\zeta(t-t'')/m} \eta(t'')$$
 (1.12)

By making the use of Eq. (1.9), we have the average of the product of the two noise factors:

$$\int_{0}^{t} dt' e^{-\zeta(t-t')/m} \eta(t') \frac{1}{m^{2}} \int_{0}^{t} dt'' e^{-\zeta(t-t'')/m} 2B\delta(t'-t'')$$
(1.13)

Hence, the mean squared velocity is

$$\langle v(t)^2 \rangle = e^{-2\zeta t/m} v(0)^2 + \frac{B}{\zeta m} (1 - e^{-2\zeta t/m})$$
 (1.14)

In the long-time limit, exponentials drop out and Eq. (1.14) proceeds to $B/\zeta m$. At equilibrium, $t \to \infty$, equipartition theorem, $\langle v(t)^2 \rangle = k_B T/m$ must hold. Hence the equality:

$$\lim_{t \to \infty} \langle v(t)^2 \rangle = \frac{B}{\zeta m} = \frac{k_B T}{m}$$
 (1.15)

$$B = \zeta k_B T \tag{1.16}$$

The Eq. (1.16) is named as the fluctuation-dissipation theorem. The magnitude of the random or fluctuating force, B, is balanced by the strength of the dissipation, ζ . Hence, the Langevin's model accurately captures the system's temperature.

1.5 Numerical method for Langevin equation simulation

It is often difficult to get an exact solution of Langevin equation analytically. So, we are using numerical methods for solving the Langevin equation. The corresponding equations Eq. (1.5) and Eq. (1.6) can be solved using Predictor-Corrector method (also known as Heun's method) which is a modified Euler's method. For solving, initially we discretize time t and use predictor-corrector method to proceed the Brownian particle from $x(t_n)$ to $x(t_{n+1})$ and also $v(t_n)$ to $v(t_{n+1})$ as:

$$x_1(t_{n+1}) = x(t_n) + v\Delta t$$
 (1.17)

$$v_1(t_{n+1}) = v(t_n) - \gamma v(t_n) \Delta t - U'(x(t_n) \Delta t + (2B\Delta t)^{1/2} g_w$$
 (1.18)

$$x(t_{n+1}) = x(t_n) + \frac{1}{2} [v(t_n) + v(t_{n+1})] \Delta t$$
(1.19)

$$v(t_{n+1}) = v(t_n) - \frac{1}{2} \left[\gamma v(t_n) + \gamma v(t_{n+1}) + U'(x(t_n)) + U'(x(t_{n+1})) \right] \Delta t$$

$$+ (2B\Delta t)^{1/2} g_w$$
(1.20)

Eq. (1.18) and Eq. (1.19) represents the predictor step, where the predicted value, $x_1(t_{n+1})$, and $v_1(t_{n+1})$ is calculated using Euler's method and then slopes at the points, $x(t_n)$, and $v(t_n)$ is calculated. Δt is the step size of each increment. Eq. (1.19) and Eq. (1.20) implies the corrector method. Here, the average of the slopes is calculated and added to $x(t_n)$ and $v(t_n)$ to calculate the corrected value of $x(t_{n+1})$ and $v(t_{n+1})$ respectively. g_w is Gaussian white noise and has the properties, $\langle g_w(t) \rangle = 0$, and $\langle g_w(t) g_w(s) \rangle = 2B\delta(t-s)$. Box-Muller algorithm⁸ is used to generate Gaussian white noise from two uniformly distributed random numbers with unit interval.

$$g_w = \left[-4B\Delta t \ln(a)\right]^{1/2} \cos(2\pi b), a \text{ and } b \text{ are the random numbers}$$
 (1.21)

The theory of Brownian motion was further studied by, Adriaan Daniël Fokker⁹, Max Planck¹⁰ and Hans Kramers¹¹ which leads to the later development in the field of Brownian motion. These studies have sparked numerous important advances in equilibrium and non-equilibrium statistical physics¹²,¹³. Furthermore, it inspired mathematically the growth of stochastic differential equation and probability theory which further fostered the stochastic modelling of finance, and stock market¹⁴,¹⁵. Currently, the dynamics of non-equilibrium systems under stochastic influence might well be studied most simply and effectively using the theory of Brownian motion.

Next section, we are discussing about Brownian ratchets, mathematical formulation of ratchet and its applications.

1.2 Introduction to Brownian ratchets

In the first decade of the twentieth century, Marian Smoluchowski⁵ designed a thought experiment and composed a device called Brownian ratchet. It features a ratchet attached to a pawl that allows the ratchet to rotate only in one direction by preventing its rotation in both directions. The two ends of the Brownian ratchet device are maintained at two distinct temperatures, T_1 and T_2 . Ratchet can be compared to a circular saw with asymmetric saw-teeth. The ratchet is connected to, via an axel, a small paddle wheel immersed in a liquid at a temperature, T_1 . Molecules in the liquid exhibit random Brownian motion due to the collisions between each other. As the device is considered very small, the impulses coming from the random collisions of liquid molecules on the paddle, force it to turn and resulting rotation in ratchet at temperature, T_2 . Further as the bidirectional motion of the ratchet is prevented by a pawl, the random collisions on the paddle lead to the unidirectional motion of ratchet thus allowing it to perform net work by lifting a connected load (Fig. 1.1). Therefore, a Brownian

ratchet rectify the unbiased fluctuations into a directed way in a thermally equilibrated environment.

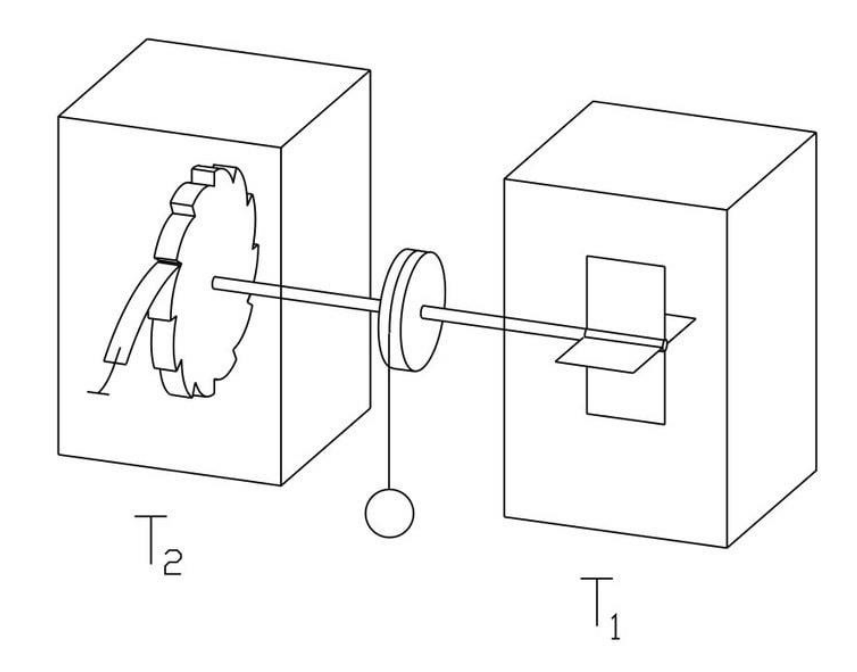


Fig. 1.1: Schematic representation of the Brownian ratchet

Although it may appear that this device will be able to generate 'something' out of 'nothing,' however close inspection reflects that this device would violate the second law of thermodynamics and create a Maxwell demon like situation. Since both the paddle and ratchet are kept in thermal equilibrium, as Richard Feynman highlighted in his renowned 'Lecture of Physics: There's plenty of room at the bottom¹⁶'in 1960 that, this device would not perform any work. According to Feynman, the pawl will be susceptible to random collisions from the medium, allowing it to move up and down, which make the ratchet teeth slip backward as well as it moves forward, thereby preventing the rotation of ratchet in one direction. He also proposed that if the paddle and the ratchet, are kept in heat baths having two different temperatures, $T_1 \neq T_2$, then net work is possible without violating the second law of thermodynamics. The key ingredients of generating net motion are breaking spatial symmetry and principle of detailed balance. The pawl mechanism and the temperature difference of two heat baths breaks the spatial symmetry and detailed balance, respectively. References [¹⁷, ¹⁸] give a critique of the Smoluchowski-Feynman construction.

The Brownian ratchet device in Fig. 1.1 can be formulated¹⁹ in a mathematical way as:

1. The ratchet (paddle) depicts a spatially periodic system. The potential it represents is one that is spatially periodic, U(x) = U(x + L).

- 2. Since the pawl attached to the ratchet, would move the teeth of it in both the directions, the symmetry of ratchet gets broken. This leads to the breaking of the reflection symmetry of the periodic potential, $U(x_0 + x) \neq U(x_0 x)$.
- Due to the collision between the molecules in the liquid, the average random force
 exerted on the vanes is found to be zero. This accords the thermal fluctuations to be, on
 average, as zero.
- 4. Heat bath with dissimilar temperature is a trivial way of breaking the detailed balance. Also, we can drive the system away from its thermal equilibrium state by applying driving force (either deterministic or stochastic kind of force) of zero mean.

1.2.1 Ratchet model - Mathematical formulation

We will discuss the analytic formulation of the ratchet model using Langevin description of the dynamics. Equation of the motion of the particle can be defined as

$$m\ddot{x} = -U'(x) - \gamma \dot{x} + \eta(t) \tag{1.22}$$

U(x) is the periodic potential with, U(x) = U(x + L), having a periodicity, L, and barrier height, $\Delta U(=U_{max}-U_{min})$. The inertial force is represented by the first component on the left-hand side of the Eq. (1.22). The force due to friction as described by the second component on the right-hand side of the Eq. (1.22), which is directly proportional to the particle's velocity, \dot{x} . γ corresponds to frictional coefficient of the described system. The potential force represented by, -U'(x), which is the negative gradient of the potential, has an average value over the periodicity, L.

$$\langle (-U'(x))\rangle_L = -\frac{1}{L} \int_x^{x+L} U'(x) \, dx = \frac{1}{L} [U(x) - U(x+L)] = 0$$
 (1.23)

The stochastic term, $\eta(t)$, denotes thermal fluctuations. It can be modeled using a δ -correlated Gaussian white noise has the following characteristics.

$$\langle \eta(t) \rangle = 0; \qquad \langle \eta(t) \eta(t') \rangle = 2\gamma k_B T \delta(t - t')$$
 (1.24)

Where T is the temperature of the system and k_B represents Boltzmann constant.

Fokker-Planck equation, corresponds to Eq. (1.23) is provided by

$$\frac{\partial P(x,\dot{x},t)}{\partial t} = \left[-\frac{\partial}{\partial x}\dot{x} + \frac{\partial}{\partial \dot{x}} \left(\frac{\gamma}{m}\dot{x} - \frac{f(x)}{m} \right) + \frac{\gamma k_B T}{m^2} \frac{\partial^2}{\partial x^2} \right] P(x,\dot{x},t) , \qquad (1.25)$$

Where f(x) = -U'(x) is the potential force. Under the stationary state, Eq. (1.25) can be resolved. As shown in Eq. (1.26), stationary probability density is

$$P_{st}(x,\dot{x}) = N \exp\left[-\frac{m\dot{x}^2}{2} + \int_0^x \frac{f(y)}{k_B T} dy\right],$$
 (1.26)

Where N stands for normalization constant, and can be calculated from the normalization condition of the stationary probability distribution

$$\int_{-\infty}^{+\infty} d\dot{x} \int_{0}^{L} dx P_{st}(x, \dot{x}) = 1 . \tag{1.27}$$

The mean velocity can be obtained as

$$\langle \dot{x} \rangle_{s} = \int_{-\infty}^{+\infty} \dot{x} d\dot{x} \int_{0}^{L} dx P_{st}(x, \dot{x}) . \tag{1.28}$$

It is straightforward to confirm that the mean velocity is zero in a stationary state. According to the principle of detailed balance, the Brownian particle in the periodic potential, U(x), does not move in a directed manner. We need to introduce a non-thermal force in order to induce transport.

In many circumstances, an overdamped condition is of interest. The equation of motion of a particle under overdamped dynamics is

$$\gamma \dot{x} = -U'(x) + \eta(t) \tag{1.29}$$

Probability density function, P(x, t), representing the Eq. (1.29), which is

$$\frac{\partial P(x,t)}{\partial t} = -\frac{\partial J(x,t)}{\partial x} \tag{1.30}$$

Where the probability current is represented by

$$J(x,t) = f(x)P(x,t) - D\frac{\partial P(x,t)}{\partial x}.$$
(1.31)

And $D = k_B T$. The current J is kept as a constant, in the stationary state $P(x) = \lim_{t \to \infty} P(x, t)$ and it can be read as

$$J = f(x)P(x) - D\frac{\partial P(x)}{\partial x}.$$
 (1.32)

The solution of Eq. (1.32) for P(x) is therefore can be written formally,

$$P(x) = -\frac{1}{R} \exp[-\psi(x)] \int_0^x \exp[\psi(y)] dy + N \exp[-\psi(x)], \qquad (1.33)$$

Where

$$\psi(x) = -\int_0^x \frac{f(y)}{D} dy \quad , \tag{1.34}$$

Else as an alternative, $\psi(x) = \frac{U(x)}{D}$, also N can be considered as a constant. In line with the periodic boundary condition:

$$\psi(x) = \psi(x+L). \tag{1.35}$$

Applying periodic boundary condition on Eq. (1.33) and from Eq. (1.35) and it follows

$$\frac{J}{D} \int_{x}^{x+1} \exp[\psi(y)] dy = 0.$$
 (1.36)

The aforementioned integral cannot be zero, hence the current, J = 0, which is given by an overdamped Langevin equation having periodic boundary condition. Hence,

$$P(x) = N \exp[-\psi(x)] \tag{1.37}$$

And normalization constant, N, can be $\left[\int_0^1 \exp\left[\int_0^x \frac{f(y)}{D}dy\right]\right]^{-1}$. The Brownian particle's zero current, J=0, can be physically interpreted as follows. There is no slope for generalized potential, $\psi(x)$, (Fig. 1.2(a)). This denotes that the rates of transition to both the right and left wells from a local minimum state of the generalised potential, $\psi(x)$, are the same. The difference between rates of transition in both the positive and negative directions, determines the stationary mean velocity. Therefore, the current, J=0, indicates the principle of detailed balance.

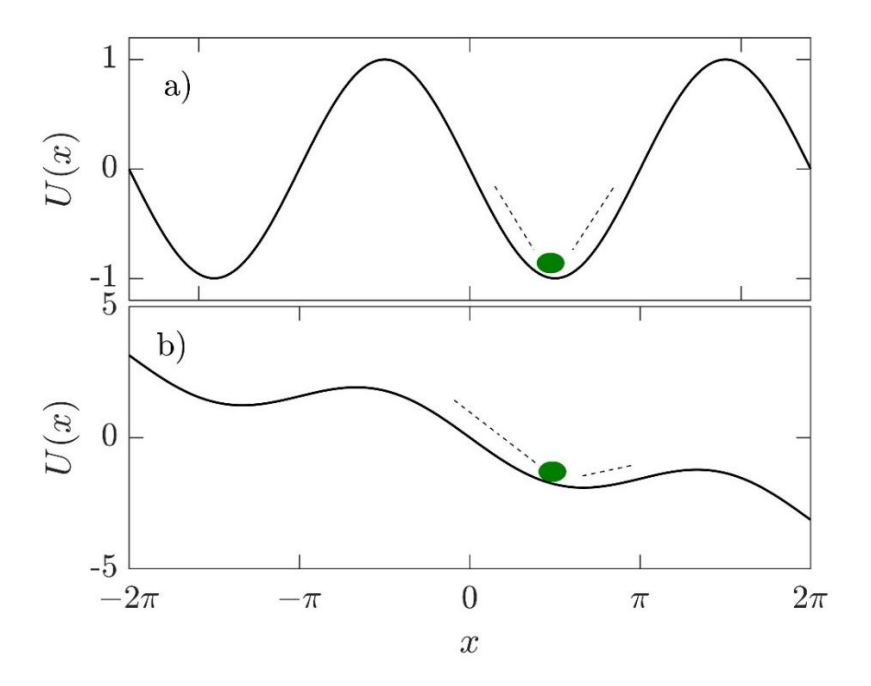


Fig. 1.2: Schematic representation of generalized potential, a) Generalized periodic potential with zero slope, Brownian particle's transition probability from local minima to both the left as well as right well are equal, so that there is no directed motion. b) Periodic potential having non zero slope and hence transition probability of particle to left and right well are unequal which results in a directed motion.

The principle of detailed balance should be broken in order to generate directed motion. The formulation for generalised potential (Eq. (1.34)) contains the explanation. The quantity, D, in the Eq.(1.34) must be space-dependent, D(x), in order for the generalised potential, $\Delta \psi \neq 0$, (Fig. 1.2(b)) to have a non-zero slope. So, to initiate a directed motion, the principle of detailed balance should be broken. It is possible to achieve this, by adding non - equilibrium fluctuation or an external load. Any external non-equilibrium fluctuation that is added to the system will not be enough to change the detailed balancing principle and initiate directed transport. Instead, in order to make the diffusion coefficient spatially dependent and generate an asymmetric generalised potential, the external non-equilibrium fluctuation force must be properly correlated.

1.2.1 Different types of Brownian ratchets

Inspired from the theme of directed transport from Brownian ratchet leads to several studies in statistical and biological physics, in both theoretical $^{19-34}$ and experimental $^{36-42}$. There is plethora of literatures which cover different classes of ratchet systems. One such example includes- pulsating ratchets – where the potential is switched on or off $^{43-48}$ (Fig 1.3). Here the

potential is not shifting in space over time, that is the spatial periodicity of the potential remains intact. Rather, the amplitude of the ratchet potential is modulated with time. In other words, these ratchets deliver directed motion through 'potential oscillations.'

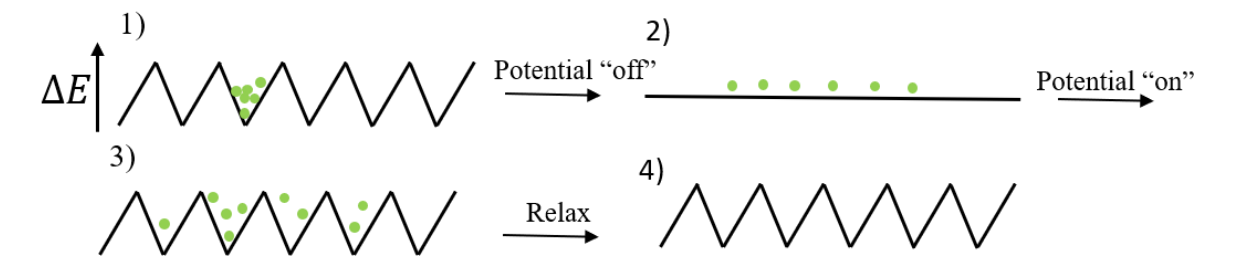


Fig1.3: Graphical representation of pulsating ratchet

This can experimentally be mimicked in the case of identical colloidal Brownian particles in the symmetric periodic potential. Colloidal particles placed like in two parallel straight lines forming a one-dimensional channel of locally variable width, with space-dependent oscillation periods⁴⁹. The other examples include tilting ratchet in which the unbiased additive driving force will take over the role of non-equilibrium perturbation which will drive the system out of thermal equilibrium. When the applied external perturbation is heat, then those ratchet systems are categorized as temperature or diffusion ratchet^{43,50} (Fig 1.4). Here, when the temperature is increased, the particles located at the energy-minima of the ratchet potential cross the energy barrier ($\ll kT$) and diffuse across the surface for a shorter period of time. In an asymmetric potential energy surface, there can be of higher likelihood of the particles getting trapped to the right of their original position as temperature is lowered. And this leads to their directional transport. This mechanism is similar to the on-off mechanism of pulsating ratchets.

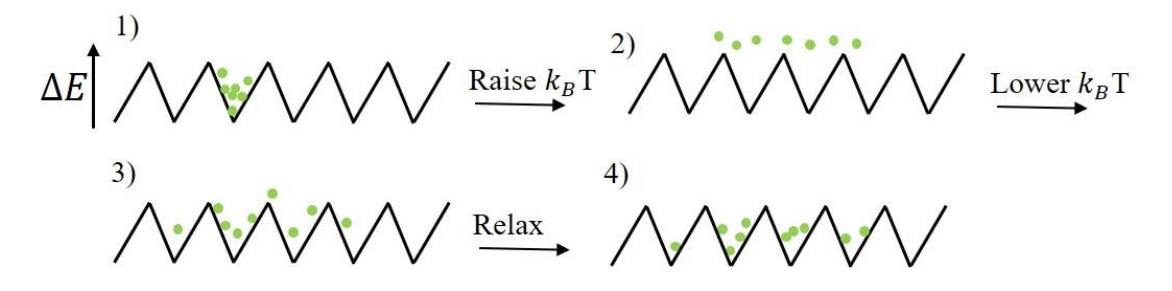


Fig1.4: Graphical representation of temperature or diffusion ratchet

Another category of ratchets is rocking ratchets^{51–58}, where a periodic directional force is applied to a potential surface which is asymmetric, to generate directional transport (Fig 1.5). Even though the average of the net directional force is zero, due to having a asymmetry in the potential energy surface, system is able to generate the directed motion.

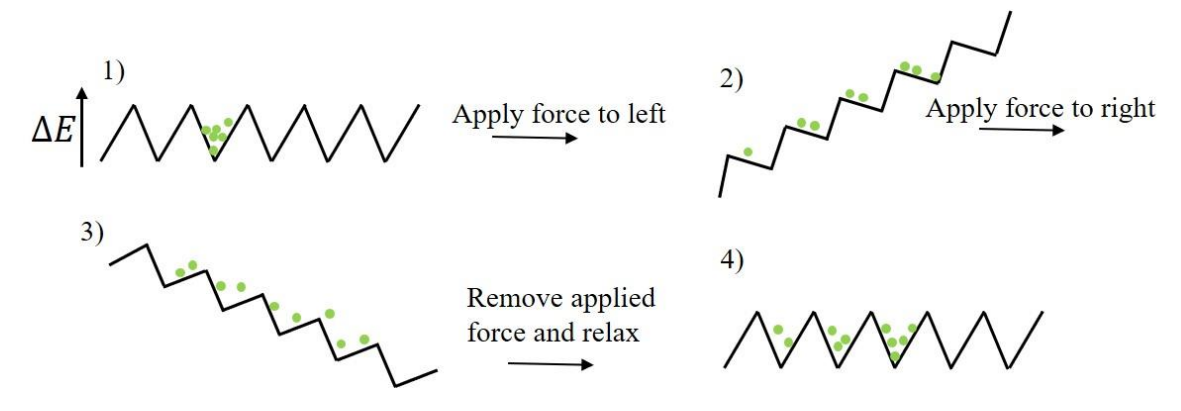


Fig1.5: Graphical representation of rocking ratchet

Energy ratchets⁵⁹ are another classes of ratchets. They modulate the potential energy surface's peaks and minima regardless of the position of the Brownian particle. Meanwhile, information ratchets^{43,60,61} operate by lifting or lowering the potential energy barrier with respect to the location of the particle, which leads to distribution of particles in a non-equilibrium condition. Similar to the famous Maxwell's demon¹⁰, this process requires information handover from the particle to the ratchet potential surface. Rotaxane1, which consists of dibenzo-24-crown-8-based macrocycle is considered as the first example of synthetic molecular information ratchet^{60,61}. Other examples of ratchet systems include correlation ratchets^{62–64}, quantum ratchets³³ and so on.

1.2.2 Applications of Brownian ratchets

The theoretical concept of rectification of noise and converting those unbiased thermal fluctuations into a unidirectional motion, by such a device called "Brownian motors" have been experimentally realized in several systems. Examples includes cold atoms in a dissipative optical lattice⁶⁵, diffusion of colloidal particles in a cycle of three holographic optical trapping patterns⁶⁶, Josephson Junction arrays^{67–69}, vortex lattice ratchet effect in superconducting films with periodic arrays of asymmetric potential^{70,71}, to name only a few. The Brownian ratchet model has been used for studying many biological processes which includes intracellular of cargo on microtubule networks, metastasis of cancer cells, transport of ions through nanopores among many. The functioning of protein-based molecular motors in cell can be explain using the ratchet theory. Molecular motors are either natural or synthetic molecular machines, which are capable of continuously transforming one form of energy into another. They use random thermal motion as their energy input and generate unidirectional motion^{33,72–79}. In biological systems, molecular motors are made up of nucleic acids and proteins and they use the chemical energy of ATP (adenosine triphosphate) as the energy source. Protein kinesin, an example of

biological motor, which uses the energy of ATP hydrolysis to move along the surface of microtubule filaments. This can be mapped into the transport of Brownian particles moving in an one-dimensional ratchet potential with period of about 8.2nm. Here, the nonequilibrium energy is provided by the catabolic reaction process involving the hydrolysis of ATP which occur near to kinesin. Myosin⁸⁰ and dyneins⁸¹ are some other examples of ATP-driven molecular motors. These motors and also, kinesin⁸² is responsible for the cellular activities such as intracellular transport and muscle contraction.

Synthetic molecular motors⁸³ are another class of molecular machines which rotate only in one direction under an energy input. The concept of synthetic molecular motors was first promoted by Richard Feynman's on his remark that "There's plenty of room at the bottom"⁸⁴. After half a century, the Nobel Prize in 2016 was awarded to Jean-Pierre Sauvage, Sir J. Fraser Stoddart and Bernard L. Feringa for their design and synthesis of molecular machines^{85–87}. Over the past decades, both biological and synthetic motors have been topic of intense study. Also, creation and understanding as well as engineering of molecular motors is the one of the research topics in various disciplines of science^{79,88}.

Thus, the concept of Brownian motors does provide the concept of noise-induced transport from random thermal fluctuations. It has many potential technological applications in different contexts ranging from optimising and controlling transport on the nanoscale²⁶, particle separation and trapping at microscale^{89–91}, nanoscale friction^{92,93} and so on. So, in the context of transport of particles rectifying the thermal fluctuations, it is worth to ask the question that what will be the nature of diffusive process. In the next section, discussion will be on the types of diffusion and their research importance.

1.3 Anomalous diffusion and research scenario

Brownian motion, an archetypal example of random walk⁹⁴ is commonly quantified by the trajectory mean squared displacement (MSD), $\langle \Delta x^2(t) \rangle$, which linearly increases with time, t. It is also, directly proportional to the diffusion coefficient, D, of the fluid. In one dimension, with, x(t), as the position of the random walker at time, t, then MSD is:

$$<\Delta x^{2}(t)> = <[x(t)-]^{2}> = 2Dt$$
 (1.5)

Where <. > indicates the ensemble averaging. For Brownian walkers, MSD grows linearly in time ($MSD \propto t$). Deviations from Brownian motion and showing an asymptotic power-law dependence ($MSD \propto t^{\alpha}$) are referred to as anomalous diffusion. The exponent α indicates

the type of diffusion. For normal diffusion, $\alpha = 1$ as in Brownian motion. Sub-diffusion and super-diffusion are characterized by the range of values of α . The value of α lies in the range of $0 < \alpha < 1$ for sub-diffusion and for super-diffusion $\alpha > 1$ (Fig.1.6).

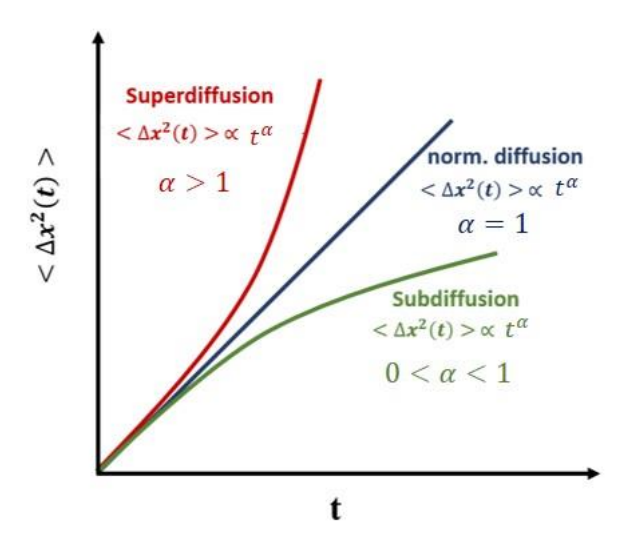


Fig1.6: Schematic representation of various types of diffusion from the time dependence of MSD.

There are lot of instances where MSD deviates from linear temporal evolution such as in the economic fluctuations of stock market⁹⁵, anomalous diffusion in the cytoplasm of mammalian cells⁹⁶, dynamics of sleep-wake transitions during sleep⁹⁷, in the foraging and mating strategies of animals⁹⁸, enhanced diffusion in intracellular transport induced by protein motors⁹⁹, Levy flight facilitated diffusion on DNA polymeric chains¹⁰⁰, migratory dynamics of cells in monolayers¹⁰¹, inverse-friction expansion for Brownian motion in an inhomogeneous medium in the overdamped limit¹⁰², transient anomalous diffusion in periodic systems¹⁰³, crossover from sub diffusive motion to diffusive motion in glass forming liquids¹⁰⁴, to name a few. There are many formalism that describe the mechanistic aspects of anomalous diffusion ranging from thermodynamics^{105–107}, fractional derivatives^{108,109} to generalized Langevin equations^{110,111}.

1.7 Scope of our chosen problems in the current research background

The vast majority of all these research studies with this theoretical background, look at the overdamped Brownian dynamics of the system in the energy landscapes that are not solely periodic but also smooth. However, it is well established that there are numerous circumstances when spatial heterogeneity in the potential exists^{112–118}.

Zwanzig first simulated the rough energy landscape by overlaying a rapidly - oscillating trigonometric function over the baseline potential energy function in a seminal paper ¹¹⁹. There, he pointed out the reduction of diffusion coefficient because of the roughness in the periodic potential in compared to smooth potential especially at low temperatures, which lead to the reduction of thermally activated barrier crossing rate of the particle. He also provides an analytical tool to explain the properties of roughness in his model. Recent studies showed that roughness hinders current notably in overdamped dynamics¹²⁰. Ansari developed a robust numerical approach to solve the Smoluchowski equation describing diffusion along a spatially rough potential¹²¹. Pollak et. al. used master equation for studying the rate theory for rugged energy landscape¹²². Mondal et. al. calculated directed current and efficiency of a thermal ratchet moving in a rough periodic potential and found that roughness holds back the current in a ratchet potential in the presence of Gaussian noise¹²⁰. All these studies showed the adverse effect of the spatial heterogeneity in the transport as well diffusive characteristics of the Brownian particle. Does roughness always act as a hindrance to the transport of Brownian particle, even if it is inertially driven in its dynamical level. The notion of this question directs a research gap in the area of transport in driven ratchet systems. So, in this thesis, we looked out to the effects of rough periodic potential on the noise-induced directed transport of a ratchet system in underdamped dynamics aided by Gaussian noise, in the chapters 2-4.

1.8 Reference

- 1. Holland, M. *The change agent. Achieving Cultural Change in Networked Libraries* (2017). doi:10.4324/9781315263434-16.
- 2. Brown, R. XXVII. A brief account of microscopical observations made in the months of June, July and August 1827, on the particles contained in the pollen of plants; and on the general existence of active molecules in organic and inorganic bodies . *Philos. Mag.* **4**, 161–173 (1828).
- 3. Einstein, A. *Investigations on the theory of the Brownian movement, translated by A. D. Cowper. Dover publications, INC* (Dover publications, INC., 1956).
- Einstein, A. Zur Theorie der Brownschen Bewegung [AdP 19, 371 (1906)]. *Ann. Phys.* 14, 248–258 (2005).
- 5. von Smoluchowski, M. Zur kinetischen Theorie der Brownschen Molekularbewegung und der Suspensionen. *Ann. Phys.* **326**, 756–780 (1906).
- 6. Perrin, J. Les atomes. C. R. Acad. Sci. (France) vol. 158 (1914).
- 7. Lemons, D. S. & Gythiel, A. Paul Langevin's 1908 paper "On the Theory of Brownian Motion" ["Sur la théorie du mouvement brownien," C. R. Acad. Sci. (Paris) 146, 530–533 (1908)]. *Am. J. Phys.* **65**, 1079–1081 (1997).
- 8. Fox, R. F., Gatland, I. R., Roy, R. & Vemuri, G. Fast, accurate algorithm for numerical simulation of exponentially correlated colored noise. *Phys. Rev. A* **38**, (1988).
- 9. Fokker, A. D. Die mittlere Energie rotierender elektrischer Dipole im Strahlungsfeld. *Ann. Phys.* **348**, 810–820 (1914).
- 10. Maxwell, J. C. Theory of heat. *Green, New York* (1902).
- 11. Kramers, H. A. Brownian motion in a field of force and the diffusion model of chemical reactions. *Physica* **7**, 284–304 (1940).
- 12. Hänggi, P. & Marchesoni, F. Introduction: 100 years of Brownian motion. *Chaos* **15**, 1–5 (2005).
- 13. Kubo, R. Brownian motion and nonequilibrium statistical mechanics. *Science* (80-.).

- **233**, 330–334 (1986).
- 14. Lewis, J. T. & Pulè, J. V. Dynamical theories of Brownian motion. *Int. Symp. Math. Probl. Theor. Phys.* 294–296 (2005) doi:10.1007/bfb0013344.
- 15. Gardiner, C. W. Handbook of stochastic methods for physics, chemistry, and the natural sciences. *Springer-Verlag, Berlin, Heidelb.* (2004).
- 16. Feynman, R. P., Leighton, R. B., Sands, M. & Hafner, E. M. The Feynman Lectures on Physics; Vol. I. *Am. J. Phys.* **33**, 750–752 (1965).
- 17. Parrondo, J. M. R. & Español, P. Criticism of Feynman's analysis of the ratchet as an engine. *Am. J. Phys.* **64**, 1125–1130 (1996).
- 18. Magnasco, M. O. & Stolovitzky, G. Feynman's ratchet and pawl. *J. Stat. Phys.* **93**, 615–632 (1998).
- 19. Luczka, J. Application of statistical mechanics to stochastic transport. *Phys. A Stat. Mech. its Appl.* **274**, 200–215 (1999).
- 20. B. M. & Leibler, S. NEWS AND VIEWS Moving forward noisily. (1994).
- 21. Luczka, J., Bartussek, R. & Hanggi, P. White-noise-induced transport in periodic structures. *EPL* **31**, (1995).
- 22. Speer, D., Eichhorn, R. & Reimann, P. Directing brownian motion on a periodic surface. *Phys. Rev. Lett.* **102**, 2–5 (2009).
- 23. Bartussek, R. & Hänggi, P. Brownian Rectifiers: H o w to Convert Brownian M o t i o n into Directed Transport. *Lect. Notes Phys.* **476**, 294–308 (1996).
- 24. Chauwin, J. F., Ajdari, A. & Prost, J. Force-free motion in asymmetric structures: A mechanism without diffusive steps. *Epl* **27**, 421–426 (1994).
- 25. Bier, M. Brownian ratchets in physics and biology. *Contemp. Phys.* **38**, 371–379 (1997).
- 26. Hänggi, P. & Marchesoni, F. Artificial Brownian motors: Controlling transport on the nanoscale. *Rev. Mod. Phys.* **81**, 387–442 (2009).
- 27. Rousselet, J., Salome, L., Ajdarit, A. & Prostt, J. periodic asymmetric potential: I j. **370**, 446–448 (1994).

- 28. Chen, R. & Jiang, L. Directed transport of symmetrically periodic system induced by 'color' breaking of noise. *Chaos* **30**, (2020).
- 29. Derényi, I. & Vicsek, T. Cooperative transport of brownian particles. *Phys. Rev. Lett.* **75**, 374–377 (1995).
- 30. Reimann, P. Thermally activated escape with potential fluctuations driven by an Ornstein-Uhlenbeck process. *Phys. Rev. E* **52**, 1579–1600 (1995).
- 31. Derényi, I. & Astumian, R. D. Brownian Ratchets and Their Application to Biological Transport Processes and Macromolecular Separation. *Struct. Dyn. Confin. Polym.* 281–294 (2002) doi:10.1007/978-94-010-0401-5_17.
- 32. Speer, D., Eichhorn, R. & Reimann, P. Brownian motion: Anomalous response due to noisy chaos. *Epl* **79**, (2007).
- 33. Lau, B., Kedem, O., Schwabacher, J., Kwasnieski, D. & Weiss, E. A. An introduction to ratchets in chemistry and biology. *Mater. Horizons* **4**, 310–318 (2017).
- 34. Bartussek, R., Hänggi, P. & Kissner, J. G. Periodically rocked thermal ratchets. *Epl* **28**, 459–464 (1994).
- 35. Thibado, P. M. *et al.* Fluctuation-induced current from freestanding graphene. *Phys. Rev. E* **102**, 1–12 (2020).
- 36. Kümmel, F. *et al.* Circular motion of asymmetric self-propelling particles. *Phys. Rev. Lett.* **110**, 1–5 (2013).
- 37. Galajda, P., Keymer, J., Chaikin, P. & Austin, R. A wall of funnels concentrates swimming bacteria. *J. Bacteriol.* **189**, 8704–8707 (2007).
- 38. Kaiser, A. *et al.* Transport powered by bacterial turbulence. *Phys. Rev. Lett.* **112**, 1–5 (2014).
- 39. Koumakis, N., Lepore, A., Maggi, C. & Di Leonardo, R. Targeted delivery of colloids by swimming bacteria. *Nat. Commun.* **4**, 1–6 (2013).
- 40. Schwarz-Linek, J. *et al.* Phase separation and rotor self-assembly in active particle suspensions. *Proc. Natl. Acad. Sci. U. S. A.* **109**, 4052–4057 (2012).
- 41. Bricard, A., Caussin, J. B., Desreumaux, N., Dauchot, O. & Bartolo, D. Emergence of macroscopic directed motion in populations of motile colloids. *Nature* **503**, 95–98

(2013).

- 42. Mijalkov, M., McDaniel, A., Wehr, J. & Volpe, G. Engineering sensorial delay to control phototaxis and emergent collective behaviors. *Phys. Rev. X* **6**, 1–16 (2016).
- 43. Reimann, P. Brownian motors: Noisy transport far from equilibrium. *Phys. Rep.* **361**, 57–265 (2002).
- 44. Semenov, S. & Schimpf, M. Non-Feynman Deterministic Pulsing Ratchet Based on a Symmetric Periodic Potential with Harmonic Time Modulation. *J. Phys. Chem. C* **121**, 22621–22627 (2017).
- 45. Reimann, P. & Evstigneev, M. Pulsating potential ratchet. *Epl* **78**, (2007).
- 46. Rozenbaum, V. M., Shapochkina, I. V., Teranishi, Y. & Trakhtenberg, L. I. Symmetry of Pulsating Ratchets. *JETP Lett.* **107**, 506–511 (2018).
- 47. Feito, M. & Cao, F. J. Time-delayed feedback control of a flashing ratchet. *Phys. Rev. E Stat. Nonlinear, Soft Matter Phys.* **76**, 1–10 (2007).
- 48. Kedem, O., Lau, B., Ratner, M. A. & Weiss, E. A. Light-responsive organic flashing electron ratchet. *Proc. Natl. Acad. Sci. U. S. A.* **114**, 8698–8703 (2017).
- 49. Bleil, S., Reimann, P. & Bechinger, C. Directing Brownian motion by oscillating barriers. *Phys. Rev. E Stat. Nonlinear, Soft Matter Phys.* **75**, 1–5 (2007).
- 50. Reimann, P., Bartussek, R., Häußler, R. & Hänggi, P. Brownian motors driven by temperature oscillations. *Phys. Lett. Sect. A Gen. At. Solid State Phys.* **215**, 26–31 (1996).
- 51. Zhao, T., Cao, T., Zhan, Y. & Zhuo, Y. Rocking ratchets with stochastic potentials. *Phys. A Stat. Mech. its Appl.* **312**, 109–118 (2002).
- 52. Arzola, A. V., Volke-Sepúlveda, K. & Mateos, J. L. Dynamical analysis of an optical rocking ratchet: Theory and experiment. *Phys. Rev. E Stat. Nonlinear, Soft Matter Phys.* **87**, 1–9 (2013).
- 53. Arzola, A. V., Volke-Sepúlveda, K. & Mateos, J. L. Experimental control of transport and current reversals in a deterministic optical rocking ratchet. *Phys. Rev. Lett.* **106**, 20–23 (2011).
- 54. Grossert, C., Leder, M., Denisov, S., Hänggi, P. & Weitz, M. Experimental control of

- transport resonances in a coherent quantum rocking ratchet. Nat. Commun. 7, (2016).
- 55. Schwemmer, C., Fringes, S., Duerig, U., Ryu, Y. K. & Knoll, A. W. Experimental Observation of Current Reversal in a Rocking Brownian Motor. *Phys. Rev. Lett.* **121**, 104102 (2018).
- 56. Skaug, M. J., Schwemmer, C., Fringes, S., Rawlings, C. D. & Knoll, A. W. Nanofluidic rocking Brownian motors. *Science* (80-.). **359**, 1505–1508 (2018).
- 57. Schreier, M., Reimann, P., Hänggi, P. & Pollak, E. Giant enhancement of diffusion and particle selection in rocked periodic potentials. *Europhys. Lett.* **44**, 416–422 (1998).
- 58. Zarlenga, D. G., Larrondo, H. A., Arizmendi, C. M. & Family, F. Complex synchronization structure of an overdamped ratchet with discontinuous periodic forcing. *Phys. Rev. E Stat. Nonlinear, Soft Matter Phys.* **80**, 1–9 (2009).
- 59. Wang, H. Y. & Bao, J. D. Brownian free energy ratchets. *Phys. A Stat. Mech. its Appl.*323, 197–212 (2003).
- 60. Serreli, V., Lee, C. F., Kay, E. R. & Leigh, D. A. A molecular information ratchet. *Nature* **445**, 523–527 (2007).
- 61. Carlone, A., Goldup, S. M., Lebrasseur, N., Leigh, D. A. & Wilson, A. A three-compartment chemically-driven molecular information ratchet. *J. Am. Chem. Soc.* **134**, 8321–8323 (2012).
- 62. Doering, C. R., Horsthemke, W. & Riordan, J. Nonequilibrium fluctuation-induced transport. *Phys. Rev. Lett.* **72**, 2984–2987 (1994).
- 63. Ai, B. Q. *et al.* Efficiency optimization in a correlation ratchet with asymmetric unbiased fluctuations. *Phys. Rev. E Stat. Physics, Plasmas, Fluids, Relat. Interdiscip. Top.* **68**, 1–5 (2003).
- 64. Ai, B. Q. *et al.* Efficiency and current in a correlated ratchet. *Chaos* **14**, 957–962 (2004).
- 65. Jones, P. H., Goonasekera, M. & Renzoni, F. Rectifying fluctuations in an optical lattice. *Phys. Rev. Lett.* **93**, 1–4 (2004).
- 66. Lee, S. H., Ladavac, K., Polin, M. & Grier, D. G. Observation of flux reversal in a

- symmetric optical thermal ratchet. *Phys. Rev. Lett.* **94**, 1–4 (2005).
- 67. Beck, M. *et al.* High-efficiency deterministic Josephson vortex ratchet. *Phys. Rev. Lett.* **95**, 2–5 (2005).
- 68. Trías, E., Mazo, J. J., Falo, F. & Orlando, T. P. Depinning of kinks in a Josephson-junction ratchet array. *Phys. Rev. E Stat. Physics, Plasmas, Fluids, Relat. Interdiscip. Top.* **61**, 2257–2266 (2000).
- 69. Menditto, R. et al. Tunable φ Josephson junction ratchet. Phys. Rev. E 94, 1–5 (2016).
- 70. Villegas, J. E., Gonzalez, E. M., Gonzalez, M. P., Anguita, J. V. & Vicent, J. L. Experimental ratchet effect in superconducting films with periodic arrays of asymmetric potentials. *Phys. Rev. B Condens. Matter Mater. Phys.* **71**, 1–5 (2005).
- 71. Van De Vondel, J., De Souza Silva, C. C., Zhu, B. Y., Morelle, M. & Moshchalkov, V. V. Vortex-rectification effects in films with periodic asymmetric pinning. *Phys. Rev. Lett.* **94**, 2–5 (2005).
- 72. Kolomeisky, A. B. & Fisher, M. E. Molecular motors: A theorist's perspective. *Annu. Rev. Phys. Chem.* **58**, 675–695 (2007).
- 73. Jülicher, F., Ajdari, A. & Prost, J. Modeling molecular motors. *Rev. Mod. Phys.* **69**, 1269–1281 (1997).
- 74. Iino, R., Kinbara, K. & Bryant, Z. Introduction: Molecular Motors. *Chem. Rev.* **120**, 1–4 (2020).
- 75. Astumian, R. D. & Bier, M. Fluctuation driven ratchets: Molecular motors. *Phys. Rev. Lett.* **72**, 1766–1769 (1994).
- 76. Ait-Haddou, R. & Herzog, W. Brownian ratchet models of molecular motors. *Cell Biochem. Biophys.* **38**, 191–213 (2003).
- 77. Astumian, R. D. & Hänggi, P. B Rownian. 33–39 (2002).
- 78. Erbas-Cakmak, S., Leigh, D. A., McTernan, C. T. & Nussbaumer, A. L. Artificial Molecular Machines. *Chem. Rev.* **115**, 10081–10206 (2015).
- 79. Gross, M. The unstoppable march of the machines. *Curr. Biol.* **25**, R255–R258 (2015).
- 80. Spudich, J. A. Nat. Rev. Mol. Cell Biol. 2001 Spudich. 2, (2001).

- 81. Bhabha, G., Johnson, G. T., Schroeder, C. M. & Vale, R. D. How Dynein Moves Along Microtubules. *Trends Biochem. Sci.* **41**, 94–105 (2016).
- 82. Block, S. M. Kinesin motor mechanics: Binding, stepping, tracking, gating, and limping. *Biophys. J.* **92**, 2986–2995 (2007).
- 83. Davis, A. P. Synthetic molecular motors. *Nature* **401**, 120–121 (1999).
- 84. Landauer, R. There's Plenty of Room at the Bottom. *Feynman and Computation* 77–92 (2018) doi:10.1201/9780429500459.
- 85. Sauvage, J. P. From Chemical Topology to Molecular Machines (Nobel Lecture). *Angew. Chemie Int. Ed.* **56**, 11080–11093 (2017).
- 86. Feringa, B. L. The Art of Building Small: From Molecular Switches to Motors (Nobel Lecture). *Angew. Chemie Int. Ed.* **56**, 11060–11078 (2017).
- 87. Stoddart, J. F. Mechanically Interlocked Molecules (MIMs)—Molecular Shuttles, Switches, and Machines (Nobel Lecture). *Angew. Chemie Int. Ed.* **56**, 11094–11125 (2017).
- 88. Service, R. F. Chemistry Nobel heralds age of molecular machines. *Science* (80-.). **354**, 158–159 (2016).
- 89. Gorre-Talini, L., Spatz, J. P. & Silberzan, P. Dielectrophoretic ratchets. *Chaos* **8**, 650–656 (1998).
- 90. Derényi, I. & Dean Astumian, R. AC separation of particles by biased Brownian motion in a two-dimensional sieve. *Phys. Rev. E Stat. Physics, Plasmas, Fluids, Relat. Interdiscip. Top.* **58**, 7781–7784 (1998).
- 91. Duke, T. A. J. & Austin, R. H. Microfabricated sieve for the continuous sorting of macromolecules. *Phys. Rev. Lett.* **80**, 1552–1555 (1998).
- 92. Daikhin, L. & Urbakh, M. Roughness effect on the frictional force in boundary lubrication. *Phys. Rev. E* **49**, 1424–1429 (1994).
- 93. Daly, C. & Krim, J. Sliding friction of solid xenon monolayers and bilayers on Ag(111). *Phys. Rev. Lett.* **76**, 803–806 (1996).
- 94. Pearson, K. The problem of the random walk [3]. *Nature* vol. 72 (1905).

- 95. Plerou, V., Gopikrishnan, P., Amaral, L. A. N., Gabaix, X. & Stanley, H. E. Economic fluctuations and anomalous diffusion. *Phys. Rev. E Stat. Physics, Plasmas, Fluids, Relat. Interdiscip. Top.* **62**, 3023–3026 (2000).
- 96. Sabri, A., Xu, X., Krapf, D. & Weiss, M. Elucidating the Origin of Heterogeneous Anomalous Diffusion in the Cytoplasm of Mammalian Cells. *Phys. Rev. Lett.* **125**, 58101 (2020).
- 97. Lo, C. C. *et al.* Dynamics of sleep-wake transitions during sleep. *Europhys. Lett.* **57**, 625–631 (2002).
- 98. Humphries, N. E., Weimerskirch, H., Queiroz, N., Southall, E. J. & Sims, D. W. Foraging success of biological Lévy flights recorded in situ. *Proc. Natl. Acad. Sci. U. S. A.* **109**, 7169–7174 (2012).
- 99. Santamaría-Holek, I., Vainstein, M. H., Rubí, J. M. & Oliveira, F. A. Protein motors induced enhanced diffusion in intracellular transport. *Phys. A Stat. Mech. its Appl.* **388**, 1515–1520 (2009).
- 100. Lomholt, M. A., Ambjörnsson, T. & Metzler, R. Optimal target search on a fast-folding polymer chain with volume exchange. *Phys. Rev. Lett.* **95**, 1–4 (2005).
- 101. Palmieri, B., Bresler, Y., Wirtz, D. & Grant, M. Multiple scale model for cell migration in monolayers: Elastic mismatch between cells enhances motility. *Sci. Rep.* 5, 1–13 (2015).
- 102. Ryter, D. Brownian motion in inhomogeneous media and with interacting particles. *Zeitschrift für Phys. B Condens. Matter* **41**, 39–42 (1981).
- 103. Spiechowicz, J., Luczka, J. & Hänggi, P. Transient anomalous diffusion in periodic systems: Ergodicity, symmetry breaking and velocity relaxation. *Sci. Rep.* **6**, 1–11 (2016).
- 104. Haxton, T. K. & Liu, A. J. Kinetic heterogeneities at dynamical crossovers. *EPL* (*Europhysics Lett.* **90**, 66004 (2010).
- 105. Rubi, J. M. & Bedeaux, D. Brownian motion in a fluid in elongational flow. *J. Stat. Phys.* **53**, 125–136 (1988).
- 106. Pérez-Madrid, A. Gibbs entropy and irreversibility. *Phys. A Stat. Mech. its Appl.* **339**,

- 339-346 (2004).
- 107. Kuśmierz, Ł., Dybiec, B. & Gudowska-Nowak, E. Thermodynamics of superdiffusion generated by Lévy-Wiener fluctuating forces. *Entropy* **20**, 1–16 (2018).
- 108. Metzler, R. & Klafter, J. The random walk's guide to anomalous diffusion: A fractional dynamics approach. *Phys. Rep.* **339**, 1–77 (2000).
- 109. Metzler, R. & Klafter, J. The restaurant at the end of the random walk: Recent developments in the description of anomalous transport by fractional dynamics. *J. Phys. A. Math. Gen.* **37**, (2004).
- 110. Hänggi, P., Talkner, P. & Borkovec, M. Reaction-rate theory: Fifty years after Kramers. *Rev. Mod. Phys.* **62**, 251–341 (1990).
- 111. Lapas, L. C., Costa, I. V. L., Vainstein, M. H. & Oliveira, F. A. Entropy, non-ergodicity and non-Gaussian behaviour in ballistic transport. *Epl* **77**, 1–9 (2007).
- 112. Nevo, R., Brumfeld, V., Kapon, R., Hinterdorfer, P. & Reich, Z. Direct measurement of protein energy landscape roughness. *EMBO Rep.* **6**, 482–486 (2005).
- 113. Frauenfelder, H., Sligar, S. G. & Wolynes, P. G. The energy landscapes and motions of proteins. *Science* (80-.). **254**, 1598–1603 (1991).
- 114. Charbonneau, P., Kurchan, J., Parisi, G., Urbani, P. & Zamponi, F. Fractal free energy landscapes in structural glasses. *Nat. Commun.* **5**, 1–6 (2014).
- 115. Delemotte, L., Kasimova, M. A., Klein, M. L., Tarek, M. & Carnevale, V. Free-energy landscape of ion-channel voltage-sensor-domain activation. *Proc. Natl. Acad. Sci. U. S. A.* **112**, 124–129 (2015).
- 116. Heuer, A., Doliwa, B. & Saksaengwijit, A. Potential-energy landscape of a supercooled liquid and its resemblance to a collection of traps. *Phys. Rev. E Stat. Nonlinear, Soft Matter Phys.* **72**, 1–13 (2005).
- 117. Linder, T., de Groot, B. L. & Stary-Weinzinger, A. Probing the Energy Landscape of Activation Gating of the Bacterial Potassium Channel KcsA. *PLoS Comput. Biol.* **9**, 1–9 (2013).
- 118. Debenedetti, P. G. & Stillinger, F. H. Review article Supercooled liquids and the glass transition. *Nature* **410**, 259 (2001).

- 119. Zwanzig, R. Diffusion in a rough potential. *Proc. Natl. Acad. Sci. U. S. A.* **85**, 2029–2030 (1988).
- 120. Mondal, D., Ghosh, P. K. & Ray, D. S. Noise-induced transport in a rough ratchet potential. *J. Chem. Phys.* **130**, (2009).
- 121. Ansari, A. Mean first passage time solution of the Smoluchowski equation:
 Application to relaxation dynamics in myoglobin. *J. Chem. Phys.* **112**, 2516–2522 (2000).
- 122. Pollak, E., Auerbach, A. & Talknerz, P. Observations on rate theory for rugged energy landscapes. *Biophys. J.* **95**, 4258–4265 (2008).

INTRODUCTION: Part 2

THERMAL TRANSPORT IN LOW-DIMESNIONAL LATTICE

1.2.1 Introduction

One of the persistent problem in statistical thermodynamics, is how to understand heat conduction in insulator systems at the microscopic level. According to the Fourier law of heat conduction (named after the French Physicist Joseph Fourier), the heat flux, J, is proportional to the negative gradient of temperature, T, as

$$J = -\kappa \nabla T \tag{1.2.1}$$

and κ , is the thermal conductivity, which is the proportionality constant. This phenomenological equation was proposed by Fourier about almost 200 years ago to understand the thermal gradient inside the Earth. One key finding of Fourier's law is that the thermal conductivity is an inherent quality of the system and it does not depend on the system size. According to the Fourier law, with increasing chain length, the heat flux, $I \sim N^{-1}$, under a temperature difference. The main problem is, there is yet no first-principle derivation of this straightforward law. Also, the validity of Fourier's law in low dimension is not entirely certain. One of the long-standing challenges in nonequilibrium statistical mechanics is to comprehend the microscopic dynamical genesis of heat conduction. Numerous investigations have been inspired by the heat conductivity of low-dimensional systems¹⁻¹³. It is still an open and challenging problem to understand the macroscopic law of heat conduction and their statistical properties in terms of determistic microscopic dynamics. To simulate the transport processes in lattices, two heat baths with varying temperatures are combined with the vibrations of the atoms in the lattice with nearest neighbour interactions. Based on the numerical modelling of lattices, statistical observables from the microscopic Hamiltonians will be obtained, and the results will provide essential hints for the formulation of the microscopic theory of heat conduction.

It is important to note that this topic is not just an academic one. Researchers have already been able to experimentally quantify the size dependent of the heat conductivity in numerous one
14 and two-dimensional 15-17 microscopic materials due to the rapid progress in nanotechnology. Despite the fact that the microscopic mechanism of heat conduction remains uncertain, simulations have already been used to investigate the possible uses of nonlinear lattice chains for designing thermal devices. Through simulations, solid state thermal diode 18-23 and thermal

transistor ²⁴ prototypes have been developed by leveraging the nonlinear characteristics of onedimensional lattice models. These thermal devices manage heat current in a manner similar to how transistors and semiconductor diodes regulate electric current. The definitions and characteristics of lattices model, temperature, heat flux, and heat baths—all of which are employed in numerical simulations—will be covered in the section that follows. Later, origin of the research problem will be discussed followed by references.

1.2.2 Basic definitions

In this thesis, we are discussing one research problem related to heat conduction in one dimensional (1D) lattice, which will be in chapter 5. A schematic representation of a 1D lattice can be seen in Fig 1.2.1, where a chain of N particles are interacting with each other. Terminal particles come into contact with heat bath at left and right ends, having two different temperatures T_L and T_R respectively.

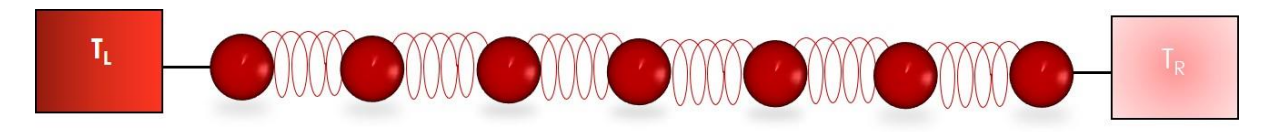


Fig. 1.2.1: Schematic representation of a one-dimensional (1D) chain attached to heat bath at left and right ends with two different temperatures.

The potential consists of a nearest-neighbour interaction potential, $V(x_i - x_{i-1})$, and an external on-site potential, $U(x_i)$, and, thus the corresponding Hamiltonian for a general one-dimensional lattice model is:

$$H = \sum_{i=1}^{N} \left[\frac{p_i^2}{2m_i} + U(x_i) \right] + \sum_{i=1}^{N} V(x_i - x_{i-1})$$
 (1.2.2)

Where x_i and p_i are the displacement from equilibrium position and momentum of the i^{th} particle, respectively. The m_i and N stands for the mass and the number of particles on the lattice chain respectively. The general lattice models can be categorised on to two different classes based on on-site potential, lattices with on-site potential, $U(x_i) \neq 0$, and without, $U(x_i) = 0$. In lattices, without on-site potential, total momentum is conserved, but not in those with on-site potential.

Fermi-Pasta-Ulam (FPU) lattice models are very famous examples for lattices without on-site potential²⁵. The one with quadratic plus cubic ($k_4 = 0$) and quadratic plus quartic ($k_3 = 0$)

are known as FPU- α and FPU- β models, respectively. The Hamiltonian is for FPU chain is represented as

$$H = \sum_{i=1}^{N} \frac{p_i^2}{2m_i} + \sum_{i=1}^{N-1} k_2 \frac{(x_i - x_{i-1})^2}{2} + k_3 \frac{(x_i - x_{i-1})^3}{3} + k_4 \frac{(x_i - x_{i-1})^4}{4}$$
(1.2.3)

Examples for the lattices with on-site potential includes Frenkel–Kontrova (FK) model as well as discrete ϕ^4 model. Hamiltonian corresponds to Frenkel–Kontrova model includes:

$$H = \sum_{i=1}^{N} \left[\frac{p_i^2}{2m_i} + \frac{k}{2} (x_i - x_{i-1})^2 + \frac{V}{4\pi^2} (1 - \cos 2\pi x_i) \right]$$
 (1.2.4)

This model ^{26,27} reflects a chain of particles harmonically connected with their nearest neighbours and subjected to a sinusoidal on-site (substrate) potential.

And Hamiltonian for the discrete ϕ^4 model²⁸ corresponds to:

$$H = \sum_{i=1}^{N} \left[\frac{p_i^2}{2m_i} + \frac{k}{2} (x_i - x_{i-1})^2 + \frac{\beta}{4} x_i^4 \right]$$
 (1.2.5)

This model mimics both the quadratic inter-particle interaction as well as quartic non-linear on-site potential.

1.2.3 Temperature

According to equilibrium statistical physics, the ensemble average of the particle's kinetic energy defines the system's temperature:

$$T = \langle \frac{\sum_{i=1}^{N} p_i^2}{Nm} \rangle = \langle \frac{p_i^2}{m} \rangle \tag{1.2.6}$$

Where $\langle . \rangle$ defines canonical ensemble average. The value of Boltzmann constant is chosen as one. The averages can be simply determined in simulations, by tracing single trajectories over time, which is the time average of the corresponding system.

$$T = \lim_{t \to \infty} \frac{\sum_{t=1}^{N_t m} p_i^2(t)}{N_t} = \frac{\overline{p_i^2}}{m}$$
 (1.2.7)

Here, the systems under examination must be ergodic in order for ensemble average to be equivalent to time average.

We require a different explanation for the local temperature equilibrium (LTE) in non-equilibrium situations, which are precisely the situations in which heat conduction occurs with a temperature gradient. In simulations, the time averages of the kinetic energy of the particles along the lattice chain changes gradually, with an exception of the two ends of the chain coming into contact with heat baths. This will make sure that system reaches non-equilibrium steady state. The interaction of the system with heat baths leads to contact resistances due to the effect of boundary conditions. This can be seen as the jumps in the temperature profile of the system.

1.2.3 Heat flux

We require a precise description of heat flux at the microscopic level in order to quantify the heat conductivity²⁹. The continuity equation of energy flow in the system can be used to describe the heat flux, j(x, t), at time, t, in the position, x, implicitly as:

$$\frac{dh(x,t)}{dt} + \frac{\partial j(x,t)}{\partial x} = 0 \tag{1.2.8}$$

Where h(x, t) is the energy density. The energy density for the general one-dimensional lattice chains can be defined as the total of the individual contributions situated in the instantaneous position of each particle.

$$h_i = \frac{p_i^2}{2m_i} + U(x_i) + \frac{1}{2} [V(x_{i+1} - x_i) + V(x_i - x_{i-1})]$$
(1.2.9)

Both kinetic and potential energy, $U(x_i)$, related to the (possible) interaction with an external field are represented by the first two terms on the right hand side of the equation Eq. (1.2.9). Half of the potential energy of pairwise interactions with adjacent particles is given by the final term in the Eq. (1.2.9).

In the case of modest oscillations around the equilibrium location, density fluctuations can be disregarded, in which case h_i equals the energy density multiplied by the lattice spacing, 'a'. Time derivative of the ith particle's energy contribution, h_i

$$\frac{dh_i}{dt} = m_i \dot{x}_i \ddot{x}_i + \dot{x}_i U'(x_i)
- \frac{1}{2} [(\dot{x}_{i+1} - \dot{x}_i) F(x_{i+1} - x_i) + (\dot{x}_i - \dot{x}_{i-1}) F(x_i - x_{i-1})]$$
(1.2.10)

function, F, can be defined as F(x) = -V'(x). Equations of motion can be written as

$$m_i \ddot{x}_i = -U'(x_i) - F(x_{i+1} - x_i) + F(x_i - x_{i-1})$$
(1.2.11)

$$\frac{dh_i}{dt} = -\frac{1}{2} [(\dot{x}_{i+1} + \dot{x}_i) F(x_{i+1} - x_i) - (\dot{x}_i - \dot{x}_{i-1})]$$
(1.2.12)

This equation can be rewritten as,

$$\frac{dh_i}{dt} + \frac{j_i - j_{i-1}}{a} = 0 ag{1.2.13}$$

with the physical significance that heat flux into and out of the particle at the i^{th} particle equals the rate of change in energy at this particle. By comparing eq. (1.2.12) and Eq. (1.2.13), we obtained the following formula for the local heat flux, j_i , in one dimensional lattice chains as

$$j_i = \frac{1}{2}a(\dot{x}_{i+1} + \dot{x}_n)F(x_{i+1} - x_i)$$
(1.2.14)

1.2.3 Heat bath

The thermal reservoirs connecting to the system's two ends are called heat baths (Thermostats) Fig. 1.2.1. They depict how noise and environmental dissipation affect systems from both ends. The literatures have discussed a variety of bath models to simulate the mechanism of thermal reservoir and in this section, we will discuss one such stochastic heat bath.

Langevin heat bath

By including the force terms in the equation of motion of the particles in contact with the baths, we may simulate the heat bath. Additional forces include both dissipative as well as a stochastic term. Stochastic part will be modeled using Gaussian white noise. So, the corresponding equations of motions for the particles i = 1 and i = N in the lattice chain connected to Langevin reservoirs as:

$$\dot{p}_{1} = f_{1} - \frac{\gamma_{L}}{m_{1}} p_{1} + \eta_{L}(t)$$

$$\dot{p}_{i} = f_{i} \text{ for } i = 2, 3, \dots, N - 1,$$

$$\dot{p}_{N} = f_{N} - \frac{\gamma_{R}}{m_{N}} p_{N} + \eta_{R}(t)$$
(1.2.15)

Where

$$f = -\frac{\partial H}{\partial x_i} \tag{1.2.16}$$

is the Newtonian force on the i^{th} particle. The noise $\eta_{L,R}$ is given by Gaussian with zero mean and fluctuation-dissipation relation connect them to the dissipation coefficients $\gamma_{L\gamma,R}$.

$$\langle \eta_L(t)\eta_L(t')\rangle = 2k_BT_L\gamma_L\delta(t-t')$$

$$\langle \eta_R(t)\eta_R(t')\rangle = 2k_B T_R \gamma_R \delta(t - t')$$

$$\langle \eta_L(t)\eta_R(t')\rangle = 0$$
(1.2.17)

Where T_L , T_R represents the temperature at the left and right heat bath respectively.

1.2.4 Origin of the research problem

The primary focus of all the research studies related to heat conduction in low dimensional systems has been on the prerequisites and conditions for the validity of Fourier law of heat conduction in one-dimensional (1D) systems. Consider a one-dimensional shaped material with length, N, which is maintained at two different temperatures, T_L , and T_R at both ends. Now, the Fourier law for one-dimensional chain length, N, as:

$$J = \kappa (T_L - T_R) / (N - 1)a \tag{1.2.18}$$

Where a is the chain period and $T_{L,R}$ is the temperature of the left or right chain end respectively. Using Eq. (1.2.18), we can determine how the length, N = (N-1)a, affects the thermal conductivity and temperature, T, of the one-dimensional chain, for a small temperature difference, $\Delta T = (T_L - T_R) \ll T = (T_L + T_R)/2$, as:

$$\kappa(N,T) = J(N-1)\alpha/T\delta T, \quad \delta = (T_L - T_R)/T \ll 1 \tag{1.2.19}$$

The Fourier law Eq. (1.2.18) is satisfied if the given finite limit exists.

$$\bar{\kappa}(T) = \lim_{N \to \infty} \kappa(N, T) \tag{1.2.20}$$

Thermal conductivity for the chain in this case has a finite value. On the other hand, chain has an anomalous thermal conductivity, where it will diverge with the chain length N, for $\kappa \to \infty$ for $N \to \infty$.

To date, a vast number of studies have been carried out on the numerical modelling of heat transfer in one-dimensional (1D) lattices. Heat transport anomalies in 1D nonlinear systems have been well understood, since the time of the illustrious work of Fermi, Pasta, and Ulam²⁵. In integrable systems (such as harmonic chain, Toda chain, and chain of rigid disks) Lebowitz *et al.* ³⁰ shown that no temperature gradient can be formed which leads to divergent thermal conductivity and thus Fourier law is not valid. Here, the value of heat flux, J, is independent on the chain length of the lattice, N, $\kappa(N) \sim N$ for $N \to \infty$. Since noninteracting quasiparticles do the heat transport in this case, energy transports freely along the chain without any loss (energy is not dissipated) and so temperature gradient is not established throughout the heat transfer. Presence of temperature gradient in non-integrable systems suggests the existence of scattering. The problem is far more challenging with nonintegrable systems, though. Some nonintegrable

systems obey the Fourier law, while the others do not. In some non-integrable systems like Lorentz gas model^{4,7}, Frenkel-Kontorova (FK) model ^{11,26,27}, the ding -a- ling and alike models^{8,9,31,32}, the heat flux, J, is proportional to N^{-1} and thus thermal conductivity, κ , is independent of system size, N, and thereby Fourier's law is obeyed. While in other non-integrable systems like Fermi – Pasta – Ulam chain^{33,34}, diatomic Toda chain³⁵, Heisenberg spin chain⁵, the disordered harmonic chain^{35–37}, diatomic 1D gas of colliding particles^{38–40} and so on, it is the other way around. Their heat flux, J, is proportional to $N^{\alpha-1}$, with α as the divergent exponent and corresponding thermal conductivity is divergent, $\kappa \sim N^{\alpha}$, as one approaches thermodynamic limit $N \to \infty$ with $0 < \alpha < 1$. So, the distinct heat conduction behaviours in the two groups of nonintegrable systems suggest that the basic mechanism of heat transfer must be different. Also, these observation direct the fact that, although nonintegrability is required for a temperature gradient, it is insufficient to ensure that a one-dimensional lattice will have normal thermal conductivity.

On the other hand, convergence in thermal conductivity with the system size was observed for chain with on-site potential. Examples include Frenkel-Kontorova chain 11,41 , chain with ϕ^4 on-site potential 42,43 , chain having sine-Gordon on-site potential 44 , and the chain of hard disks with the substrate potential 45 and so on, which have normal thermal conductivity. The external potential, which simulates how the chain interacts with the substrate, is the key element of all these models. The total momentum is not conserved in these systems, because they lack translational invariance. According to Ref. [13], having an external potential may be a crucial for the system's thermal conductivity to converge. It was proposed that, all isolated one-dimensional lattices have an anomalous thermal conductivity in which the absence of an external potential results in the total momentum conservation of system. This conjecture was invalidated in Refs. [46,47], which established that the isolated chain of connected rotators (a chain with a periodic interparticle potential) has a normal (finite) thermal conductivity.

In this thesis, we are focussing on the one-dimensional momentum conserving systems, especially lattice model with Fermi-Pasta-Ulam (FPU) interaction potential. Both theoretical calculations $^{1,48-55}$ and numerical simulations $^{2,34,42,50,56-59}$ predicted the anomalous behaviour of thermal conductivity, κ , in these models. Even though, the divergence value of the scaling exponent, α , lies in the range of $0 \le \alpha \le 1$, specific values of α varies in all the calculations 2 . Generally, three different values, $\alpha = 1/2$ 51,52,54,55 , $\alpha = 1/3$ 32,49,50,53,56,58 , and $\alpha = 2/5$ 31,53 have been obtained in different calculations. In the case of FPU- lattices with symmetric double – well (DW) neighbouring interaction potential, two different temperature regimes of thermal

transport has been observed with, $\alpha = 0.33$, at high temperature and weak divergence was observed at low temperature ⁵⁶. Similar observation was also made for FPU $-\alpha\beta$ lattice with divergence exponent, $\alpha = 0.4$, at high temperature and weak divergence at low temperature ⁶⁰. So, with this research scenario, we investigated the temperature dependent divergence in an asymmetric double -well potential for nearest neighbour interaction potential using non-equilibrium simulation method.

1.2.5 Reference

- 1. Lepri, S., Livi, R. & Politi, A. Thermal conduction in classical low-dimensional lattices. *Phys. Rep.* **377**, 1–80 (2003).
- 2. Dhar, A. Heat transport in low-dimensional systems. *Adv. Phys.* **57**, 457–537 (2008).
- 3. Sepehri, S., Mosavi, M., Seyyed, M. M., Bloch, I. & Zoller, P. Thermal conductivity of one- and two-dimensional lattices lattices. (1989).
- 4. Alonso, D., Artuso, R., Casati, G. & Guarneri, I. Heat conductivity and dynamical instability. *Phys. Rev. Lett.* **82**, 1859–1862 (1999).
- 5. Dhar, A. & Dhar, D. Absence of local thermal equilibrium in two models of heat conduction. *Phys. Rev. Lett.* **82**, 480–483 (1999).
- 6. Lepri, S., Livi, R. & Politi, A. Heat transport in low dimensions: Introduction and phenomenology. *Lect. Notes Phys.* **921**, 1–37 (2016).
- 7. Lebowitz, J. L. & Spohn, H. Transport properties of the Lorentz gas: Fourier's law. *J. Stat. Phys.* **19**, 633–654 (1978).
- 8. Casati, G., Ford, J., Vivaldi, F. & Visscher, W. M. One-dimensional classical many-body system having a normal thermal conductivity. *Phys. Rev. Lett.* **52**, 1861–1864 (1984).
- 9. Prosen, T. & Robnik, M. Energy transport and detailed verification of Fourier heat law in a chain of colliding harmonic oscillators. *J. Phys. A Gen. Phys.* **25**, 3449–3472 (1992).
- 10. Mimnagh, D. J. R. & Ballentine, L. E. Thermal conductivity in a chain of alternately free and bound particles. *Phys. Rev. E Stat. Physics, Plasmas, Fluids, Relat. Interdiscip. Top.* **56**, 5332–5342 (1997).
- 11. Hu, B., Li, B. & Zhao, H. Heat conduction in one-dimensional chains. *Phys. Rev. E Stat. Physics, Plasmas, Fluids, Relat. Interdiscip. Top.* **57**, 2992–2995 (1998).
- 12. Fillipov, A., Hu, B., Li, B. & Zeltser, A. Energy transport between two attractors connected by a Fermi-Pasta-Ulam chain. *J. Phys. A. Math. Gen.* **31**, 7719–7728 (1998).

- 13. Hatano, T. Heat conduction in the diatomic Toda lattice revisited. *Phys. Rev. E Stat. Physics, Plasmas, Fluids, Relat. Interdiscip. Top.* **59**, 1–4 (1999).
- 14. Chang, C. W., Okawa, D., Garcia, H., Majumdar, A. & Zettl, A. Breakdown of fourier's law in nanotube thermal conductors. *Phys. Rev. Lett.* **101**, 1–4 (2008).
- 15. Ghosh, S. *et al.* Dimensional crossover of thermal transport in few-layer graphene. *Nat. Mater.* **9**, 555–558 (2010).
- 16. Wang, Z. *et al.* Supported Few-Layer Graphene. 113–118 (2011) doi:10.1021/nl102923q.
- 17. Nika, D. L., Askerov, A. S. & Balandin, A. A. Anomalous Size Dependence of the Thermal Conductivity of Graphene Ribbons. (2012).
- 18. Terraneo, M., Peyrard, M. & Casati, G. Controlling the Energy Flow in Nonlinear Lattices: A Model for a Thermal Rectifier. 2–5 (2002) doi:10.1103/PhysRevLett.88.094302.
- 19. Li, B., Wang, L. & Casati, G. Thermal Diode: Rectification of Heat Flux. 1–4 (2004) doi:10.1103/PhysRevLett.93.184301.
- 20. Li, B., Lan, J. & Wang, L. Interface Thermal Resistance between Dissimilar Anharmonic Lattices. **104302**, 1–4 (2005).
- 21. Segal, D. & Nitzan, A. Spin-Boson Thermal Rectifier. **034301**, 10–13 (2005).
- 22. Lan, J. & Li, B. Thermal rectifying effect in two-dimensional anharmonic lattices. 1–9 (2006) doi:10.1103/PhysRevB.74.214305.
- 23. Hu, B., Yang, L. & Zhang, Y. Asymmetric heat conduction in nonlinear lattices. *Phys. Rev. Lett.* **97**, 2–5 (2006).
- 24. Wang, L. & Casati, G. Negative differential thermal resistance and thermal transistor. **143501**, 1–4 (2017).
- 25. Fermi, E., Pasta, J. R. & Ulam, S. M. Studies of Non-Linear Prolems (Technical Report). *Collect. Work. E. Fermi* **2**, 978–988 (1955).
- 26. Hu, B. & Yang, L. Heat conduction in the Frenkel-Kontorova model. *Chaos* **15**, (2005).

- 27. Braun, O. M. & Kivshar, Y. S. Nonlinear dynamics of the Frenkel-Kontorova model. *Phys. Rep.* **306**, (1998).
- 28. Ding, C., Aubry, S. & Tsironis, G. P. Breather mobility in discrete φ4 nonlinear lattices. *Phys. Rev. Lett.* **77**, 4776–4779 (1996).
- 29. Hardy, R. J. Energy-flux operator for a lattice. *Phys. Rev.* **132**, (1963).
- 30. Rieder, Z., Lebowitz, J. L. & Lieb, E. Properties of a harmonic crystal in a stationary nonequilibrium state. *J. Math. Phys.* **8**, 1073–1078 (1967).
- 31. Lepri, S., Livi, R. & Politi, A. On the anomalous thermal conductivity of one-dimensional lattices. *Europhys. Lett.* **43**, 271–276 (1998).
- 32. Posch, H. A. & Hoover, W. G. Heat conduction in one-dimensional chains and nonequilibrium Lyapunov spectrum. *Phys. Rev. E Stat. Physics, Plasmas, Fluids, Relat. Interdiscip. Top.* **58**, 4344–4350 (1998).
- 33. Kaburaki, H. & Machida, M. Thermal conductivity in one-dimensional lattices of Fermi-Pasta-Ulam type. *Phys. Lett. A* **181**, 85–90 (1993).
- 34. Lepri, S., Livi, R. & Politi, A. Heat Conduction in Chains of Nonlinear Oscillators. *Phys. Rev. Lett.* **78**, 1896–1899 (1997).
- 35. Dhar, A. Heat conduction in the disordered harmonic chain revisited. *Phys. Rev. Lett.* **86**, 5882–5885 (2001).
- 36. Rubin, R. J. & Greer, W. L. Abnormal lattice thermal conductivity of a one-dimensional, harmonic, isotopically disordered crystal. *J. Math. Phys.* **12**, 1686–1701 (1971).
- 37. Casher, A. & Lebowitz, J. L. Heat flow in regular and disordered harmonic chains. *J. Math. Phys.* **12**, 1701–1711 (1971).
- 38. Dhar, A. Heat conduction in a one-dimensional gas of elastically colliding particles of unequal masses. *Phys. Rev. Lett.* **86**, 3554–3557 (2001).
- 39. Savin, A. V., Tsironis, G. P. & Zolotaryuk, A. V. Heat Conduction in One-Dimensional Systems with Hard-Point Interparticle Interactions. *Phys. Rev. Lett.* **88**, 4 (2002).
- 40. Grassberger, P., Nadler, W. & Yang, L. Heat Conduction and Entropy Production in a

- One-Dimensional Hard-Particle Gas. Phys. Rev. Lett. 89, 1–4 (2002).
- 41. Savin, A. V & Gendelman, O. V. Heat conduction in one-dimensional lattices with on-site potential. *Phys. Rev. E. Stat. Nonlin. Soft Matter Phys.* **67**, 041205 (2003).
- 42. Hu, B., Li, B. & Zhao, H. Heat conduction in one-dimensional nonintegrable systems. *Phys. Rev. E Stat. Physics, Plasmas, Fluids, Relat. Interdiscip. Top.* **61**, 3828–3831 (2000).
- 43. Aoki, K. & Kusnezov, D. Bulk properties of anharmonic chains in strong thermal gradients: Non-equilibrium φ4 theory. *Phys. Lett. Sect. A Gen. At. Solid State Phys.*265, 250–256 (2000).
- 44. Tsironis, G. P., Bishop, A. R., Savin, A. V. & Zolotaryuk, A. V. Dependence of thermal conductivity on discrete breathers in lattices. *Phys. Rev. E Stat. Physics*, *Plasmas, Fluids, Relat. Interdiscip. Top.* **60**, 6610–6613 (1999).
- 45. Gendelman, O. V & Savin, A. V. Heat Conduction in a One-Dimensional Chain of Hard Disks with Substrate Potential. 1–4 (2004) doi:10.1103/PhysRevLett.92.074301.
- 46. Gendelman, O. V & Savin, A. V. Normal Heat Conductivity of the One-Dimensional Lattice with Periodic Potential of Nearest-Neighbor Interaction. 2381–2384 (2000).
- 47. Giardinà, C., Livi, R., Politi, A. & Vassalli, M. Finite thermal conductivity in 1d lattices. *Phys. Rev. Lett.* **84**, 2144–2147 (2000).
- 48. Prosen, T. & Campbell, D. K. Momentum Conservation Implies Anomalous Energy Transport in 1D Classical Lattices. 2857–2860 (2000).
- 49. Narayan, O. & Ramaswamy, S. Anomalous Heat Conduction in One-Dimensional Momentum-Conserving Systems. *Phys. Rev. Lett.* **89**, 2–5 (2002).
- 50. Wang, J. S. & Li, B. Intriguing Heat Conduction of a Chain with Transverse Motions. *Phys. Rev. Lett.* **92**, 5–8 (2004).
- 51. Lee-Dadswell, G. R., Nickel, B. G. & Gray, C. G. Thermal conductivity and bulk viscosity in quartic oscillator chains. *Phys. Rev. E Stat. Nonlinear, Soft Matter Phys.* **72**, 1–8 (2005).
- 52. Delfini, L., Lepri, S., Livi, R. & Politi, A. Self-consistent mode-coupling approach to one-dimensional heat transport. *Phys. Rev. E Stat. Nonlinear, Soft Matter Phys.* **73**,

- 17–20 (2006).
- 53. Mai, T. & Narayan, O. Universality of one-dimensional heat conductivity. *Phys. Rev. E Stat. Nonlinear, Soft Matter Phys.* **73**, 1–7 (2006).
- 54. Van Beijeren, H. Exact results for anomalous transport in one-dimensional hamiltonian systems. *Phys. Rev. Lett.* **108**, 1–5 (2012).
- 55. Mendl, C. B. & Spohn, H. Dynamic correlators of fermi-pasta-ulam chains and nonlinear fluctuating hydrodynamics. *Phys. Rev. Lett.* **111**, 1–5 (2013).
- 56. Roy, D. Crossover from Fermi-Pasta-Ulam to normal diffusive behavior in heat conduction through open anharmonic lattices. *Phys. Rev. E Stat. Nonlinear, Soft Matter Phys.* **86**, 1–5 (2012).
- 57. You, A., Be, M. A. Y. & In, I. Anomalous heat conduction and anomalous diffusion in nonlinear lattices, single walled nanotubes, and billiard gas channels. **015121**, (2005).
- 58. Delfini, L., Lepri, S., Livi, R. & Politi, A. Comment on: Equilibration and universal heat conduction in fermi-pasta-ulam chains. *Phys. Rev. Lett.* **100**, 2–5 (2008).
- 59. Li, Y., Liu, S., Li, N., Hänggi, P. & Li, B. 1D momentum-conserving systems: the conundrum of anomalous versus normal heat transport 1D momentum-conserving systems: the conundrum of anomalous versus normal heat transport. (2015) doi:10.1088/1367-2630/17/4/043064.
- 60. Savin, A. V. & Kosevich, Y. A. Thermal conductivity of molecular chains with asymmetric potentials of pair interactions. *Phys. Rev. E Stat. Nonlinear, Soft Matter Phys.* **89**, 1–12 (2014).

CHAPTER 2

Effect of roughness in the periodic potential in the transport of a driven inertial ratchet aided by Gaussian noise.

2.1 Introduction

Fluctuations and random perturbations have a dominant role on the transport in the microscale realm. It is not always true that randomness restrains the transport properties of the particle. However, positive role of both equilibrium and non-equilibrium fluctuations can be seen in many instances such as in the area of fluctuation-induced transport which includes Brownian ratchets ¹ stochastic resonance ², intracellular transport ³, molecular motors ⁴⁻⁶ biochemical and genetic regulatory systems ⁷ and so forth. In which, Brownian ratchets can rectify the unbiased random thermal fluctuations and generate directed motion of particle through the mechanism of breaking the spatial symmetry of periodic potential as well as the principle of detailed balance. In recent years, anomalous transport properties of ratchet systems have been one of the research topics in the various disciplines ^{8–14}. In particular, directed transport and diffusion anomalies of Brownian particles in a driven ratchet moving in a smooth periodic potential have been investigated widely ^{11,15–20}. Most of the Brownian ratchet models, researchers have considered the smooth periodic potential. However, it is quite well established that potential can have fine structures and these microscopic spatial heterogeneity in the potential energy landscape is known as the roughness in the potential. This can be visualized as hills and valleys of various heights and widths. Examples includes in the protein folding pathway ^{21–23}, where the potential surface of protein have hierarchical structures holding a number of minima and maxima revealing spatial heterogeneity of the potential landscape. Rough periodic potential is known to exist in many other systems such as diffusion in structural glasses²⁴, activation gating of ion channels^{25,26} and supercooled liquids^{27,28}.

Zwanzig modeled the rough potential by super imposing an oscillating trigonometric function in a background of smooth potential function. He studied mean first passage time and found that roughness reduces the effective diffusion coefficient at low temperatures and thereby the thermally activated barrier crossing rate of the particle²⁹. Ansari developed a robust numerical approach to solve the Smoluchowski equation describing diffusion along a spatially rough potential³⁰. Pollak *et. al.* used master equation for studying the rate theory for rugged energy landscape³¹. Mondal *et. al.* calculated directed current and efficiency of a thermal ratchet

moving in a rough periodic potential and found that roughness holds back the current in a ratchet potential in the presence of Gaussian noise³². However, under Lévy noise particle exhibits quite different transport characteristics in rough periodic potential. There, roughness help to accelerate barrier crossing leading to enhanced current ^{33–35}. Most of the works on rough periodic potential considered only overdamped systems leaving the inertial term due to the mass of the particle. How spatial heterogeneity in the periodic potential affects the transport in a driven inertial ratchet under the Gaussian environment has not been considered yet. This class of model dealing with a periodic system has been discussed in several problems including Josephson junctions³⁶ dynamics of adatoms under the influence of a time-periodic force³⁷, transport of cold and ultracold atoms in optical potentials³⁸, to name but a few. In this chapter we discuss the effects of roughness in an asymmetric periodic potential on the diffusion as well as the transport of a Brownian particle in a time-based-periodic force driven inertial ratchet aided by Gaussian noise.

2.2 Model

We considered motion of an inertial Brownian particle of mass M moving in a spatially asymmetric periodic potential, U(x). The particle is driven by an unbiased time-periodic force $A\cos(\Omega t)$ with an amplitude A and an angular frequency Ω . This force drives the particle away from thermal equilibrium and thereby the break the principle of detailed balance. The presence of unbiased random thermal fluctuations is modeled by δ -correlated Gaussian white noise $\eta(t)$ of zero mean $\langle \eta(t) \rangle = 0$, which satisfy Einstein's fluctuation-dissipation relation $\langle \eta(t) \eta(t') \rangle = 2\Gamma k_B T \delta(t-t')$, where k_B , Γ and T are the Boltzmann's constant, frictional coefficient and temperature, respectively.

Dynamics of the driven inertial Brownian particle is described using the Langevin equation,

$$M\ddot{x} = -U'(x) - \Gamma \dot{x} + A\cos(\Omega t) + \eta(t). \tag{2.1}$$

The dot and prime represents the derivative with respect to time (t) and position (x), respectively. The ratchet potential, U(x), is a combination of asymmetric smooth $U_0(x)$ and rough periodic potential $U_1(x)$.

$$U(x) = U_0(x) + U_1(x) (2.2)$$

The smooth potential with periodicity $2\pi L$ and barrier height ΔU has the form,

$$U_0(x) = -\Delta U \left[\sin\left(\frac{x}{L}\right) + \frac{1}{4}\sin\left(\frac{2x}{L} + \psi - \frac{\pi}{2}\right) \right]. \tag{2.3}$$

Reflection symmetry of the periodic potential $U_0(x_0 + x) = U_0(x_0 - x)$ is broken by the asymmetry parameter ψ of the potential. The rectification of the unbiased nonequilibrium fluctuations into a noise-induced directed current requires breaking the spatial symmetry of the periodic potential. $U_1(x)$ has the form,

$$U_1(x) = \varepsilon_0(c_1 \sin \Lambda_1 x + c_2 \sin \Lambda_2 x). \tag{2.4}$$

 ε_0 measures the amplitude of the roughness in the periodic potential. Λ and c terms represent the periodicities and relative amplitudes of the two sine components in the rough part of the potential, respectively. The periodicity of the rough potential should typically be higher than the periodicity of the smooth potential, and the amplitude of the roughness should typically be low.

In order to decrease the number of parameters in the model equation, we nondimensionalized the Langevin equation (2.1) using the previous method²⁰ and the nondimensional version of the Langevin equation in given as

$$m\ddot{\hat{x}} = -\hat{U}'(\hat{x}) - \dot{\hat{x}} - a\cos(\omega\hat{t}) + \hat{\eta}(\hat{t}) \tag{2.5}$$

The hat (Λ) symbolises the rescaled variables, where $\hat{x}=x/L$, and $\hat{t}=t/\tau_0$ with $\tau_0=\Gamma L^2/\Delta U$ were used to scale the position and the time, respectively. Rescaled values for the particle's mass, the periodic driving's amplitude, and the frequency of the driving are $m=M/\Gamma\tau_0$, $\alpha=AL/\Delta U$, and $\omega=\Omega\tau_0$, respectively. The roughness amplitude and rough potential periodicity were rescaled as $\varepsilon=\varepsilon_0/\Delta U$, $\lambda_1=\Lambda_1/L$, and $\lambda_2=\Lambda_2/L$, respectively. The potential was rescaled to have a periodicity of 2π and in the form of $\widehat{U}(\widehat{x})=U(x)/\Delta U=U(L\widehat{x})/\Delta U$. The rough portion of the potential has also changed due to the rescaling of the variables as

$$\widehat{U}_1(\widehat{x}) = \varepsilon(c_1 \sin \lambda_1 \widehat{x} + c_2 \sin \lambda_2 \widehat{x})$$
 (2.6)

Throughout the study, 1, 50, 100, 1, and 0.5 were chosen as the values for ΔU , λ_1 , λ_2 , c_1 and c_2 respectively. Fig. 2.1 depicts the asymmetric periodic potential with ($\varepsilon = 0.1$) and without ($\varepsilon = 0.1$) roughness for the asymmetric parameter $\psi = 0.5\pi$.

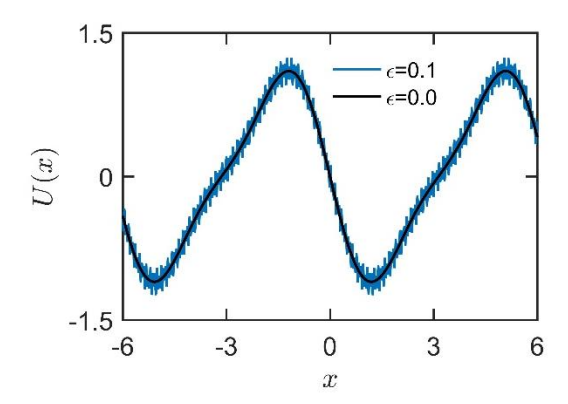


Fig. 2.1: Schematic representation of the asymmetric periodic potential U(x) without ($\epsilon = 0$) and with roughness ($\epsilon = 0.1$).

The fluctuation-dissipation relation has now changed to $\langle \hat{\eta}(\hat{t}) \rangle = 0$ and $\langle \hat{\eta}(\hat{t}) \hat{\eta}(\hat{t}') \rangle = 2Q\delta(\hat{t} - \hat{t}')$, where the thermal noise has been rescaled as $\hat{\eta}(\hat{t}) = (L/\Delta U)\eta(\tau_0\hat{t})$. The dimensionless strength of thermal noise is defined as $Q = k_B T/\Delta U$. We used the dimensionless Langevin equation (Eq. (2.5)) for all calculations, and for convenience's sake, we do not explicitly display the (Λ) in the remaining sections of the study.

The quantifier we used to study the diffusion process of the Brownian particle position x(t) and its spread of trajectories is Mean square displacement (MSD) was used to study the diffusion process of the Brownian particle. MSD was calculated by averaging over a set of trajectories with random initial positions and velocities and defined as

$$\langle \Delta x^2(t) \rangle = \langle [x(t) - \langle x(t) \rangle]^2 \rangle. \tag{2.7}$$

The power-law scaling of the MSD generally be used to depict the nature of the diffusive process as

$$\langle \Delta x^2(t) \rangle \propto t^{\alpha}$$
 (2.8)

The scaling exponent $\alpha = 1, 0 < \alpha < 1$ and $\alpha > 1$ signify normal diffusion, sub-diffusion, and super-diffusion of the particle, respectively. As a result, the rate of rise of the MSD is greater in the super-diffusive domain of anomalous diffusion than it is in the sub-diffusion regime. The ballistic motion of the particle is represented by $\alpha = 2$. Consequently, the time dependent diffusion coefficient D(t) can be expressed as

$$D(t) = \frac{\langle \Delta x^2(t) \rangle}{2t} \tag{2.9}$$

According to Eq. (2.8) and (2.9), D(t) for normal diffusion must be time independent, whereas D(t) for super- and sub-diffusion must change over time.

Next, we estimated the time-dependent ensemble- and period- average velocity v(t) to quantify the directed transport of the particle under asymmetric rough potential and it is defined as

$$v(t) = \frac{1}{T_p} \int_t^{t+T_p} ds \langle \dot{x}(s) \rangle$$
 (2.10)

Where $T=2\pi/\omega$ is the period of the time-periodic force. Using the second-order predictor-corrector method, we numerically solved the Langevin equation (Eq. (2.5)) in order to quantify D(t) and v(t). The ensemble averaging was carried out over 20,000 trajectories with initial conditions of x and \dot{x} , which were uniformly distributed in the ranges $[0,2\pi]$ and [-2,2], respectively. In order to capture the impact of fine structures of roughness in the potential, a very small (10^{-4}) integration time step was used. The parameters of m, a, ω , and were selected as 6.0, 1.899, 0.403, and 0.5π , respectively, in accordance with earlier research on the transient anomalous diffusion²⁰.

2.3 Results and Discussions

This study mainly presents the effect of roughness in the asymmetric periodic potential on the transport properties of a Brownian particle driven by a time-based periodic force. Systematic study of time-dependent diffusion coefficient of the same in a smooth periodic potential was undertaken in previous studies²⁰. It was shown that diffusion anomalies can be observed in finite times. In related work, it was shown that transient anomalous diffusion can occur from low to moderate noise intensity¹⁹.

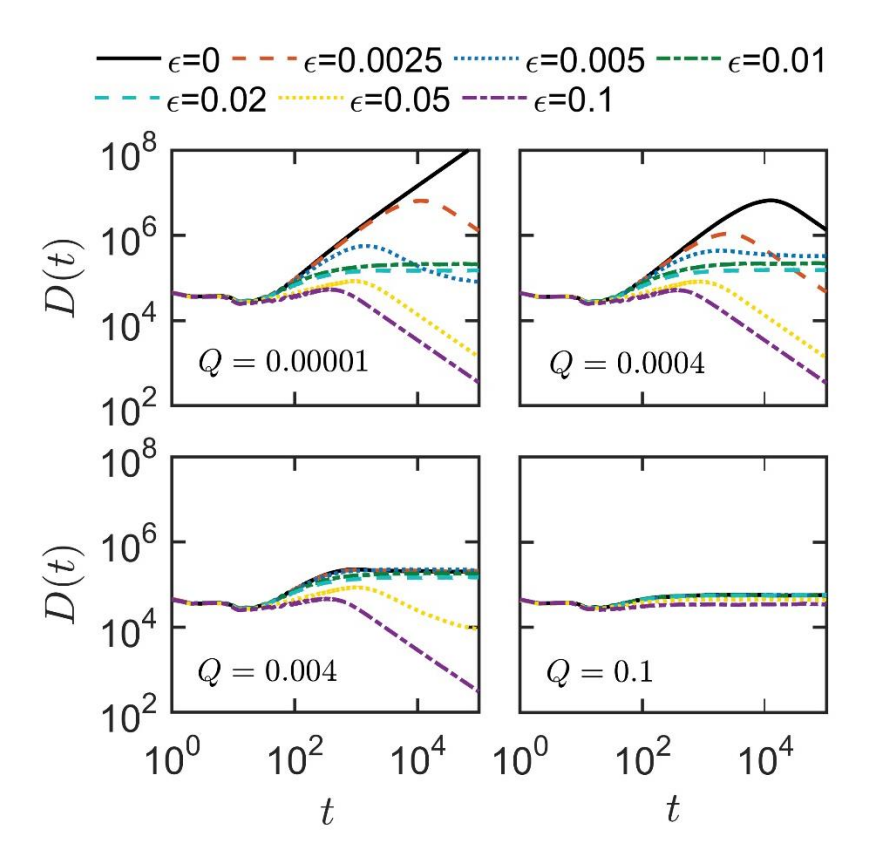


Fig. 2.2: Impact of roughness on the diffusion process. Time dependent diffusion coefficient D(t) for different values of roughness ε and noise strength Q.

In order to have an understanding on how roughness affects the diffusive nature of the particle, we studied the time-dependent diffusion coefficient, D(t), (Eq. (2.9)). In Fig. 2.2, we present the diffusive behavior of the particle for different amplitudes of roughness ranging from $\varepsilon=0$ to $\varepsilon=0.1$ for different values of noise intensity, Q. A considerable change on the diffusive behaviour of the particle with roughness is observed, especially at lower noise intensity regime. At Q=0.00001, D(t) shows an increasing nature with respect to time t for smooth ($\varepsilon=0$) periodic potential. This shows that, the particle is at super-diffusive stage of motion which gets gradually change with the introduction of roughness. We noted a crossover from super diffusive to sub diffusive motion for $\varepsilon>0.005$. Then, for small amplitude of roughness, we observed a crossover of three stages of diffusion as reflected like super-diffusion to sub-diffusion to normal diffusion of driven Brownian particle. So hereby, we infer that intermediate range of roughness $(0.01 \le \varepsilon \le 0.02)$ enforces the particle to have normal diffusion at asymptotic time limit, where D(t) is time independent. With higher roughness the particle undergoes sub-diffusion. This kind of diffusive behaviour of particle stays till at noise intensity, Q=0.0004. For the intermediate to higher noise intensity, Q>0.004, the impact of

roughness is negligible in compared to the diffusive nature of the particle in a smooth periodic potential. This can be due to the consequence of particle's own diffusive motion at higher noise intensity which over power in compare to the effect of roughness. Normal diffusion is established at higher noise intensity irrespective of the amplitude of roughness.

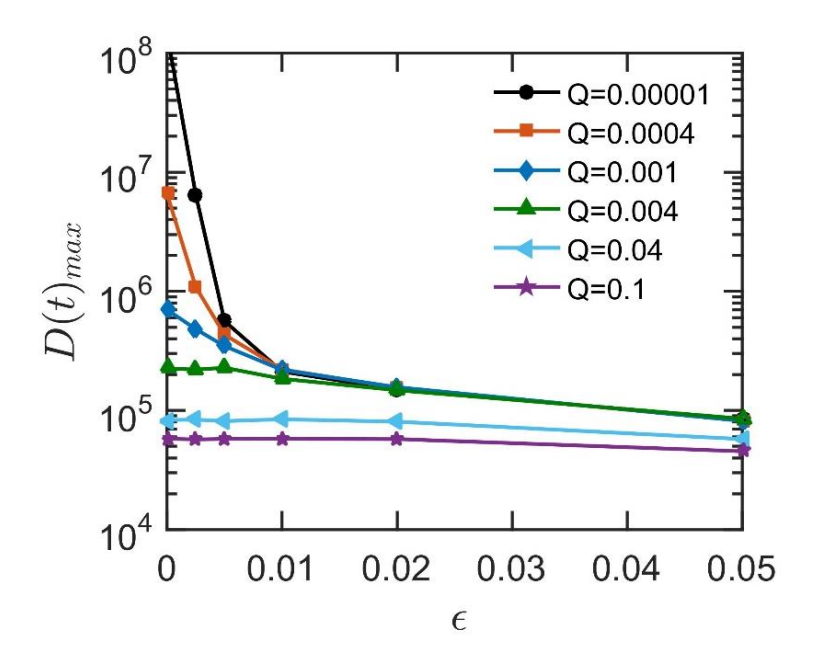


Fig. 2.3: Maximum value of time dependent diffusion coefficient D(t) as function of amplitude of roughness ε for different values of noise intensity Q.

In order to find the extent of diffusion, we present, the dependence of the maximum value of time dependent diffusion coefficient D(t) on the amplitude of roughness ε for different noise intensity Q (Fig.2.3). There, we observed the reduction of D(t) at weak noise intensity and at higher noise intensity, the effect of rough periodic potential on the diffusion process is trivial.

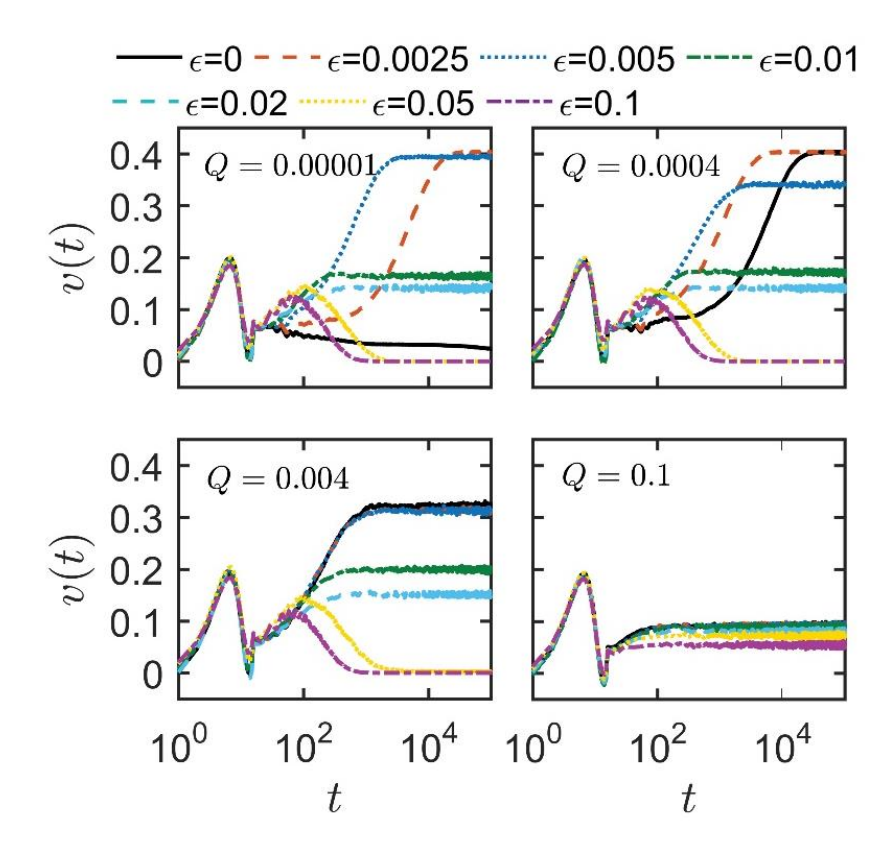


Fig. 2.4: Ensemble- and period-averaged velocity, v(t), as a function of time t for different values of Q and ε .

In Fig. 2.4, we numerically investigate the ensemble- and period-averaged velocity v(t) defined by the Eq. (2.10) in order to have a detailed study on the changes that occur over a longer period of time. In smooth periodic potential $\varepsilon=0$, the system relaxes to $v(t)\approx 0$ at lower noise intensity Q=0.00001. On the introduction of roughness ($\varepsilon\neq 0$), the long-time v(t) increases considerably and it shows decreasing trend with the amplitude of roughness. This nature of the transport, however, depends on the strength of the noise intensity. At Q=0.0004, the particle shows a non-zero steady state velocity of particle even in smooth potential ($\varepsilon=0$) which shows that the particle is having directed transport and the transport gradually decreases with the amplitude of roughness. Similar behaviour is followed at higher noise strength also. Introduction of roughness makes a considerable changes in the mode of transport as well as in the velocity relaxation process.

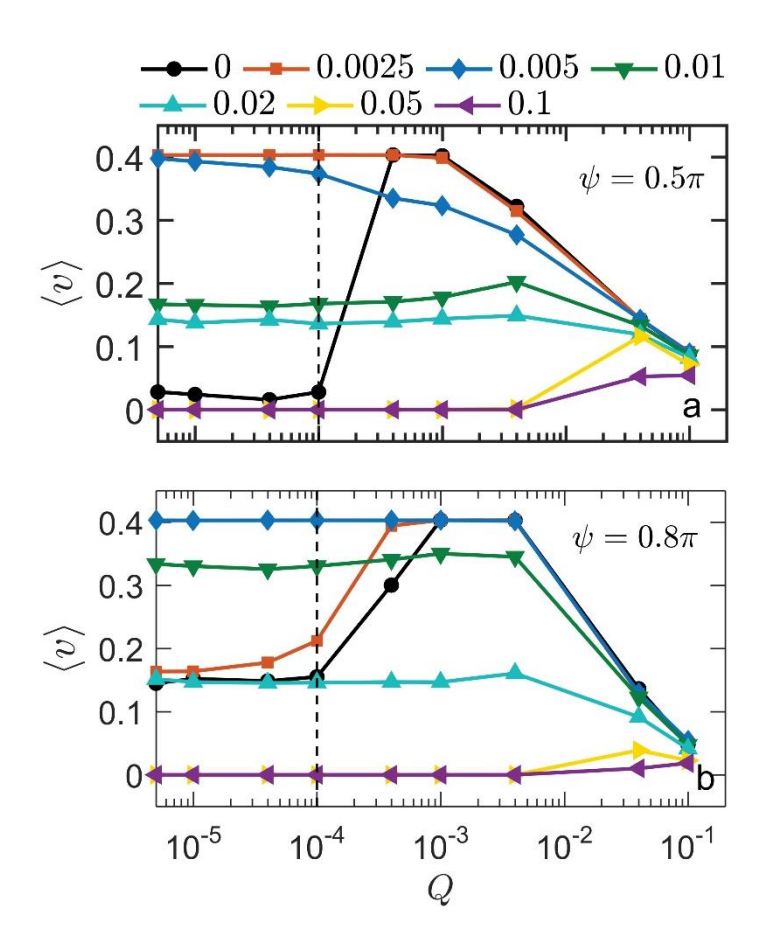


Fig. 2.5: Asymptotic ensemble- and period-averaged asymptotic velocity, $\langle v \rangle$, as a function of Q for the indicated values of ε and two different values of asymmetric parameter, ψ . The vertical line dashed lines separate the lower and higher noise regimes.

Now, in order to study the consequences of roughness along with the role of noise intensity on the directed transport of the driven Brownian particle, we next studied the asymptotic long-time velocity, $\langle v \rangle$, $[=\lim_{t \to \infty} v(t)]$ and the impacts of these two parameters on $\langle v \rangle$. In Fig. 2.5, we choose two different values of asymmetric parameter ψ , and plotted $\langle v \rangle$ as a function of noise strength Q for different values of roughness amplitude ε . The particle has very low magnitude of asymptotic velocity in smooth periodic potential, below the noise strength Q < 0.0001. Beyond this Q, we can see the magnitude of $\langle v \rangle$ suddenly increase and then decreases with the strength of the noise intensity. In the presence of roughness, particle shows altogether different behaviour in terms of $\langle v \rangle$ at weak noise intensity ($Q \le 0.0001$). The asymptotic velocity increased with the introduction of roughness and then it decreased at large roughness. The reversed scenario is observed at higher noise strength, where the $\langle v \rangle$ without roughness is higher than with roughness. Similar behaviour is observed for higher asymmetric parameter $\psi = 0.8\pi$ (Fig. 2.5 (b)).

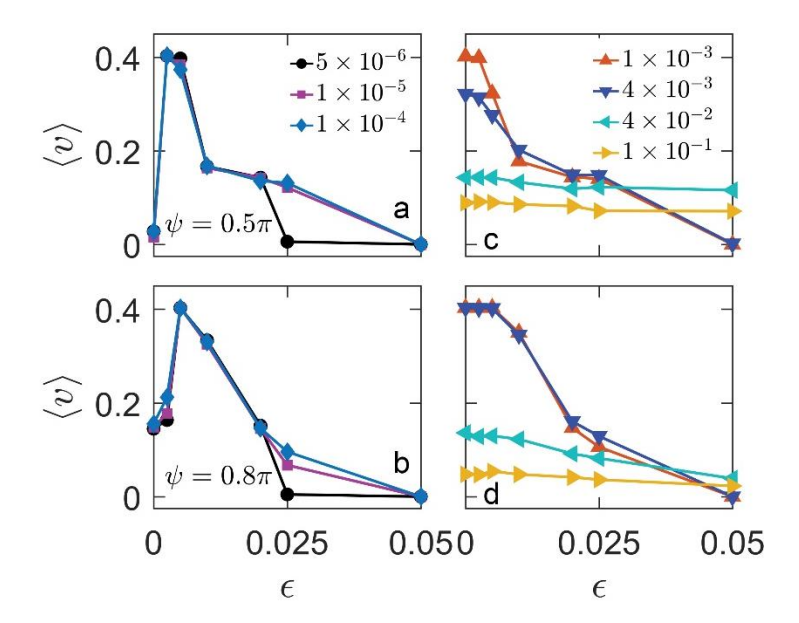


Fig. 2.6: Ensemble- and period averaged asymptotic velocity $\langle v \rangle$ as a function of roughness amplitude ε for different values of noise strength Q for two different values of ψ . Left and right column correspond to weak and strong noise limits, respectively.

In order to better visualize the effect of roughness at the weak and strong noise regime on the directed transport, we next studied the asymptotic velocity $\langle v \rangle$ as a function of ε and presented in Fig. 2.6. At the weaker noise strength, displayed in panel (a) ($\psi = 0.5\pi$) and panel (b) ($\psi =$ 0.8π), for two different values of asymmetric parameters, $\langle v \rangle$ increases with increasing roughness, and after reaching a maximum, it drops. We observed similar behaviour for higher asymmetry of the rough periodic potential [Fig. 2.6(a) and (b)]. In comparison to the smooth case, the particle transport is noticeably higher in the presence of roughness. For moderate to large noise strength, the asymptotic velocity decreases with the roughness in the lower and higher asymmetry of the potential [Figs. 2.6(c)-2.6(d)]. These findings demonstrate that in the weak noise limit, small to moderate roughness in the potential permits the particle to move effectively in one direction, however at the moderate to high noise limit, the roughness hinder the directed transport. Small wells due to the spatial heterogeneity in the periodic potential serve as steps in a ladder to cross the potential energy barrier. The roughness causes the particle to temporarily become caught inside these tiny wells in the weak noise limit, which improves the directional motion. The particle trapping is lost in the high noise limit, though, because the intensity of noise is greater compared to the depth of these tiny wells. The transport is reduced at higher noise strength, because the particles are now trapped in the potential wells for a longer time, which reduces their directional mobility.

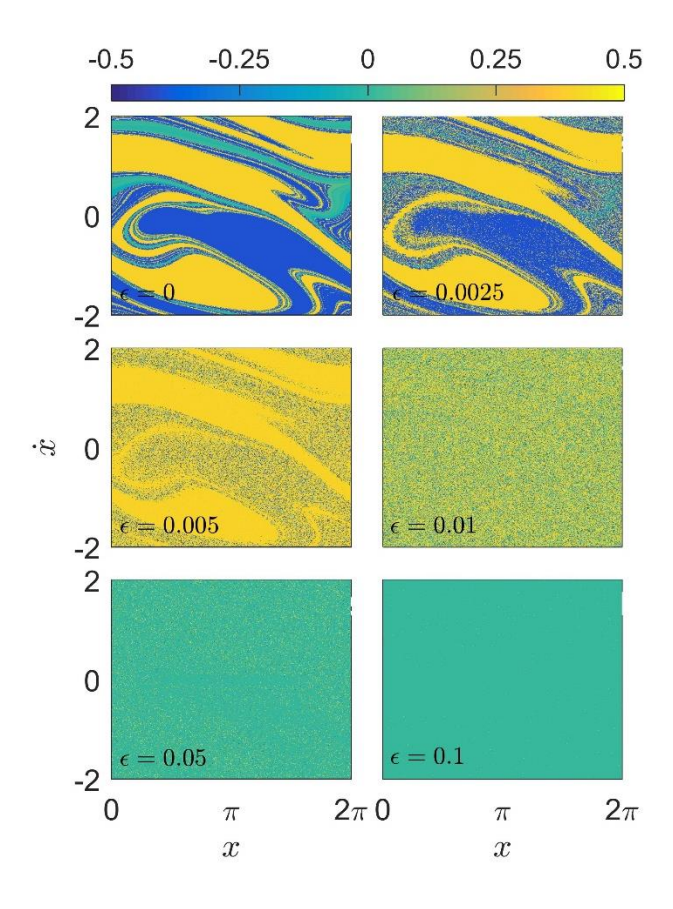


Fig. 2.7 Basins of attraction of asymptotic velocity $\langle v \rangle$ from the deterministic dynamics for different values of roughness amplitude ε . The colour bar at the top represents the magnitude of asymptotic velocity $\langle v \rangle$.

In order to comprehend the behaviour of the system at the weak noise limit, we explored the deterministic dynamics of the system by setting Q=0. We integrated the Langevin equation (Eq. (2.5)) with Q=0 with random initial positions and velocities to obtain the particle's steady-state asymptotic velocity. The basins of attraction of the asymptotic velocity change significantly due to the spatial heterogeneity in the periodic potential. There are three basins of attractors for the particle under smooth periodic potential – two with large positive and negative velocities which will be categorized as running states of the particle and one with nearly zero velocity where the particle remains in locked states (Fig. 2.7, $\varepsilon=0$). The area occupied by the positive and negative velocities are almost equal. Small roughness in the periodic potential causes tiny positive velocity regions to percolate into the negative velocity regions while leaving the positive velocity regions unaffected. When the amplitude of roughness reaches $\varepsilon=0.005$, the frequency of these small regions of positive velocity in the negative regions got rise, dramatically expanding the region of positive velocity as a whole. These small regions

demonstrate the chaotic aspect of the dynamical system, which increase with roughness. The majority of the region is covered by zero asymptotic velocity at large roughness ($\varepsilon \ge 0.05$). The reduction of the tiny regions shows that the system is not chaotic at high levels of roughness.

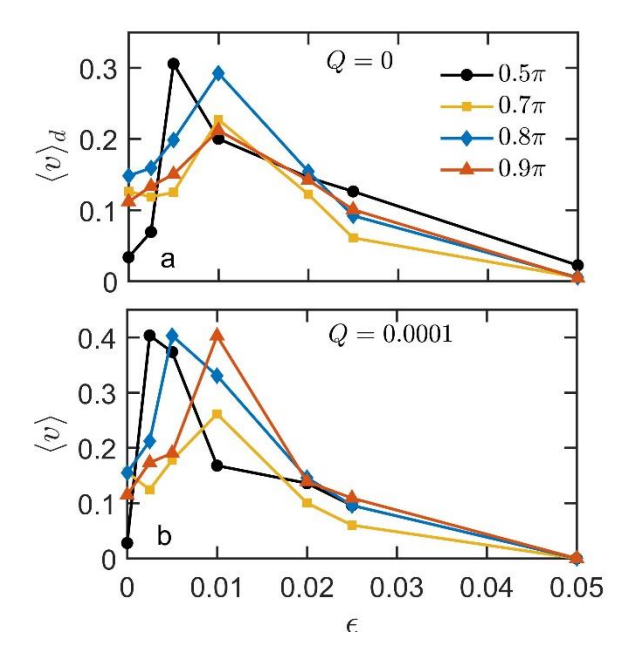


Fig. 2.8 Comparison of asymptotic velocity $\langle v \rangle$ with ε from the deterministic (top) and stochastic systems with weak noise strength Q=0.0001 (bottom) for the different values of asymmetric parameter ψ .

The asymptotic condition of the Brownian particle in the weak noise limit is strongly influenced by the basins of attraction. In this case, the deterministic forces will greatly influence the particle's behaviour. As a result, we determined the particle's asymptotic average velocity $(\langle v \rangle_a)$ by averaging the velocities from the deterministic calculations. By adjusting the asymmetry parameter ψ , we can see in how the deterministic dynamics depend on roughness in the potential. Across various values of the asymmetric parameter, ψ , the average asymptotic velocity rises and falls after reaching a maximum with roughness (Fig. 2.8(a)). Based on this calculation, we predict that the stochastic system in the weak noise intensity will behave similarly to the deterministic system. In Fig. 2.8(b), we plot the ensemble- and period-averaged asymptotic velocity, $\langle v \rangle$, as a function of roughness amplitude ε , with Q=0.0001 for different values of ψ . These calculations imply that, both in deterministic and stochastic dynamics, the directed transport of the Brownian particle increases dramatically in the presence of roughness.

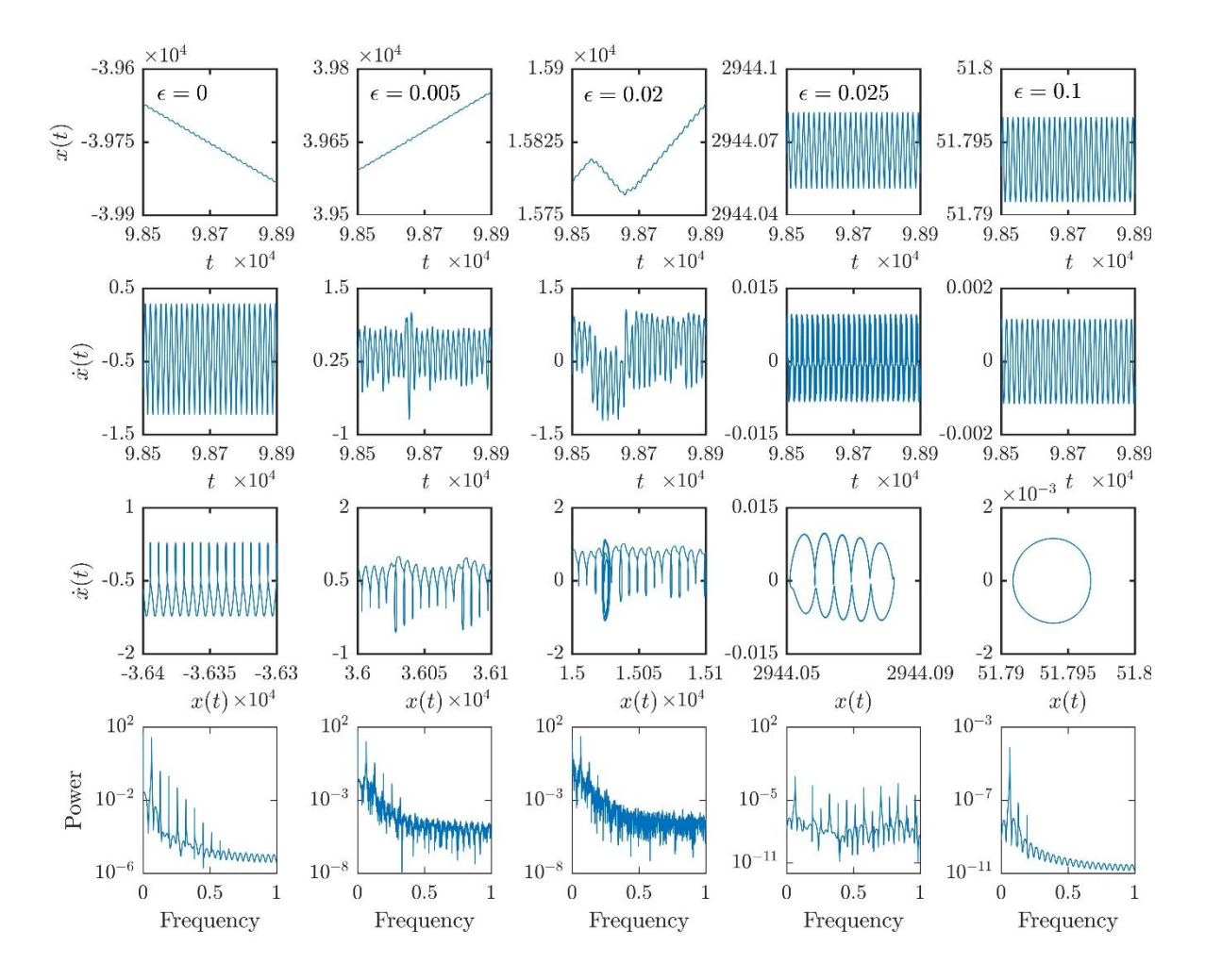


Fig. 2.9: The time series of position (first row) and velocity (second row), phase-space map (third row), and the power spectra of velocity (fourth row) in the absence of noise Q=0 for varying amplitude of roughness, ε . The initial value chosen for position and velocity were 0.1 and 0, respectively.

The asymptotic velocity's basins of attraction (Fig. 2.7) estimated from deterministic dynamics suggest that the chaotic dynamics of the system have a significant role in determining the nature of the transport of a driven Brownian particle moving under rough periodic potential. In order to better understand the physical picture behind enhancement of roughness induced current in the weak noise limit, we analysed time series of position and velocity, phase-space map and power spectra of the deterministic dynamical system (Q = 0) (Fig. 2.9). When $\varepsilon = 0$, the system displays a running state in which the particle moves with a net negative velocity while showing oscillatory dynamics in velocity (first and second rows). The resulting phase-space contains the signature of the running state (third row). The velocity power spectrum (fourth row) displays a discrete spectrum with sharp peaks at distinct frequencies signifies the purely

oscillatory (nonchaotic) behaviour of the system. In the presence of roughness ($\varepsilon = 0.005$), the particle switches to the running state in which they are "climbing" in a positive direction by overcoming the barrier of the potential well. However, the irregular oscillatory velocity profile and phase space indicate the chaotic nature of the dynamical system under roughness. The upward and downward spikes in the power spectrum indicates that the attractor might be weakly chaotic. The velocity profile of the particle with $\varepsilon = 0.02$ indicates that it traverses from one potential well to another and the spectrum is overwhelmed by downward spikes. These two characteristic features clearly indicate the strongly chaotic nature of the system. At $\varepsilon = 0.025$, the system stays in locked states, in which particle oscillates inside the potential well and average velocity is zero. The phase space maps shows that the trajectory of the particle winds arounds in a particular direction and leads to almost a torus-like structure. The spectrum for this case consists of sharp peaks at discrete frequencies which contains both upward and downward spikes. These findings suggests that system is quasi-periodic at this regime. For $\varepsilon =$ 0.1, the particle stays in one particular well and follows locked state. The time series of both position and velocity shows periodic behaviours. The spectrum shows definite peaks at discrete frequencies suggesting a periodic attractor for this particular regime.

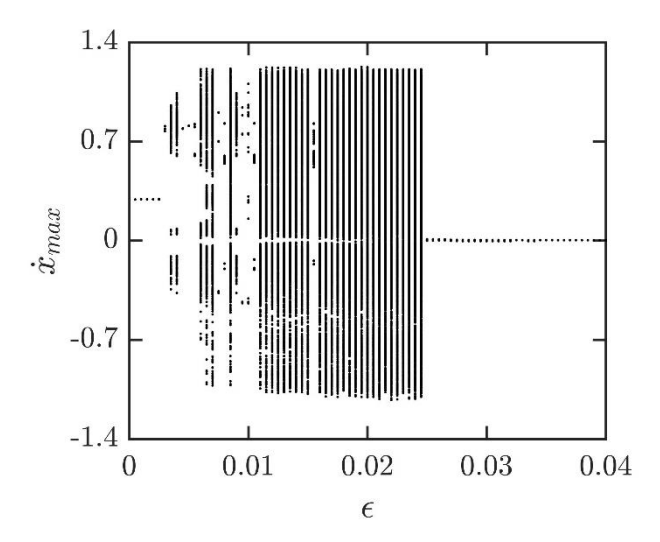


Fig. 2.10 Bifurcation plot as a function of amplitude of ε for the deterministic system.

In order to demonstrate the qualitative change in the dynamics, which transitions from strictly periodic to chaotic and then back to periodic with the rise in roughness, we plotted the bifurcation diagram of the deterministic system (Fig. 2.10). This shows that the probable cause of the rise in directed transport with the introduction of modest amplitude of roughness is the system's chaotic behaviour.

2.4 Conclusion

Physical and chemical systems often have spatial heterogeneity in the smooth potential. Previous studies looked into how roughness affected particle transport^{32,39} and barrier-crossing dynamics²⁹ in overdamped systems. These studies shown that roughness in the potential, hinders the dynamics of crossing barriers²⁹ and can play opposing roles in the movement of overdamped particles under periodic potential^{32,39}. Here, we looked at diffusion and transport of a Brownian particle in a driven inertial ratchet when the spatial periodic potential is rough in nature. We demonstrate that the roughness of the potential has a significant impact on the nature of diffusion. The phenomenon of transient anomalous diffusion in the driven inertial ratchet becomes less under roughness²⁰. Due to the roughness, the particle's transition from a super-diffusive to sub-diffusive motion occurs much earlier. The particle which displays transient anomalous diffusion under the smooth potential in the weak noise limit, exhibits normal diffusion, due to moderate roughness in their periodic potential. We demonstrate that the roughness has different kinds of impact on the transport of the particle in the weak and moderate-strong noise limits, as measured by the ensemble- and period-averaged asymptotic velocity. Small amplitude roughness considerably increases the transport of particles across different levels of asymmetry in the periodic potential in the weak noise limit. However, in the moderate-strong noise limit, roughness significantly decreases the transport. Therefore, we demonstrate here a constructive role of small amplitude roughness in the movement of particle in an inertial driven ratchet. Study on the deterministic dynamics of the system, reveals that under smooth potential, a nonchaotic system transforms into a chaotic system as roughness increases, but in the large roughness limit, the system reverts to its nonchaotic state of dynamics. These, results underline the fact that in the situation of driven inertial ratchet in a Gaussian heat bath, moderate roughness increase the directed transport due to the chaotic dynamics of the system caused by the roughness.

Previous research has demonstrated that inertial Brownian particles under periodic potential controlled by time-periodic forces can exhibit chaotic dynamics depending on the parameter space of the system^{20,40}. According to a recent study, driven inertial ratchet systems can exhibit chaotic dynamics depending on the form parameter of the smooth periodic potential⁴¹.

According to these researches, the chaotic dynamics displayed by the particle moving in a rough periodic potential are caused by the potential's related parameters.

2.5 Reference

- 1. Hänggi, P. & Marchesoni, F. Artificial Brownian motors: Controlling transport on the nanoscale. *Rev. Mod. Phys.* **81**, 387–442 (2009).
- 2. Gammaitoni, Luca & Hänggi, P,Peter & Jung, Peter & Marchesoni, Fabio. Stochastic resonance. *Rev. Mod. Phys.* **70**, 223–287 (1998).
- 3. Bressloff, P. C. & Newby, J. M. Stochastic models of intracellular transport. *Rev. Mod. Phys.* **85**, 135–196 (2013).
- 4. Ann, S. O. Molecular Motors. *Mol. Mot.* **422**, 759–765 (2007).
- 5. Kay, E. R., Leigh, D. A. & Zerbetto, F. Synthetic molecular motors and mechanical machines. Angewandte Chemie International Edition vol. 46 (2007).
- 6. Machura, L., Kostur, M. & Łuczka, J. Transport characteristics of molecular motors. *BioSystems* **94**, 253–257 (2008).
- 7. Steuer, R., Zhou, C. & Kurths, J. Constructive effects of fluctuations in genetic and biochemical regulatory systems. *BioSystems* **72**, 241–251 (2003).
- 8. Kosturf, M. Title: Transport in ratchet-type systems Author: Marcin Kostur, Jerzy Łuczka Citation style: Kostur Marcin, Łuczka Jerzy. (1996). Transport in ratchet-type systems. "Acta Physica Polonica. B" (1996, no. 3, s. 663-675). (1996).
- 9. Bier, M. Brownian ratchets in physics and biology. *Contemp. Phys.* **38**, 371–379 (1997).
- Hänggi, P. & Bartussek, R. Brownian rectifiers: How to convert brownian motion into directed transport. *Nonlinear Phys. Complex Syst.* 294–308 (2008) doi:10.1007/bfb0105447.
- 11. Spiechowicz, J. & Łuczka, J. Diffusion anomalies in ac-driven Brownian ratchets. *Phys. Rev. E Stat. Nonlinear, Soft Matter Phys.* **91**, 1–6 (2015).
- 12. Salgado-García, R. Noise-induced rectification in out-of-equilibrium structures. *Phys. Rev. E* **99**, 1–9 (2019).
- 13. Metzler, R. & Klafter, J. The random walk's guide to anomalous diffusion: A fractional dynamics approach. *Phys. Rep.* **339**, 1–77 (2000).

- 14. Metzler, R., Jeon, J. H., Cherstvy, A. G. & Barkai, E. Anomalous diffusion models and their properties: Non-stationarity, non-ergodicity, and ageing at the centenary of single particle tracking. *Phys. Chem. Chem. Phys.* **16**, 24128–24164 (2014).
- 15. Machura, L. *et al.* Brownian motors: Current fluctuations and rectification efficiency. *Phys. Rev. E Stat. Physics, Plasmas, Fluids, Relat. Interdiscip. Top.* **70**, 8 (2004).
- 16. Ai, B. Q., He, Y. F. & Zhong, W. R. Transport in periodic potentials induced by fractional Gaussian noise. *Phys. Rev. E Stat. Nonlinear, Soft Matter Phys.* **82**, 3–7 (2010).
- 17. Li, J. hui, Łuczka, J. & Hänggi, P. Transport of particles for a spatially periodic stochastic system with correlated noises. *Phys. Rev. E Stat. Physics, Plasmas, Fluids, Relat. Interdiscip. Top.* **64**, 6 (2001).
- 18. Kula, J., Czernik, T. & Łuczka, J. Brownian ratchets: Transport controlled by thermal noise. *Phys. Rev. Lett.* **80**, 1377–1380 (1998).
- 19. Spiechowicz, J., Kostur, M. & Łuczka, J. Brownian ratchets: How stronger thermal noise can reduce diffusion. *Chaos* **27**, (2017).
- 20. Spiechowicz, J., Luczka, J. & Hänggi, P. Transient anomalous diffusion in periodic systems: Ergodicity, symmetry breaking and velocity relaxation. *Sci. Rep.* **6**, 1–11 (2016).
- 21. Frauenfelder, H., Sligar, S. G. & Wolynes, P. G. The energy landscapes and motions of proteins. *Science* (80-.). **254**, 1598–1603 (1991).
- Hyeon, C. & Thirumalai, D. Can energy landscape roughness of proteins and RNA be measured by using mechanical unfolding experiments? *Proc. Natl. Acad. Sci. U. S. A.* 100, 10249–10253 (2003).
- 23. Nevo, R., Brumfeld, V., Kapon, R., Hinterdorfer, P. & Reich, Z. Direct measurement of protein energy landscape roughness. *EMBO Rep.* **6**, 482–486 (2005).
- 24. Charbonneau, P., Kurchan, J., Parisi, G., Urbani, P. & Zamponi, F. Fractal free energy landscapes in structural glasses. *Nat. Commun.* **5**, 1–6 (2014).
- 25. Delemotte, L., Kasimova, M. A., Klein, M. L., Tarek, M. & Carnevale, V. Free-energy landscape of ion-channel voltage-sensor-domain activation. *Proc. Natl. Acad. Sci. U.*

- S. A. **112**, 124–129 (2015).
- 26. Linder, T., de Groot, B. L. & Stary-Weinzinger, A. Probing the Energy Landscape of Activation Gating of the Bacterial Potassium Channel KcsA. *PLoS Comput. Biol.* **9**, 1–9 (2013).
- 27. Debenedetti, P. G. & Stillinger, F. H. Review article Supercooled liquids and the glass transition. *Nature* **410**, 259 (2001).
- 28. Heuer, A., Doliwa, B. & Saksaengwijit, A. Potential-energy landscape of a supercooled liquid and its resemblance to a collection of traps. *Phys. Rev. E Stat. Nonlinear, Soft Matter Phys.* **72**, 1–13 (2005).
- 29. Zwanzig, R. Diffusion in a rough potential. *Proc. Natl. Acad. Sci. U. S. A.* **85**, 2029–2030 (1988).
- 30. Ansari, A. Mean first passage time solution of the Smoluchowski equation: Application to relaxation dynamics in myoglobin. *J. Chem. Phys.* **112**, 2516–2522 (2000).
- 31. Pollak, E., Auerbach, A. & Talknerz, P. Observations on rate theory for rugged energy landscapes. *Biophys. J.* **95**, 4258–4265 (2008).
- 32. Mondal, D., Ghosh, P. K. & Ray, D. S. Noise-induced transport in a rough ratchet potential. *J. Chem. Phys.* **130**, (2009).
- 33. Li, Y., Xu, Y., Kurths, J. & Yue, X. Lévy-noise-induced transport in a rough triple-well potential. *Phys. Rev. E* **94**, 1–9 (2016).
- 34. Li, Y., Xu, Y., Kurths, J. & Yue, X. Transports in a rough ratchet induced by Lévy noises. *Chaos* **27**, (2017).
- 35. Li, Y., Xu, Y. & Kurths, J. Roughness-enhanced transport in a tilted ratchet driven by Lévy noise. *Phys. Rev. E* **96**, 1–9 (2017).
- 36. Kautz, R. L. Noise, chaos, and the Josephson voltage standard. *Reports Prog. Phys.* **59**, 935–992 (1996).
- 37. Guantes, R., Vega, J. L. & Miret-Artés, S. Chaos and anomalous diffusion of adatoms on solid surfaces. *Phys. Rev. B Condens. Matter Mater. Phys.* **64**, 1–11 (2001).
- 38. Denisov, S., Flach, S. & Hänggi, P. Tunable transport with broken space-time

- symmetries. *Phys. Rep.* **538**, 77–120 (2014).
- 39. Camargo, S. & Anteneodo, C. Impact of rough potentials in rocked ratchet performance. *Phys. A Stat. Mech. its Appl.* **495**, 114–125 (2018).
- 40. Mateos, J. L. Chaotic transport and current reversal in deterministic ratchets. *Phys. Rev. Lett.* **84**, 258–261 (2000).
- 41. Luo, Y., Zeng, C. & Ai, B. Q. Strong-chaos-caused negative mobility in a periodic substrate potential. *Phys. Rev. E* **102**, 1–14 (2020).

CHAPTER 3

Effect of roughness in the periodic potential in the transport of a driven Brownian ratchet in the presence of external load

3.1 Introduction

Among many kinds of anomalous transport properties of the Brownian ratchets, ^{1–5} the surprising phenomenon of absolute negative mobility (ANM) of Brownian particles, where the particle moves in a direction opposite to the external load has attracted attention of a lot of researchers ^{6–15}. Such a physical phenomenon would be in opposition to Newton's equations of motion at equilibrium, however in many experimental systems, negative mobility has been seen under non-equilibrium condition. It has been experimentally observed in variety of systems such as the non-linear response in p-modulation-doped quantum wells ¹⁶, absolute negative conductance in sequential resonant tunnelling semi-conductor super lattices ^{17,18}, absolute negative resistance in a three terminal configuration in a two dimensional electron gas ¹⁹, negative absolute resistance in a Josephson junction ²⁰. Additionally, ANM has been seen in classical systems such charged colloidal particles in microfluidic channels ^{21,22}. Potential technological benefits of ANM include particle separation based on mass ^{23–25}.

In this framework of noise-induced transport, the nature of the energy landscape has an important role in the dynamics of the driven Brownian ratchets ^{26–30}. In contrast to smooth periodic potential, rough energy landscapes stand out in real physical systems such as in protein folding pathway^{31,32}, gating of ion channels in bacteria³³, slow diffusion in structural glasses^{34,35}, super cooled glasses^{36,37} and so on. The spatial heterogeneity thus became a relevant factor in the transport properties of Brownian ratchets. We can mimic rough periodic potential in simulation by super-imposing a fast-oscillating trigonometric function on background potential, where the amplitude and frequency of the imposed function should be smaller and higher than the other respectively³⁸.

The impact of roughness on a thermal ratchet under overdamped dynamics was examined in the context of Brownian ratchet, and it was observed that roughness acts as a hinder to the transport, supporting an earlier discovery by Zwanzig on the estimation of first passage time across rough potential barriers^{26,38}. Recent studies have shown that roughness enhances transport in both the underdamped as well as in the over damped dynamics in the presence of Levy noise. Here roughness in the potential surface ladders up the particle over the potential barrier^{27,28,39}. In the last chapter, we discussed that small amplitude of roughness in an

asymmetric periodic potential enhances transport relative to the smooth potential for inertially driven Brownian particle⁴⁰.

In this chapter, we studied the transport of a driven inertial Brownian particle moving in a symmetric rough periodic potential in presence of an external load. Since absolute negative mobility (ANM) has potential technological applications in the area of mass separation, our objective was to determine the fate of ANM under rough potential of a driven Brownian particle in its inertial regime.

3.2 Model

We have examined the Brownian particle of mass, M, moving in a rough symmetric periodic potential, U(x), driven by a time-periodic force, $A\cos(\Omega t)$, with an amplitude, A, and an angular frequency, Ω , in the presence of an external load, F. The dynamics of the particle is thus modeled by the Langevin equation and is given by

$$M\ddot{x} = -U'(x) + F - \Gamma \dot{x} + A\cos(\Omega t) + \eta(t)$$
(3.1)

The dot (\cdot) and prime $(\dot{})$, respectively, represent the derivative with respect to time (t) and the position (x). Thermal fluctuations, $\eta(t)$, are modeled by Gaussian white noise f zero mean $\langle \eta(t) \rangle = 0$, and follows fluctuation-dissipation relation $\langle \eta(t) \eta(t') \rangle = 2\Gamma k_B T \delta(t-t')$ where Γ , k_B , and Γ are dissipation coefficient, Boltzmann constant and temperature, respectively.

The symmetric potential, U(x), consists of two parts with a smooth part, $U_0(x)$, and a rough part, $U_1(x)$, and given as

$$U(x) = U_0(x) + U_1(x). (3.2)$$

The smooth symmetric periodic potential was taken as

$$U_0(x) = -\Delta U \sin\left(\frac{2\pi}{L}x\right) \tag{3.3}$$

Where L and ΔU are the period and barrier height, respectively. $U_1(x)$ was chosen as ³⁸

$$U_1(x) = \Delta U \,\varepsilon_0 \cos(\Lambda x) \tag{3.4}$$

Where ε_0 and Λ is the amplitude and periodicity of the rough potential, respectively. We nondimensionalized Eq. (3.1) to decrease the number of variables, and the dimensionless form of the equation of motion is given as¹⁵

$$\ddot{\hat{x}} = -\hat{U}'(\hat{x}) + f - \gamma \dot{\hat{x}} + a\cos(\omega \hat{t}) + \hat{\eta}(\hat{t})$$
(3.5)

We define coordinate \hat{x} and time \hat{t} for the dimensional analysis as follows:

$$\hat{x} = \frac{2\pi x}{L}$$
, $\hat{t} = \frac{t}{\tau_0}$, with $\tau_0 = \frac{L}{2\pi} \sqrt{M/\Delta U}$ (3.6)

In the process of nondimensionalization, we rescaled all the parameters as $\gamma = \tau_0 \Gamma/M$, $a = AL/2\pi\Delta U$, $f = FL/2\pi \Delta U$, $Q = k_B T/\Delta U$, $\varepsilon = \varepsilon_0/\Delta U$, $\lambda = \Lambda L/2\pi$, and $\omega = \tau_0 \Omega$. The rescaled thermal noise, $\hat{\eta}(\hat{t}) = (L/2\pi\Delta U)\eta(\tau_0\hat{t})$, follows zero mean, $\langle \hat{\eta}(\hat{t}) \rangle = 0$, and the fluctuation-dissipation relation, $\langle \hat{\eta}(\hat{t})\hat{\eta}(\hat{t}') \rangle = 2\gamma Q\delta(\hat{t}-\hat{t}')$. The rescaled potential is given by $\hat{U}(x) = U((L/2\pi)x)/\Delta U$ with the period $L = 2\pi$. The dimensionless rough symmetric potential is given as:

$$\widehat{U}(\widehat{x}) = -\sin(\widehat{x}) + \varepsilon \cos(\lambda \widehat{x}) \tag{3.7}$$

Where ε determines the amplitude of roughness. In this work, we set the value of λ as 50. The smooth ($\varepsilon = 0$) and rough ($\varepsilon = 0.1$) periodic potential with (f = 0.5) and without (f = 0) the external load are shown in Fig. 3.1.

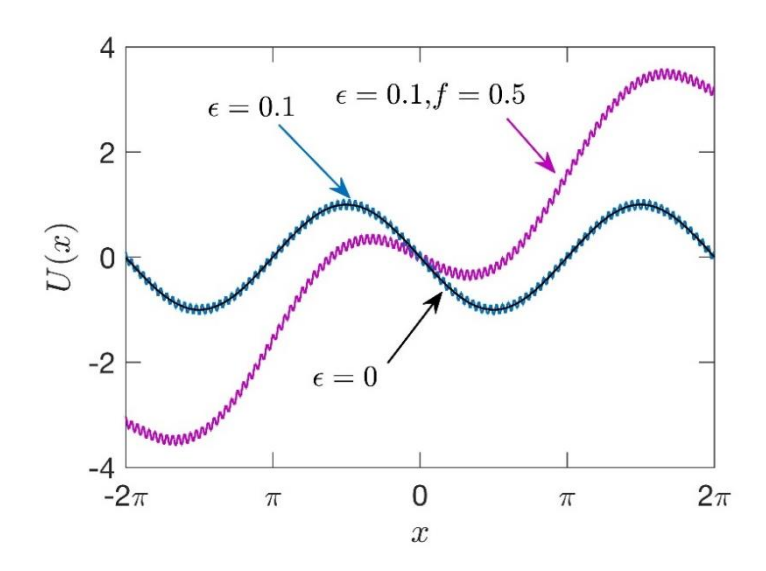


Fig. 3.1: Symmetric periodic potential, U(x), without and with roughness and the external load.

As done in the previous chapter, we calculated the asymptotic ensemble and period average velocity, $\langle v \rangle$, as⁴¹

$$\langle v \rangle = \lim_{t \to \infty} \frac{1}{T} \int_{t}^{t+T} ds \, \langle \dot{x}(s) \rangle$$
 (3.8)

Where $\langle \cdot \rangle$ indicates ensemble averaging over initial conditions for the position and velocity. The period average was calculated over one period, $T = \frac{2\pi}{\omega}$, of the external driving force. We used second-order predictor-corrector approach for numerically integrating the Langevin equation (Eq. 3.5). The initial position and velocities were uniformally distributed over the range $[0,2\pi]$ and [-2,2] respectively. We used small step size, $10^{-4} \times \frac{2\pi}{\omega}$, in order to accord the small fine structures of roughness in the potential. All the numerical calculations involved ensemble averaging of 2048 trajectories and the simulations were run for a total time of $10000 \times T$. We calculated $\langle v \rangle$ in two ways. In the first method Eq. (3.8) was used where we averaged the velocity over a period in the long-time limit and then averaged over an ensemble of trajectories. In the second method, we calculated $\langle v \rangle$ by subtracting the position of the particle at a transient time (t = 20T) from the position at final time (t = 10000T) and dividing the difference by time interval, and finally averaging it over an ensemble of trajectories. We demonstrated that both the approaches provide the same results (Fig 3.2(a) and 3.2(b)). Here we emphasize that computing the $\langle v \rangle$ from the position is computationally less costly than the calculating $\langle v \rangle$ from the first method, since it demands larger number of ensemble averaging to reduce noise.

3.3 Results and Discussions

In the previous chapter, we discussed the effect of rough asymmetric periodic potential on the transport of a driven inertial Brownian particle. There, we found smaller amplitude of roughness enhances directed transport in the inertial regime. In what follows here, we considered the combination of rough symmetric periodic potential along with the presence of a constant external load and studied the transport properties of a driven particle.

Our chosen dynamics of driven inertial ratchet is characterised by a six-dimensional parameter space $(\varepsilon, a, \omega, \gamma, f, Q)$ controlling the dynamics of the driven inertial ratchet. Previous research has demonstrated the significance of the parameters in determining the nontrivial behaviour of the same system under a smooth periodic potential⁴². We first determined the parameter space

related to the anomalous negative mobility (ANM) of the system by numerically scanning each parameter independently since our goal is to identify a roughness-induced ANM condition. Since our objective is to identify a roughness-induced ANM condition, we first identified a parameter space significant to the anomalous negative mobility of the system by quantitatively scanning each parameter individually.

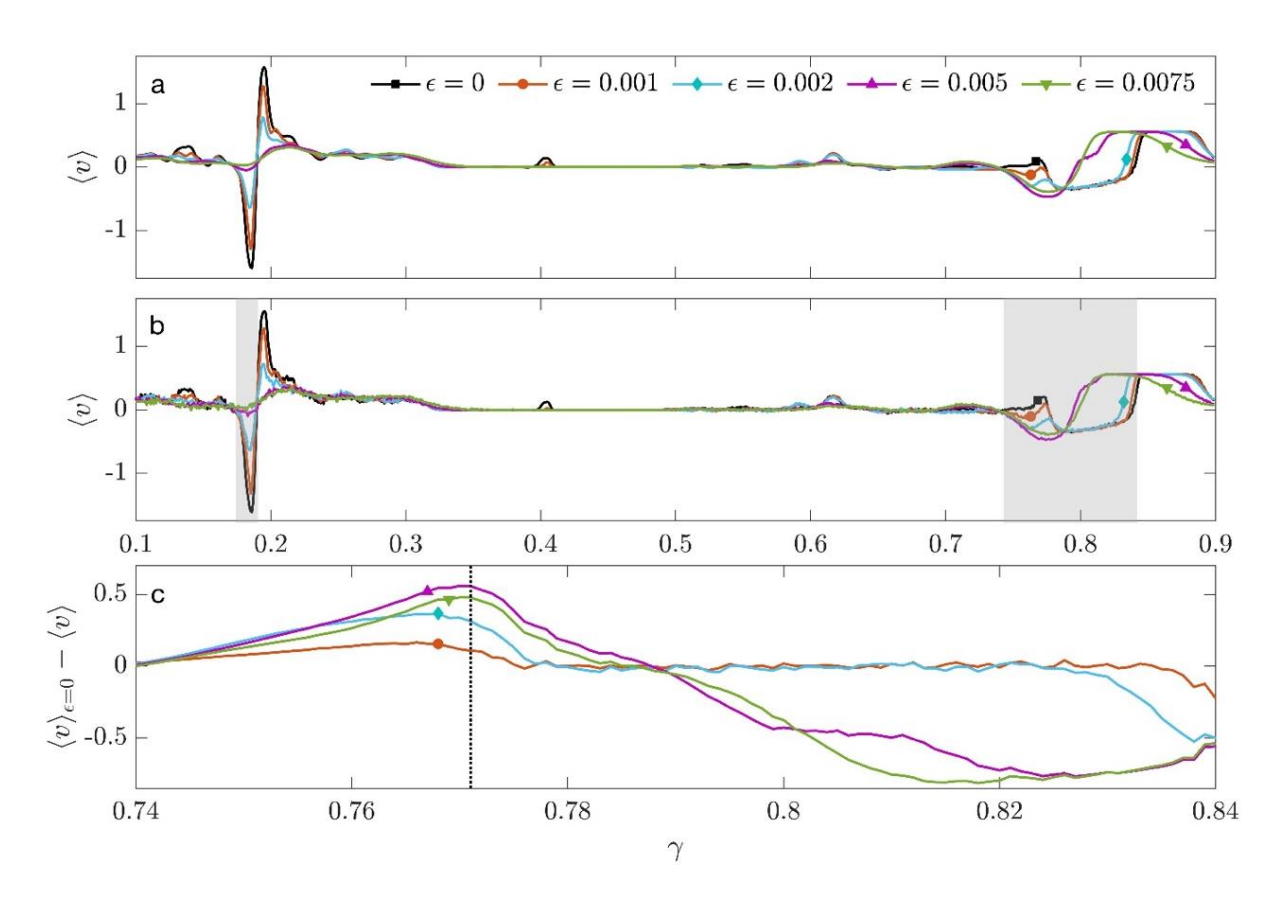


Fig. 3.2: Ensemble and period averaged asymptotic velocity, $\langle v \rangle$, calculated from x(t) (a) and $\dot{x}(t)$ (b) as a function of γ for different values of roughness amplitude ε . The shaded part indicates the region of γ where the system shows ANM. (c) The plot of difference between the $\langle v \rangle$ without and with roughness ($\langle v \rangle_{\varepsilon=0} - \langle v \rangle$) with γ . The vertical line represents maximum difference between the $\langle v \rangle$ without and with roughness. Other parameters were f=0.015, Q=0.00035, a=1.589, and $\omega=0.559$.

Fig.3.2 (a) illustrates the dependency of $\langle v \rangle$, computed from x(t), on the dissipation constant, γ , for various degrees of the roughness ε for the external load f=0.015. In Fig.3.2 (b), $\langle v \rangle$ versus γ plot, $\langle v \rangle$ was computed using Eq. (3.8). The visual comparison of these two plots reveals that the results from both methods are nearly identical. The system displays ANM in two regions (areas under shaded). The system shows ANM under smooth potential in the region

on the left, and as the potential becomes rougher, the extent of ANM decreases. Although both the smooth ($\varepsilon=0$) and the rough ($\varepsilon\neq0$) systems display ANM in the region on the right, there is a region of where ANM is only caused by the roughness in the potential, where the smooth system produces positive values of $\langle v \rangle$ against a positive load of f=0.015. So, there is a region of where ANM can only be driven by the rough potential. We evaluated the difference of $\langle v \rangle$ between the smooth and rough systems ($\langle v \rangle_{\varepsilon=0} - \langle v \rangle$) and identified the value of dissipation constant, γ , corresponding to the maximum difference (Fig. 3.2 (c)).

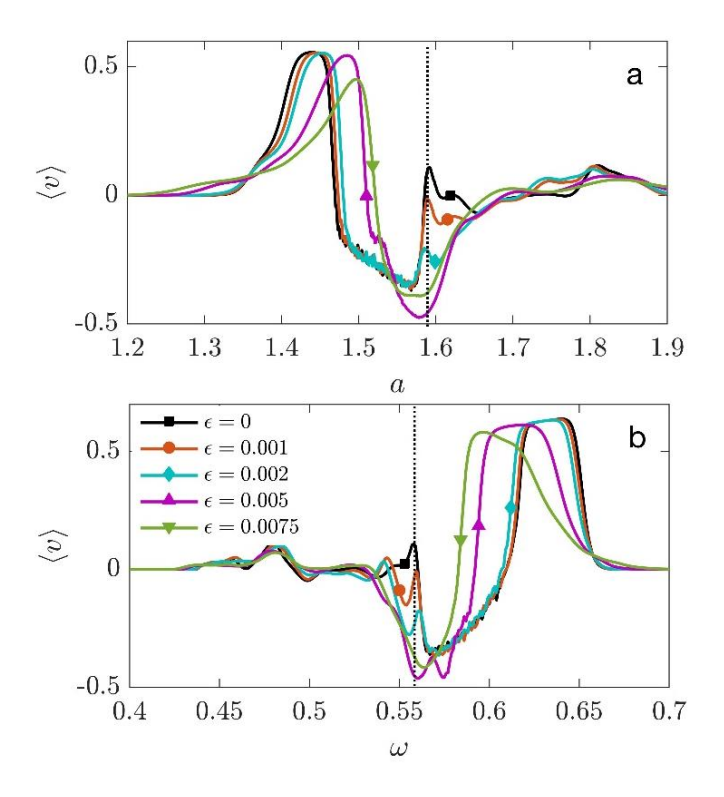


Fig. 3.3: Parameter scanning for amplitude, a, (a), frequency, ω , (b), of the external driving force. The vertical lines represent the selected values of the respective parameters where the difference between the average velocities without and with roughness was maximum. The values of γ , Q, and f were 0.7710, 0.00035, and 0.015, respectively. In the scans of a and ω , ω and a were chosen to be 0.558 and 1.589, respectively.

To determine the amplitude (a) and frequency (ω) of the external driving force, we used a similar technique of parameter scanning (Figs. 3.3(a) and 3. 3(b)). These calculations also reveal that the system does not exhibit directed transport for a large range of parameter values, indicating that even for normal transport against an external force f an optimal combination of parameters is required. Based on these calculations, we set the values of γ , α , and ω for the remaining calculations to be 0.771, 1.589, and 0.558, respectively.

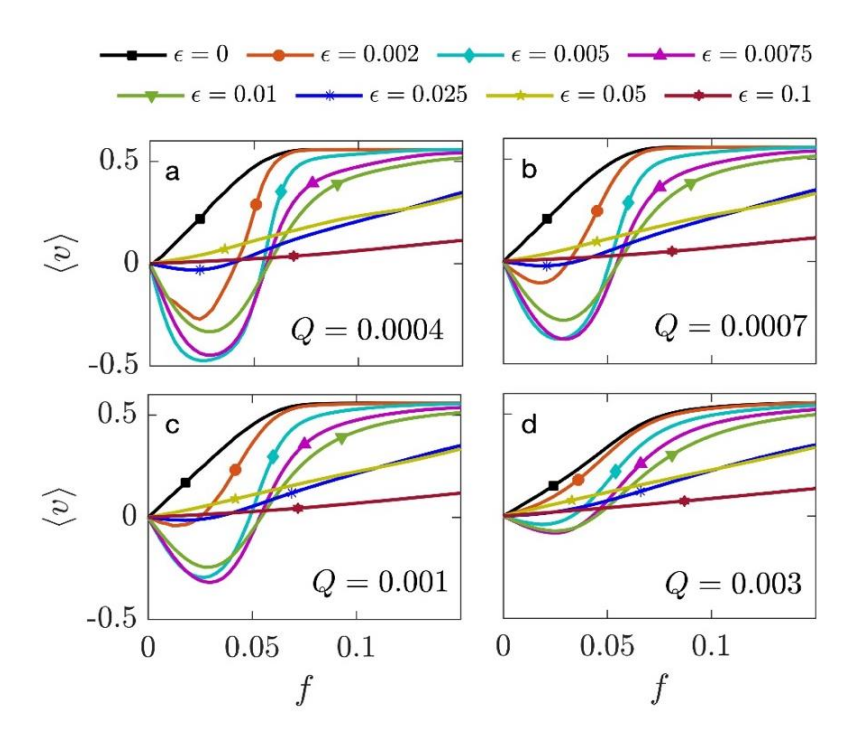


Fig. 3.4: The variation of $\langle v \rangle$ as a function of external load, f, for different values of Q and ε . Other parameters were $\gamma = 0.771$, $\alpha = 1.589$, and $\omega = 0.558$.

After establishing the parameter space necessary for roughness-driven ANM, we looked into how the external load affected the anomalous nature of the transport across various values of ε . Fig. 3.4(a) displays $\langle v \rangle$ as a function of f for various values of ε at a particular value of Q. This shows that under the smooth potential ($\varepsilon = 0$), the system does not show anomalous transport across a wide range of loads. However, the system exhibits ANM with the addition of roughness, and at higher load the particle changes the direction of current from negative to positive causing current reversal. Although the system does not exhibit ANM at higher roughness, the amount of ANM initially increases with roughness (more negative $\langle v \rangle$). Anomalous transport and current reversal are the two main features of transport that result from the introduction of roughness into the periodic potential. It also makes note of the existence of an optimal roughness at which the system exhibits the maximum ANM. Over a range of values of ε , the load corresponding to the largest negative $\langle v \rangle$ was found to be at f = 0.03. Repeating these calculations for higher noise intensities reveal that (Figs. 3.4(b-d)) the ANM and current reversal are reduced in the presence of high noise. In particular, when Q rises, the range f for which the system exhibits ANM shrinks. It is significant to notice that, for varied noise strength values, the transport feature of the system with smooth potential is mostly unaffected. As a result, it appears that ANM and current reversal due to the roughness in the potential can be observed in the weak noise limit.

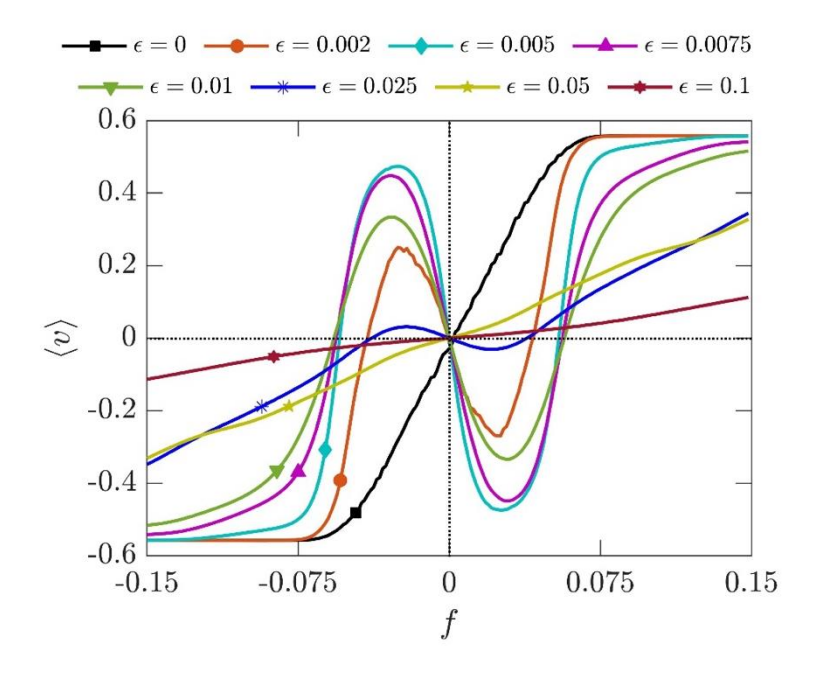


Fig 3.5: The plot of $\langle v \rangle$ as a function of external load f, at noise intensity Q = 0.0004 for different values of ε . Other parameters were the same as in Fig. 3.4.

Our calculations demonstrate that roughness-induced ANM occurs at a smaller roughness amplitude as well as for smaller range of positive load. Small amplitude of roughness in the potential surface may function as a barrier to the particle's movement in the small positive range of load, pushing the particle to move in the opposite direction and resulting in negative mobility. We calculated $\langle v \rangle$ for the same domain of roughness and other parameters in the negative range of load to confirm that (Fig. 3.5). In the negative load region, the current direction is exactly opposite to the direction of the external load, suggesting the fact that small amplitude roughness force the driven particle to travel against the load direction at smaller region of load.

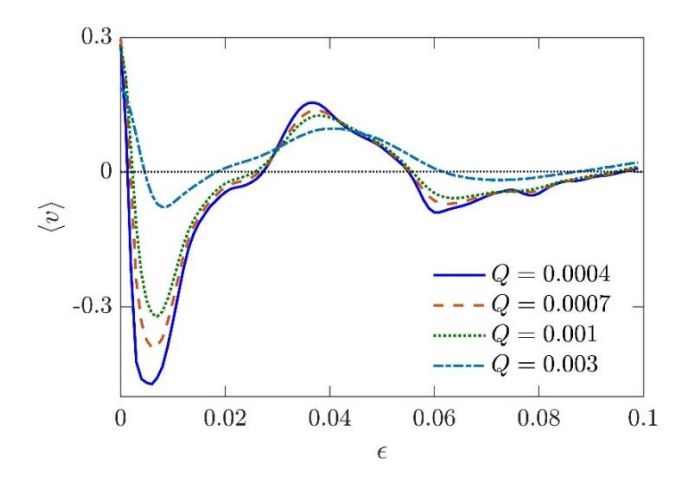


Fig. 3.6: The variation of $\langle v \rangle$ as a function of roughness amplitude, ε , for different values of Q. Other parameters were the same as in the Fig. 3.4.

Following that, we investigated the relationship between the $\langle v \rangle$ and ε at a load corresponding to the maximum negative velocity (f corresponding to the minimum in Fig. 3.4) at various values of noise intensity Q (Fig. 3.6). Across a range of noise intensities, system shows normal transport for smooth periodic potential ($\varepsilon = 0$). With increasing amplitude of roughness, it exhibits negative average velocity that dramatically drops with the increase of roughness. As the roughness increases further, the value of the negative current decreases, the direction of the current changes to positive, then back to negative when it reaches the large roughness limit. As a result, system experiences multiple current reversals as roughness in the potential increases.

ANM is more prominent around the limit of lower noise intensity Q. We calculated $\langle v \rangle$ as a function of Q for various values of ε (Fig. 3.7) at an external load (f=0.03) equivalent to the greatest ANM as shown in Fig. 3.4. The system with smooth potential displays ANM in the limit of extremely weak noise range (Q<0.0002). The area of ANM rises with the addition of small amplitude of roughness, while large roughness compels the particle to move in the direction of the external load, which reduces the ANM. In the intermediate range of noise intensity (0.0002 < Q<0.003), the rough system only moves in the opposite direction of the load exhibiting a significant amount of ANM in compared to the system in smooth potential. Therefore, roughness-induced ANM can be observed at the intermediate noise intensity.

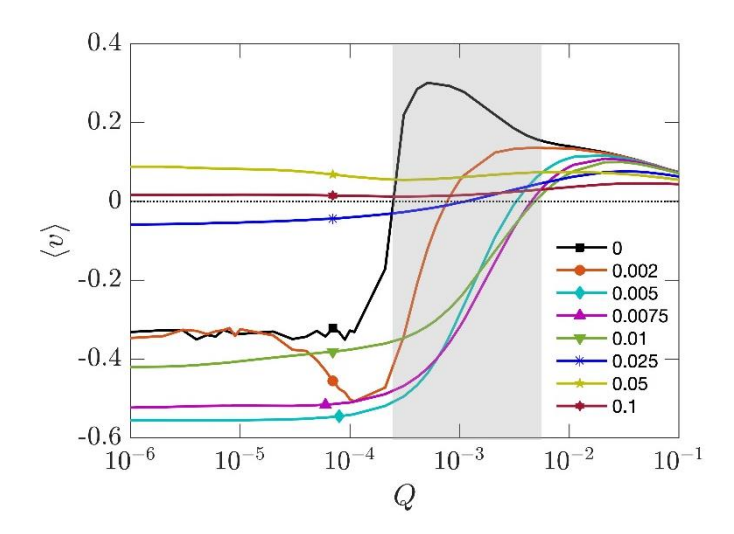


Fig. 3.7: The variation of $\langle v \rangle$ as a function of Q for the indicated values of ε . The shaded part indicates the region of Q where roughness-driven ANM occurs. Other parameters were the same as in the Fig. 3.4.

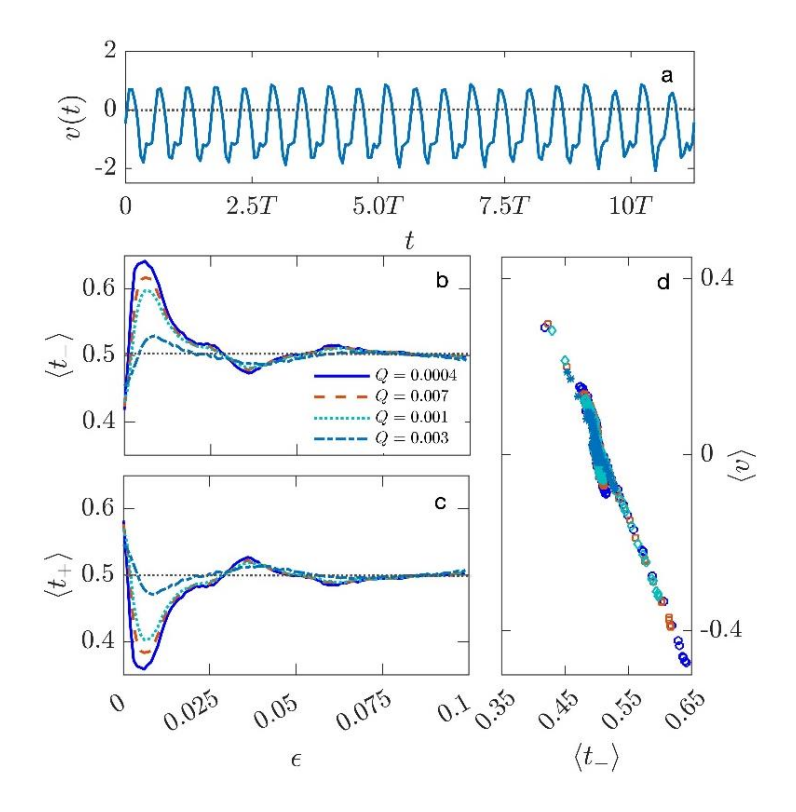


Fig. 3.8: Temporal oscillation of velocity, v(t) (a). The average fraction of time with negative $(\langle t_- \rangle)$ and positive $(\langle t_+ \rangle)$ velocity during one-time full period (T) of external driving are plotted as a function of ε for different values of Q (b, c). The correlation plots of $\langle v \rangle$ with $\langle t_- \rangle$ for different values of Q. Other parameters were the same as in the Fig. 3.4.

The direction of the current was connected to the direction of the trajectory's running states^{7,43}. In running states, x(t), typically displays a growing (or decreasing) values of x over time t,

where the average velocity is nonzero. In Fig 3.8(a) v(t) oscillates throughout time t due to the periodic driving force, regardless of the magnitude of the current. We determined the average fraction of time the system spends with positive $(\langle t_+ \rangle)$ or negative $(\langle t_- \rangle)$ velocities throughout the course of the external driving period (T) in order to establish a correlation between the ANM and the system dynamics. It makes sense that if a system spends more time in the negative velocity phase, the sign of $\langle v \rangle$ must also be negative. As a result, either $\langle t_- \rangle$ or $\langle t_+ \rangle$ must be examined in order to determine the sign of the current. Fig. 3.8(b) presents the variation of $\langle t_- \rangle$ with amplitude of roughness ε and shows that an increase in $\langle t_- \rangle$ causes an increase in the average negative velocity (Fig.3.6). As a result, variation of $\langle t_- \rangle$ with the ε in tune with the $\langle v \rangle$ versus ε plot in Fig. 3.5. Accordingly, $\langle t_+ \rangle$ behaves in a complementary manner (Fig. 3.8 (c)). Also, large negative $\langle v \rangle$ strongly correlates with large $\langle t_- \rangle$ (Fig. 3.8(d)). These indicate that the direction of the average current in the transport is ultimately determined by changes in the balance of positive and negative velocity phases in the temporal oscillation of v(t).

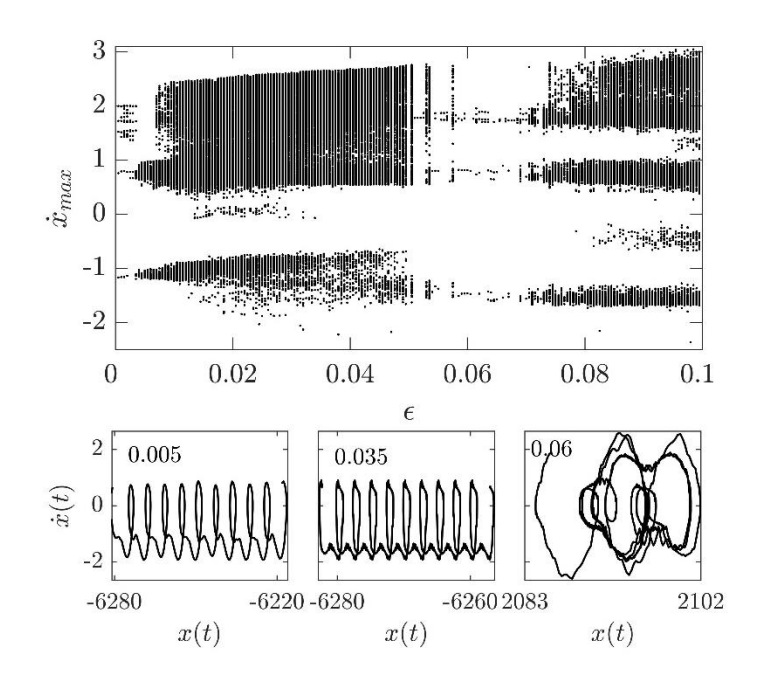


Fig. 3.9: Bifurcation diagram (\dot{x}_{max} vs ε) of the deterministic dynamical system with Q=0 and f=0.03 (top panel). Representative phase-space plots for the indicated values of ε (bottom panel).

Chaotic dynamics has been proposed as the origin of ANM in earlier studies^{7,8,44}. We generated the bifurcation diagram, where the maximal temporal velocity, \dot{x}_{max} , is plotted against the roughness parameter ε , for the deterministic (Q=0) system, to see whether chaotic dynamics

may have had any part in generating ANM (Fig. 3.9). The system's degree of chaos varies considerably with the amplitude of roughness ε . The system is relatively chaotic for extremely small ($\varepsilon > 0.0075$) and intermediate (0.05 $< \varepsilon < 0.07$) roughness ranges, and highly chaotic for other ranges of roughness. Comparison between the bifurcation diagram and $\langle v \rangle$ versus ε plot in Fig. 3.6 show a substantial association between the ANM and the system's weak chaotic dynamics. We plotted the phase-space diagram of the system for the values of ε corresponding to the maximum ANM ($\varepsilon = 0.005$ and $\varepsilon = 0.06$) and found that the system is weakly chaotic at those values of roughness. On the other hand, it is highly chaotic near the roughness ($\varepsilon = 0.035$), which is where the system exhibits its maximum positive velocity. So, it appears that the ANM caused by roughness has its roots in weak chaos.

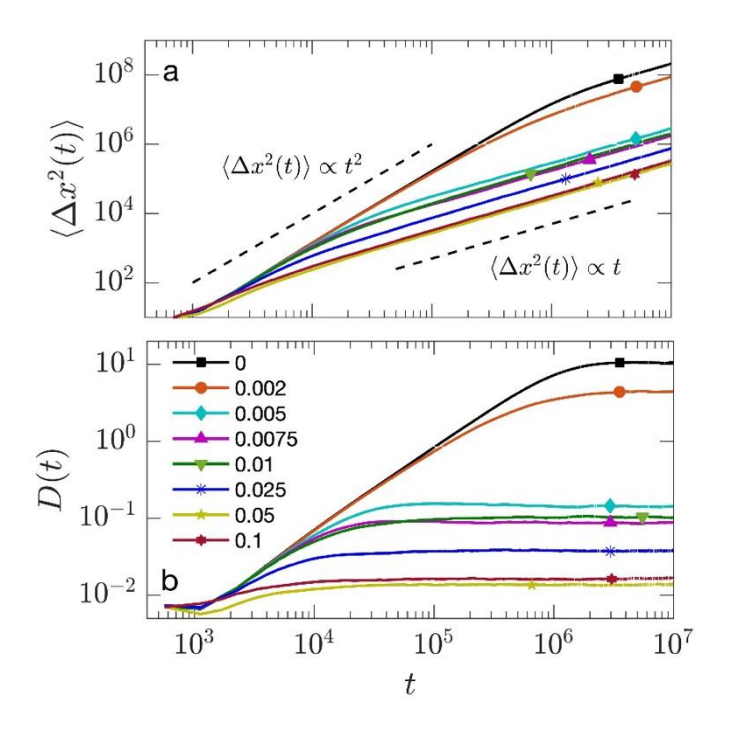


Fig. 3.10 (a) The plot of mean square displacement, $\langle \Delta x^2(t) \rangle$, as a function of time for different values of ε . The ballistic diffusion ($\langle \Delta x^2(t) \rangle \propto t^2$) in the early phase and normal diffusion in the asymptotic phase ($\langle \Delta x^2(t) \rangle \propto t$) are indicated by the dashed lines. (b) The plot of time-dependent diffusion coefficient, D(t), as a function of time. Parameters were the same as in Fig. 3.4.

It is known that driven inertial Brownian ratchets under smooth periodic potential exhibit diffusion anomalies. Previous research has suggested the presence of super- and sub-diffusive regimes at various time scales^{41,45–47}. We examined the mean square displacement, $\langle \Delta x^2(t) \rangle (= \langle [x(t) - \langle x(t) \rangle]^2 \rangle)$, and the time-dependent diffusion coefficient, $D(t) (= \langle \Delta x^2(t) \rangle / 2t)$, to

identify the nature of diffusion under roughness of the potential (Fig. 3.10). The system exhibits ballistic behaviour in the early period, and normal diffusion is established in the later time (Fig. 3.10(a)). While normal diffusion is established significantly later in the smooth system, it is enforced sooner in the rough system. As roughness increases, the ballistic phase's duration gets reduced. The D(t) plots suggest that the smooth system takes some to achieve normal diffusion, where D(t) becomes time independent in compared to the system in rough periodic potential. In light of these findings, it can be concluded that the ANM caused due to the roughness is not a by-product of anomalous diffusion.

Since it becomes essential in breaking the system's spatial symmetry in the absence of an external load, the importance of asymmetry in periodic potentials has been thoroughly investigated in the context of ratchet models. Hence, we examined how the asymmetry affected the ANM when the periodic potential was rough in nature. $U_2(x)$ was added to U(x) in Eq. (3.7) to generate asymmetry into the potential⁴⁸.

$$U_2(x) = \frac{\Delta}{2}\sin(2\pi x) \tag{3.9}$$

Where Δ is the asymmetry parameter. Asymmetry in the symmetric periodic potential can lead to the breaking of reflection symmetry of the potential, while there is no external load^{40,41}. The full form of the potential energy now becomes

$$U(x) = -\sin(x) + \varepsilon \cos(\lambda x) + \frac{\Delta}{2}\sin(2\pi x)$$
(3.10)

The impact of asymmetric parameter Δ on the transport of driven Brownian particle moving in rough periodic potential is shown in Fig. 3.11 for different values of ε . Roughness induces ANM in the range of modest asymmetry ($\Delta=0.1$). According to the change of $\langle v \rangle$ with Δ , both smooth and rough systems can experience current reversal due to asymmetry in the periodic potential. The system displays multiple current reversals, at small roughness $\varepsilon=0.001$. As the asymmetry increases, the current moves in the direction determined by the external load. According to these findings, the asymmetric periodic potential can also produce an ANM, and the directionality of the current can be adjusted by varying the asymmetric parameter of the potential.

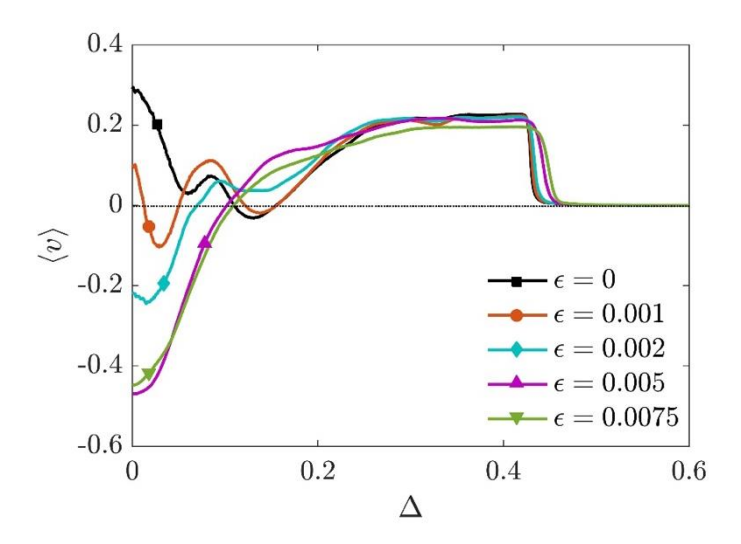


Fig. 3.11 The plot of $\langle v \rangle$ as a function of asymmetry parameter Δ , for the indicated values of ε with a load f=0.03. Other parameters were Q=0.0004, $\gamma=0.771$, $\alpha=1.589$, and $\omega=0.558$.

3.4 Conclusion

We have numerically studied the impact of roughness in the symmetric periodic potential on the transport properties of a driven inertial Brownian ratchet. Our major aim was to look at how roughness affected the absolute negative mobility ANM, a type of anomalous nature of movement, when the particle is moved in the opposite direction of external load. Given that ANM is sensitive to parameter space⁴², we have identified an ideal parameter space where ANM is solely produced by the roughness in the periodic potential. From our findings, we established that roughness-driven ANM is a feature of the system especially, in the intermediate noise intensity. We observed that the average duration of the negative velocity phase is longer than the average duration of the positive velocity phase in the temporal oscillation of velocity during a period of external driving, in the presence of roughness. This indicates that the shift of balance towards the negative velocity phase in the temporal oscillations of velocity which leads to the particle to move in opposite direction of external load. Also, we noticed that the system exhibits weak chaos in the roughness regime where ANM is found, suggesting a potential link between weak chaos and the roughness-induced ANM. Roughness-driven ANM is also feasible for the particle moving in an asymmetric periodic potential, where multiple current reversal is generated.

It has been observed that charged colloidal particles in microfluidic devices with alternating large and small gaps can induce ANM in the presence of a periodic external electric field.

Periodic physical barriers with intervening gaps can create periodic potential energy landscape. The microscopic heterogeneity of the gaps' sizes was theorised to be the source of ANM in such systems^{21,22}. We can use our roughness-induced ANM observation as an illustration of how such occurrences are theoretically taken into account. The potential energy function's involvement in generating ANM in a driven inertial ratchet was also recently highlighted in theoretical studies⁴⁹. Our research on roughness-driven ANM therefore fits under the general category of potential energy's role in ANM. Roughness has historically been seen as an annoyance since it was thought to hinder with particle transport in ratchet and barrier crossing dynamics^{26,38}. Our calculations highlight a constructive role of roughness in the anomalous transport properties of Brownian ratchet and thus may play a part in the development of mass separation and bioanalytical applications.

3.5 Reference

- 1. Hänggi, P., Marchesoni, F. & Nori, F. Brownian motors. *Ann. der Phys.* **14**, 51–70 (2005).
- 2. Reimann, P. & Hänggi, P. Introduction to the physics of Brownian motors. *Appl. Phys. A Mater. Sci. Process.* **75**, 169–178 (2002).
- 3. Reimann, P. Brownian motors: Noisy transport far from equilibrium. *Phys. Rep.* **361**, 57–265 (2002).
- 4. Astumian, R. D. & Hänggi, P. B Rownian. 33–39 (2002).
- 5. Hänggi, P. & Marchesoni, F. Artificial Brownian motors: Controlling transport on the nanoscale. *Rev. Mod. Phys.* **81**, 387–442 (2009).
- 6. Eichhorn, R., Reimann, P. & Hänggi, P. Brownian Motion Exhibiting Absolute Negative Mobility. *Phys. Rev. Lett.* **88**, 4 (2002).
- 7. MacHura, L., Kostur, M., Talkner, P., Łuczka, J. & Hänggi, P. Absolute negative mobility induced by thermal equilibrium fluctuations. *Phys. Rev. Lett.* **98**, 1–4 (2007).
- 8. Speer, D., Eichhorn, R. & Reimann, P. Transient chaos induces anomalous transport properties of an underdamped Brownian particle. *Phys. Rev. E Stat. Nonlinear, Soft Matter Phys.* **76**, 1–14 (2007).
- 9. Alatriste, F. R. & Mateos, J. L. Anomalous mobility and current reversals in inertial deterministic ratchets. *Phys. A Stat. Mech. its Appl.* **384**, 223–229 (2007).
- 10. Kostur, M., Machura, L., Talkner, P., Hänggi, P. & Łuczka, J. Anomalous transport in biased ac-driven Josephson junctions: Negative conductances. *Phys. Rev. B Condens. Matter Mater. Phys.* **77**, 1–8 (2008).
- 11. Machura, L., Kostur, M., Talkner, P., Hänggi, P. & Łuczka, J. Negative conductances of Josephson junctions: Voltage fluctuations and energetics. *Phys. E Low-Dimensional Syst. Nanostructures* **42**, 590–594 (2010).
- 12. Machura, L., Spiechowicz, J. & Łuczka, J. Directed transport in coupled noisy Josephson junctions controlled via ac signals. *Phys. Scr.* (2012) doi:10.1088/0031-8949/2012/T151/014021.
- 13. Spiechowicz, J., Łuczka, J. & Hänggi, P. Absolute negative mobility induced by white

- Poissonian noise. J. Stat. Mech. Theory Exp. 2013, (2013).
- 14. Spiechowicz, J., Hänggi, P. & Łuczka, J. Josephson junction ratchet: The impact of finite capacitances. *Phys. Rev. B Condens. Matter Mater. Phys.* **90**, 1–11 (2014).
- 15. Spiechowicz, J., Hänggi, P. & Łuczka, J. Coexistence of absolute negative mobility and anomalous diffusion. *New J. Phys.* **21**, (2019).
- 16. Höpfel, R. A., Shah, J., Wolff, P. A. & Gossard, A. C. Negative absolute mobility of minority electrons in GaAs quantum wells. *Phys. Rev. Lett.* **56**, 2736–2739 (1986).
- 17. Keay, B. J. *et al.* Dynamic localization, absolute negative conductance, and stimulated, multiphoton emission in sequential resonant tunneling semiconductor superlattices. *Phys. Rev. Lett.* **75**, 4102–4105 (1995).
- 18. Cannon, E. H., Kusmartsev, F. V., Alekseev, K. N. & Campbell, D. K. Absolute negative conductivity and spontaneous current generation in semiconductor superlattices with hot electrons. *Phys. Rev. Lett.* **85**, 1302–1305 (2000).
- 19. Kaya, I. I. & Eberl, K. Absolute negative resistance induced by directional electronelectron scattering in a two-dimensional electron gas. *Phys. Rev. Lett.* **98**, 1–4 (2007).
- 20. Nagel, J. *et al.* Observation of negative absolute resistance in a Josephson junction. *Phys. Rev. Lett.* **100**, 1–4 (2008).
- 21. Eichhorn, R., Regtmeier, J., Anselmetti, D. & Reimann, P. Negative mobility and sorting of colloidal particles. *Soft Matter* **6**, 1858–1862 (2010).
- 22. Rosa, A., Eichhorn, R., Regtmeier, J., Duong, T., Reimann, P., Anselmetti. Absolute negative particle mobility. *Nature* **436**, 7053 (2005).
- 23. Słapik, A., Łuczka, J. & Spiechowicz, J. Temperature-Induced Tunable Particle Separation. *Phys. Rev. Appl.* **12**, 1 (2019).
- 24. Słapik, A., Łuczka, J., Hänggi, P. & Spiechowicz, J. Tunable Mass Separation via Negative Mobility. *Phys. Rev. Lett.* **122**, 3–7 (2019).
- 25. Słapik, A. & Spiechowicz, J. Tunable particle separation via deterministic absolute negative mobility. *Sci. Rep.* **10**, 1–9 (2020).
- 26. Mondal, D., Ghosh, P. K. & Ray, D. S. Noise-induced transport in a rough ratchet potential. *J. Chem. Phys.* **130**, (2009).

- 27. Li, Y., Xu, Y., Kurths, J. & Yue, X. Lévy-noise-induced transport in a rough triple-well potential. *Phys. Rev. E* **94**, 1–9 (2016).
- 28. Liu, J., Li, F., Zhu, Y. & Li, B. Enhanced transport of inertial Lévy flights in rough tilted periodic potential. *J. Stat. Mech. Theory Exp.* **2019**, (2019).
- 29. Li, Y., Xu, Y., Kurths, J. & Yue, X. Transports in a rough ratchet induced by Lévy noises. *Chaos* **27**, (2017).
- 30. Li, Y., Xu, Y. & Kurths, J. Roughness-enhanced transport in a tilted ratchet driven by Lévy noise. *Phys. Rev. E* **96**, 1–9 (2017).
- 31. Frauenfelder, H., Sligar, S. G. & Wolynes, P. G. The energy landscapes and motions of proteins. *Science* (80-.). **254**, 1598–1603 (1991).
- 32. Hyeon, C. & Thirumalai, D. Can energy landscape roughness of proteins and RNA be measured by using mechanical unfolding experiments? *Proc. Natl. Acad. Sci. U. S. A.* **100**, 10249–10253 (2003).
- 33. Linder, T., de Groot, B. L. & Stary-Weinzinger, A. Probing the Energy Landscape of Activation Gating of the Bacterial Potassium Channel KcsA. *PLoS Comput. Biol.* **9**, 1–9 (2013).
- 34. Heuer, A. Exploring the potential energy landscape of glass-forming systems: From inherent structures via metabasins to macroscopic transport. *J. Phys. Condens. Matter* **20**, (2008).
- 35. Charbonneau, P., Kurchan, J., Parisi, G., Urbani, P. & Zamponi, F. Fractal free energy landscapes in structural glasses. *Nat. Commun.* **5**, 1–6 (2014).
- 36. Heuer, A., Doliwa, B. & Saksaengwijit, A. Potential-energy landscape of a supercooled liquid and its resemblance to a collection of traps. *Phys. Rev. E Stat. Nonlinear, Soft Matter Phys.* **72**, 1–13 (2005).
- 37. Debenedetti, P. G. & Stillinger, F. H. Review article Supercooled liquids and the glass transition. *Nature* **410**, 259 (2001).
- 38. Zwanzig, R. Diffusion in a rough potential. *Proc. Natl. Acad. Sci. U. S. A.* **85**, 2029–2030 (1988).
- 39. Camargo, S. & Anteneodo, C. Impact of rough potentials in rocked ratchet

- performance. Phys. A Stat. Mech. its Appl. 495, 114–125 (2018).
- 40. Archana, G. R. & Barik, D. Roughness in the periodic potential enhances transport in a driven inertial ratchet. *Phys. Rev. E* **104**, 1–8 (2021).
- 41. Spiechowicz, J., Luczka, J. & Hänggi, P. Transient anomalous diffusion in periodic systems: Ergodicity, symmetry breaking and velocity relaxation. *Sci. Rep.* **6**, 1–11 (2016).
- 42. Wiśniewski, M. & Spiechowicz, J. Anomalous transport in driven periodic systems: distribution of the absolute negative mobility effect in the parameter space. *New J. Phys.* **24**, 063028 (2022).
- 43. Machura, L. *et al.* Optimal strategy for controlling transport in inertial Brownian motors. *J. Phys. Condens. Matter* **17**, (2005).
- 44. Słapik, A., Łuczka, J. & Spiechowicz, J. Negative mobility of a Brownian particle: Strong damping regime. *Commun. Nonlinear Sci. Numer. Simul.* **55**, 316–325 (2018).
- 45. Spiechowicz, J., Talkner, P., Hanggi, P. & Łuczka, J. Non-monotonic temperature dependence of chaos-assisted diffusion in driven periodic systems. *New J. Phys.* **18**, (2016).
- 46. Spiechowicz, J. & Łuczka, J. Diffusion anomalies in ac-driven Brownian ratchets. *Phys. Rev. E Stat. Nonlinear, Soft Matter Phys.* **91**, 1–6 (2015).
- 47. Spiechowicz, J., Kostur, M. & Łuczka, J. Brownian ratchets: How stronger thermal noise can reduce diffusion. *Chaos* **27**, (2017).
- 48. Ai, B. Q. & Liu, L. G. Facilitated movement of inertial Brownian motors driven by a load under an asymmetric potential. *Phys. Rev. E Stat. Nonlinear, Soft Matter Phys.* **76**, 1–3 (2007).
- 49. Luo, Y., Zeng, C. & Ai, B. Q. Strong-chaos-caused negative mobility in a periodic substrate potential. *Phys. Rev. E* **102**, 1–14 (2020).

CHAPTER 4

Effect of roughness in the periodic potential in the transport of driven coupled inertial Brownian particles.

4.1 Introduction

Over the past years, there has been a lot of research interest in the study of transport processes for nonlinear systems that can derive useful work from unbiased nonequilibrium thermal fluctuations^{1–3}. Brownian ratchets are such non-linear systems that can rectify unbiased thermal fluctuations and generate directed motion by breaking the spatial symmetry of the periodic potential as well as the principle of detailed balance of the system^{1,3–6}. Understanding the underlying mechanism of the ratchet effects are of great importance especially in the study of molecular motors in biological systems⁷⁻¹⁸ as well as the transport process in intracellular transport of cargo on microtubule networks¹⁹, transport of ion through nanopores²⁰, metastasis of cancer cells²¹, Josephson phase in super conductors^{22–24} and so on. Also, these spatially periodic ratchet systems exhibit various anomalous transport phenomena such as stochastic resonance²⁵, anomalous diffusion^{26–29}, absolute negative mobility^{30–37}, current reversal³⁸⁻⁴⁸ and so forth. Among these, absolute negative mobility (ANM) is a form of anomalous transport behaviour, in which the particle moves in the direction opposite to the external load. This transport phenomena relies on the coexistence of both nonequilibrium and nonlinearity and ANM cannot observe in a one-dimensional system without these two characteristics^{30,49}. ANM has been experimentally observed in instances such as current voltage properties of a Josephson-Junction device^{50,51}, negative absolute mobility in GaAs quantum wells⁵², absolute negative conductance in semi-conductor super lattices^{53,54}. The separation of particles is one possible technical applications based on ANM^{55–59}.

Mostly all these research studies focussed on the directed transport of particles in periodically smooth energy landscapes. However, it is well established that there are several instances where we can observe the existence of spatial heterogeneity in the potential such as in protein folding pathway^{60,61}, diffusion in structural glasses^{62,63}, supercooled liquids^{64,65}, gating of ion channels^{66,67}. So, it will be interesting to study the effects of spatial heterogeneity in the energy landscapes in the transport of Brownian ratchets. We studied the effect of roughness in the transport of inertially driven Brownian particles in the presence of Gaussian noise. There, we found that small amplitude of roughness enhances the transport of Brownian particle in the

weak noise limit in compared to smooth periodic potential⁶⁸ as well as we found a parameter regime where ANM is observed only due to the roughness in the periodic potential⁶⁹. In both these studies, we focused on the directed transport of a single inertially driven Brownian particle moving in a rough periodic potential. However, the interaction of the particles may also affect the directed transport of particles. So, in this chapter, we investigated how the spatial heterogeneity in the potential affects the transport characteristics of inertially driven interacting Brownian particles.

4.2 Model

We considered a set of n Brownian particles of identical mass M that interact among each other through harmonic interaction moving in a symmetric rough periodic potential, U(x), in the presence of an external load, F. The system is driven out of equilibrium by an unbiased time-periodic force, $A\cos(\Omega t)$, with an amplitude of, A, and angular frequency, Ω , which will break the principle of detailed balance of the system. The equation of motion of the system can be described by Langevin equation as

$$M\ddot{x}_i = -U'(x_i) + F + A\cos(\Omega t) - \Gamma \dot{x}_i + \xi_i(t) + \sum_{j \neq i} k(x_j - x_i). \tag{4.1}$$

Where i=1,2...,n. The dot and prime represents the derivative with respect to time (t) and co-ordinate (x_i) of the i-th particle, respectively. k, Γ, k_B, T corresponds to the strength of nearest-neighbour interaction between the particles, frictional coefficient, Boltzmann constant and temperature of the heat bath respectively. The thermal fluctuations, $\xi(t)$, are modeled by δ -correlated Gaussian white noise of zero mean, $\langle \xi_i(t) = 0 \rangle$, and it follows fluctuation-dissipation relation, $\langle \xi_i(t) \xi_j(t') \rangle = 2\Gamma k_B T \delta_{ij}(t-t')$.

The ratchet potential, U(x), is a combination of symmetric smooth, $U_0(x)$, and rough periodic potential, $U_1(x)$, as

$$U(x) = U_0(x) + U_1(x) (4.2)$$

The smooth symmetric periodic potential was taken³⁵ as

$$U_0(x) = -\Delta U \sin\left(\frac{2\pi}{L}x\right) \tag{4.3}$$

Where L is the period and ΔU is the barrier height. The rough potential $U_1(x)$ was chosen as and super imposed⁷⁰ with the smooth potential $U_0(x)$.

$$U_1(x) = \Delta U \,\varepsilon_0 \cos(\Lambda x) \tag{4.4}$$

Where ε_0 and Λ are the amplitude and periodicity of the rough potential, respectively. In order to reduce the number of variables, we nondimensionalized Eq. (4.1), and the dimensionless form of the motion equation is given as

$$\ddot{\hat{x}}_i = -\hat{U}'(\hat{x}_i) + f + a\cos(\omega \hat{t}) - \gamma \dot{\hat{x}}_i + \hat{\xi}_i(\hat{t}) + \sum_{i \neq i} \hat{k}(\hat{x}_i - \hat{x}_i)$$
(4.5)

Where $\hat{x} = \frac{2\pi x}{L}$, $\hat{t} = \frac{t}{\tau_0}$ and $\tau_0 = \frac{L}{2\pi} \sqrt{\frac{M}{\Delta U}}$. Other parameters are $a = \frac{AL}{2\pi\Delta U}$, $f = \frac{FL}{2\pi\Delta U}$, $\hat{k} = \frac{kL^2}{\Delta U}$, $\omega = \Omega \tau_0$, $Q = \frac{k_B T}{\Delta U}$, $\varepsilon = \frac{\varepsilon_0}{\Delta U}$, $\lambda = \frac{\Delta L}{2\pi}$, and $\gamma = \frac{\tau_0 \Gamma}{M}$. The rescaled thermal noise is $\hat{\xi}_i(\hat{t})(=(L/2\pi\Delta U)\xi_i(\tau_0\hat{t}))$ follows zero mean, $\langle \hat{\xi}_i(\hat{t}) \rangle = 0$ and rescaled fluctuation-dissipation relation of $\langle \hat{\xi}_i(\hat{t})\hat{\xi}_j(\hat{t}') \rangle = 2\gamma Q \delta_{ij}(t-t')$. The dimensionless potential is $\hat{U}(\hat{x}) = U((L/2\pi)x)/\Delta U$ and have the period $L = 2\pi$. The rescaled version of the entire potential is now given as

$$\widehat{U}(\widehat{x}) = -\sin(\widehat{x}) + \varepsilon \cos(\lambda \widehat{x}) \tag{4.6}$$

Where ε quantifies the amplitude of roughness in the periodic potential and we set the value of rescaled frequency of rough potential λ as 50 throughout the study. The symmetric rough periodic potential is presented in Fig. 4.1.

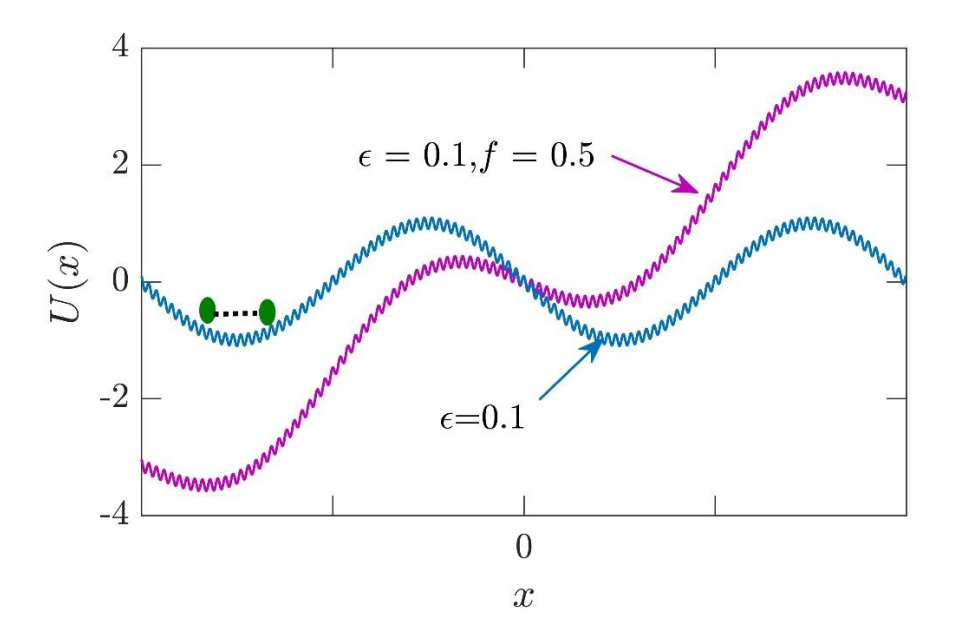


Fig. 4.1: Schematic representation of two interacting Brownian particles in rough symmetric potential.

We estimated the asymptotic ensemble average velocity⁷¹ $\langle v_i \rangle$ of the i-th particle to get an understanding on the effects of roughness in a symmetric periodic potential on the dynamical behavior of driven interacting Brownian particle in the presence of an external load.

$$\langle v_i \rangle = \lim_{t \to \infty} \langle \frac{x_i(t) - x_i(t_0)}{t - t_0} \rangle \tag{4.7}$$

Where t_0 is the initial time and the angular brackets represent averaging over an ensemble of initial position and velocities. Since the dynamics is ergodic, average velocity v_i is independent of initial position $x_i(0)$ as well as particular noise $\xi(t)$ realisation⁷². The particle-average asymptotic velocity $\overline{\langle v \rangle}$ was calculated as

$$\overline{\langle v \rangle} = \frac{1}{n} \sum_{i=1}^{n} \langle v_i \rangle \tag{4.8}$$

Where the overline denotes the averaging over the number of coupled particles. We numerically integrated the Langevin equation (Eq.(4.5)) using the second-order predictor-corrector method. The initial values of x(0) and $\dot{x}(0)$ were chosen randomly and sampled from uniform distributions over the intervals $[0,2\pi]$ and [-2,2], respectively. We used a relatively small step size $10^{-4} \times \frac{2\pi}{\omega}$ for the calculations due to the small frequency of the rough part of the periodic potential.

4.3 Results and Discussions

The dynamics of our chosen system is characterized by an eight-dimensional parameter space $(f, \gamma, a, \omega, Q, \varepsilon, k, n)$. According to earlier studies, the parameters play a significant role in determining the anomalous transport behaviour of similar systems with a smooth periodic potential^{73,74}.

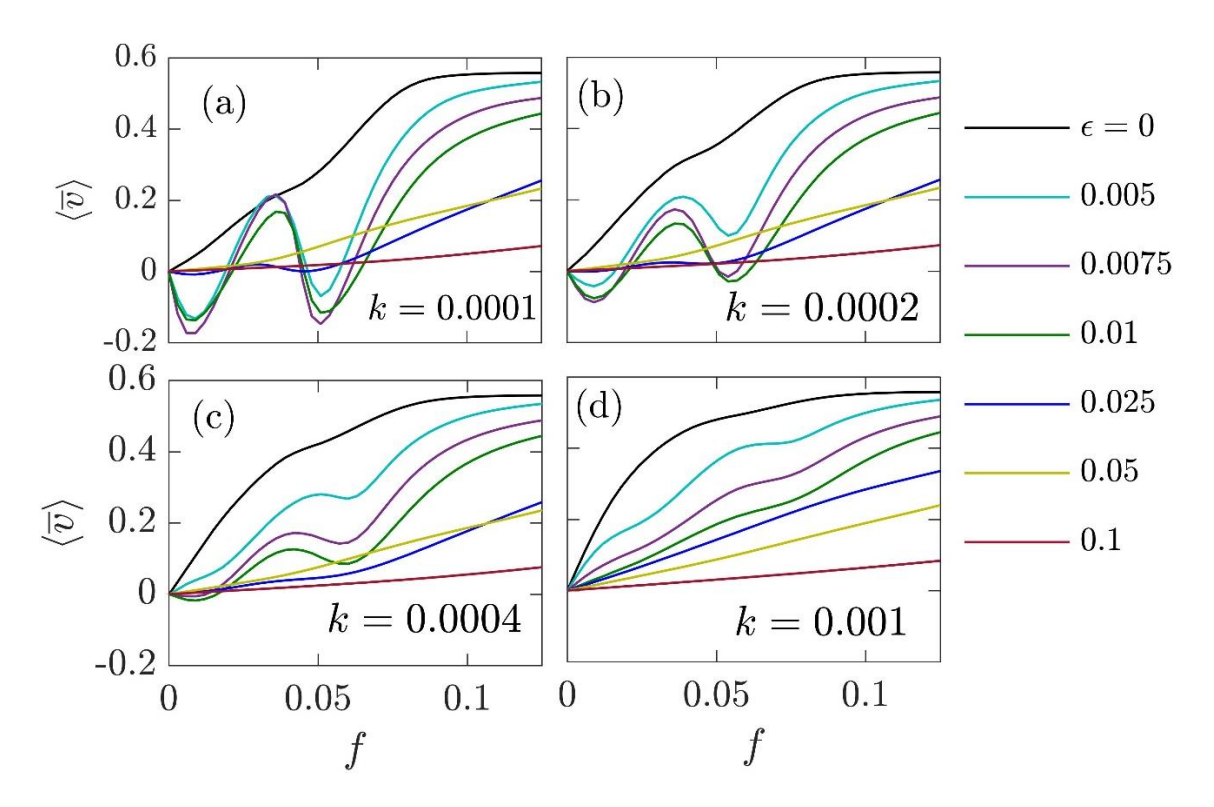


Fig. 4.2: Asymptotic average velocity $\overline{\langle v \rangle}$ vs. external load f at different values of interaction strength, k, and ε . The other parameters used in this calculation were Q=0.0004, a=1.589, $\omega=0.5580$, $\gamma=0.756$, and n=3.

Fig. 4.2 shows the dependence of particle average asymptotic velocity, $\overline{\langle v \rangle}$, on external load, f, for different strength of interaction, k, as well as for different roughness amplitude, ε , for three interacting particles (n=3). For the smooth periodic potential ($\varepsilon=0$), it is found that the particle average asymptotic velocity, $\overline{\langle v \rangle}$, has the same sign as the external load f, which is a characteristic feature of a normal transport behaviour, for every value of interaction strength k. However, the roughness in the periodic potential changes qualitative behaviour of the response of the system with respect to external load. For weak interaction between the Brownian particles with k=0.0001, the particles move opposite to the direction of external load for a range of roughness, (0.005-0.01). This is the clear signature of absolute negative mobility (ANM). It is also interesting to note that the particle changes the direction of current several times with increasing f in this regime of ε and such phenomena is called multiple current reversal. However in the regime of larger ε , the multiple current reversal start to disappear, and the system shows normal transport. Further the phenomena of multiple current reversal are limited in the regime of weakly interacting particles, as with increasing value of k the current reversals disappear. Therefore, it is concluded that particles having weak interaction

with small amplitude of roughness in the potential surface undergo multiple current reversal for a driven coupled inertial ratchet.

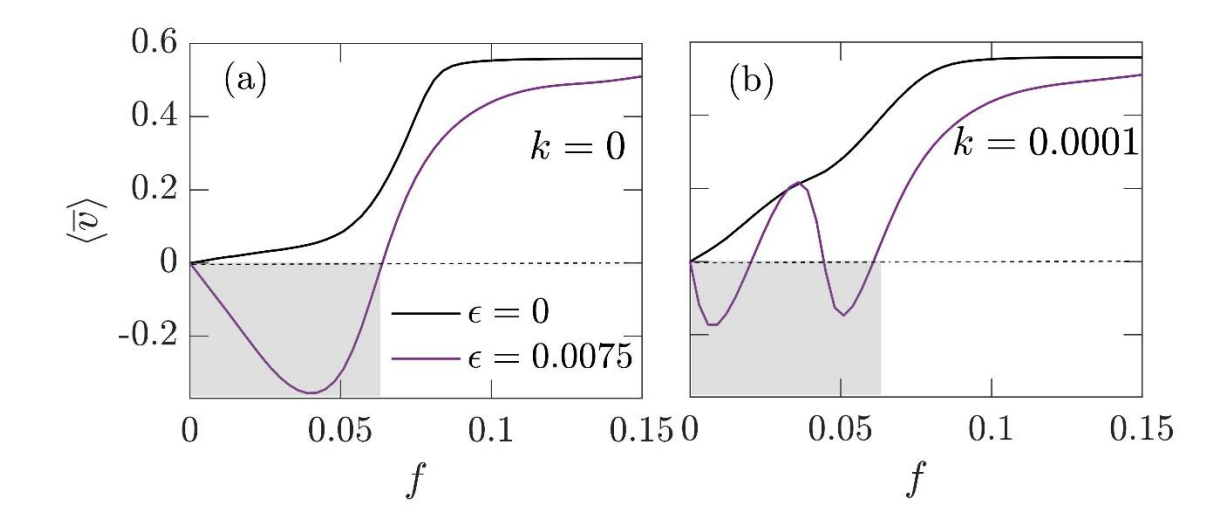


Fig. 4.3: Asymptotic average velocity $\langle v \rangle$ vs. f for smooth $\varepsilon = 0$ as well as rough $\varepsilon \neq 0$ periodic surface for both interacting $(k \neq 0)$ as well as noninteracting (k = 0) particles. The other parameters used in this calculation are Q = 0.0004, $\alpha = 1.589$, $\omega = 0.5580$, $\gamma = 0.756$ and $\alpha = 3$.

In order to establish the effect of particle-particle interaction and roughness on the transport properties, in Fig. 4.3 we compared $\overline{\langle v \rangle}$ vs. f plot for the system without (ε =0) and with (ε =0.0075) roughness for interacting ($k \neq 0$) as well as non-interacting (k = 0) particles. As shown in the previous chapters, there is a stark difference between the transport properties of the noninteracting particles with and without roughness. The roughness induces ANM for the noninteracting particles. On the contrary in the case of interacting particles, roughness leads to multiple current reversals. Therefore, small amplitude roughness in the potential can lead to nontrivial observations both in the noninteracting and interacting systems.

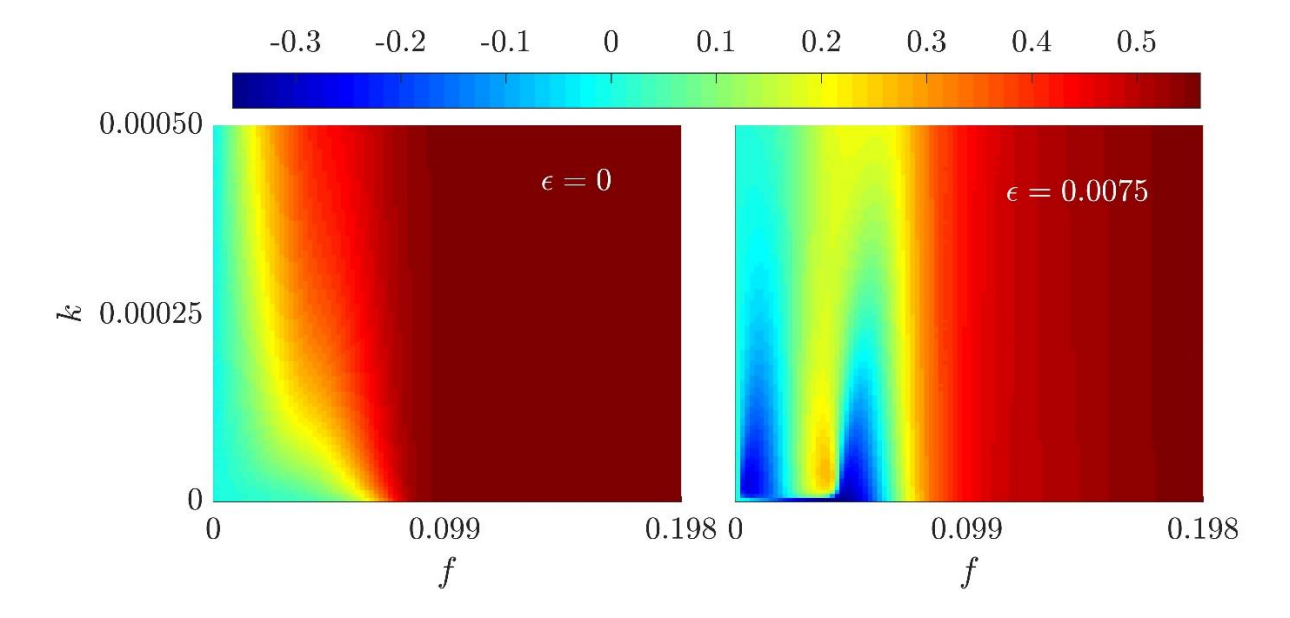


Fig4.4: The dependence of the interaction strength, k, on the transport characteristics of coupled inertial ratchet for smooth ($\varepsilon = 0$) (left) and rough periodic potential ($\varepsilon = 0.0075$) (right). The other parameters were Q = 0.0004, a = 1.589, $\omega = 0.5580$, $\gamma = 0.756$, and n = 3.

Results in the previous chapters have highlighted the importance of parameter space for ANM. With this anticipation for multiple current reversal for the interacting system under rough potential, we have probed the eight-dimensional parameter space, $(f, k, \gamma, a, \omega, Q, \varepsilon, n)$. We have performed two-dimensional parameter scanning in order to have a detailed study on the influence of each parameter on the transport behaviour. Fig. 4.4 presents the impact of interaction strength, k, on the transport characteristics of the driven coupled inertial ratchet under the smooth $(\varepsilon = 0)$ and rough $(\varepsilon = 0.0075)$ periodic potential. The coupled particles under smooth potential does not show any anomalous transport property across a range of values of k. On the contrary, the coupled particles under rough potential show multiple current reversals for large range of values of k. We extended similar two-dimensional scan of parameters with other parameters to determine the parameter dependence of multiple current reversals.

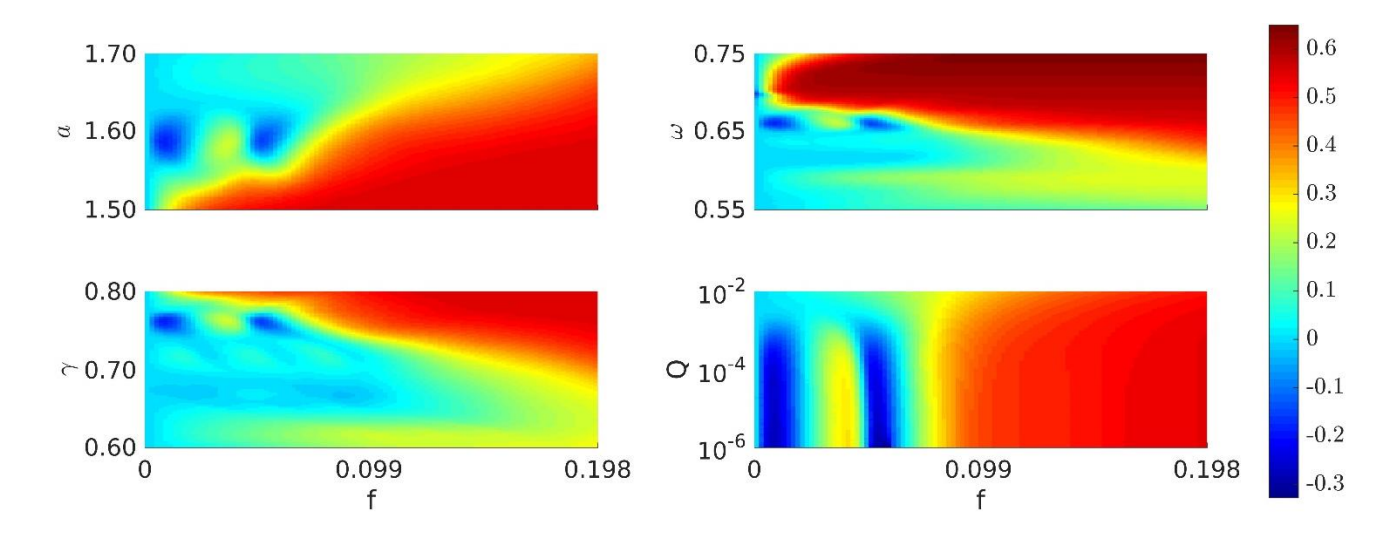


Fig. 4.5: Impact of amplitude (a) and frequency (ω) of driving force, dissipation constant (γ), and noise intensity (Q) on the multiple current reversals. The value of the parameters were $\varepsilon = 0.0075$, Q = 0.0004, k = 0.0001 and n = 3. The colour bar represents the magnitude of asymptotic velocity $\overline{\langle v \rangle}$.

In Fig. 4.5, we present the two-dimensional scans with respect to a, γ, ω and Q. These scans indicate that for small values of f, the disc-like structure indicates the negative velocity regions suggesting that multiple current reversals can be achieved for the coupled particles under rough potential. The narrow range of parameter values of a, γ and ω indicate that the multiple current reversal is highly sensitive to the choice of parameter values. Likewise, in all other parameters, the plot corresponds to the impact of noise intensity Q as a function of external load f, also shows multiple current reversal phenomenon in small range of f. However, the range of noise strength over which multiple current reversal can be observed is significantly large as compared to other parameters.

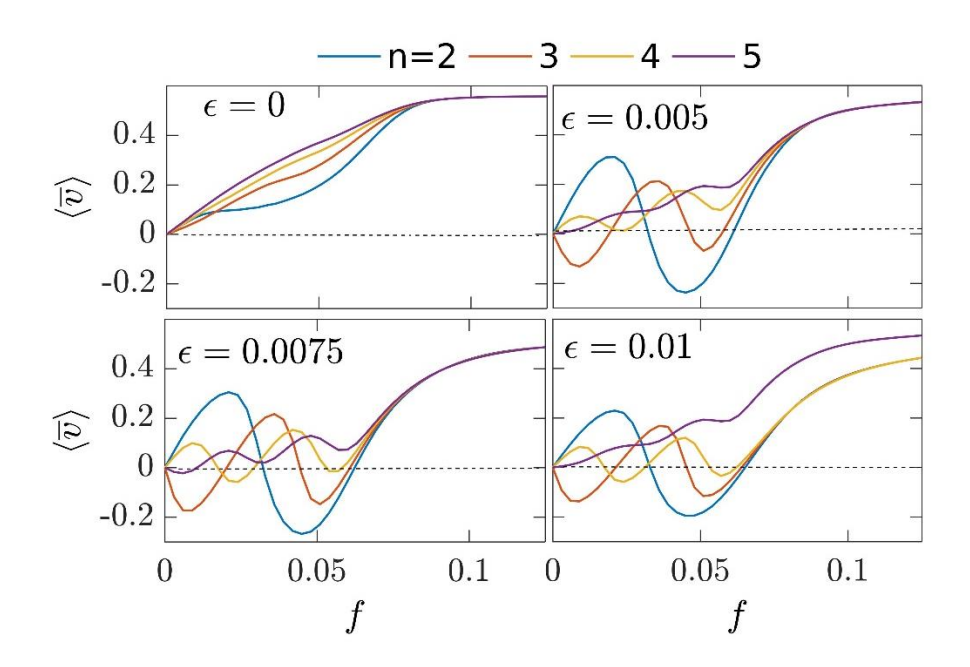


Fig. 4.6: Asymptotic average velocity $\langle v \rangle$ vs. external load f for smooth $\varepsilon = 0$ as well as rough $\varepsilon \neq 0$ periodic surface for bonding strength k = 0.0001 for different number of interacting particles, n.

To understand how does the number of interacting particles (n) affects the transport properties of the coupled inertial ratchet, we calculated the average asymptotic velocity $\langle v \rangle$ as a function of f for the indicated values of ε with the interaction strength k = 0.0001. As shown in the figure, in the absence of roughness ($\varepsilon = 0$), the direction of the transport is in accordance with the external load applied irrespective of the number of interacting particles. However, the presence of roughness in the periodic potential makes a drastic change in the transport behaviour of the system. The Brownian particles change its direction of transport with increasing f under roughness. A more striking feature is that the number of times the transport direction gets reversed is equal to the number of interacting particles, especially in the small range of roughness. For $\varepsilon = 0.005$, when there are two Brownian particles interacting, we can see one peak above and one peak below the zero velocity line which directs that two current reversals happened in that regime. We observed three current reversals for n=3 for the $\varepsilon=$ 0.005. This trend can be seen for n = 4 for $\varepsilon = 0.0075$. For higher amplitude of roughness, the multiple current reversal effect gradually disappears. This suggest that the reversal of the transport direction can be correlated with the presence of spatial heterogeneity in the periodic surface as well as the number of interacting particles.

4.4 Conclusion

In this chapter, we discussed how does the interaction between the driven Brownian particles moving in a rough periodic potential affects the directed transport properties. Here we considered, a model consisting of driven inertial Brownian particles interacting through harmonic potential moving in a rough symmetric periodic potential in the presence of external load. We numerically studied the average asymptotic velocity as a function of external load for interacting particles moving in a rough potential in order to have a detailed picture on the transport behaviour. We observed a normal transport behaviour for both interacting as well as non – interacting Brownian particles moving in a smooth periodic potential. We have shown the phenomenon of absolute negative mobility, where the particles are moving in a opposite direction of the external load applied, in the case, when the non-interacting Brownian particles are in a rough periodic potential. In the presence of interaction between the particles, we found a parameter regime where multiple current reversals are observed due to the spatial heterogeneity in the potential, in small range of external load. Also, especially in the case of weak interaction as well as the small amplitude of roughness, the number of times the transport direction gets reversed is equal to the number of interacting particles present in the system. We presented results showing that, it is possible to have multiple current reversals for interacting driven Brownian particles in the presence of roughness in under-damped dynamics.

4.5 Reference

- 1. Astumian, R. D. & Hänggi, P. Brownian motors. *Phys. Today* **55**, 33–39 (2002).
- 2. Reimann, P. Brownian motors: Noisy transport far from equilibrium. *Phys. Rep.* **361**, 57–265 (2002).
- 3. Hänggi, P., Marchesoni, F. & Nori, F. Brownian motors. *Ann. der Phys.* **14**, 51–70 (2005).
- 4. Hänggi, P. & Marchesoni, F. Artificial Brownian motors: Controlling transport on the nanoscale. *Rev. Mod. Phys.* **81**, 387–442 (2009).
- 5. Bier, M. Brownian ratchets in physics and biology. *Contemp. Phys.* **38**, 371–379 (1997).
- 6. Kula, J., Czernik, T. & Łuczka, J. Brownian ratchets: Transport controlled by thermal noise. *Phys. Rev. Lett.* **80**, 1377–1380 (1998).
- 7. Astumian, R. D. & Bier, M. Fluctuation driven ratchets: Molecular motors. *Phys. Rev. Lett.* **72**, 1766–1769 (1994).
- 8. Derényi, I. & Astumian, R. D. Brownian Ratchets and Their Application to Biological Transport Processes and Macromolecular Separation. *Struct. Dyn. Confin. Polym.* 281–294 (2002) doi:10.1007/978-94-010-0401-5_17.
- 9. Sauvage, J. P. From Chemical Topology to Molecular Machines (Nobel Lecture). *Angew. Chemie Int. Ed.* **56**, 11080–11093 (2017).
- 10. Davis, A. P. Synthetic molecular motors. *Nature* **401**, 120–121 (1999).
- 11. Gross, M. The unstoppable march of the machines. *Curr. Biol.* **25**, R255–R258 (2015).
- 12. Iino, R., Kinbara, K. & Bryant, Z. Introduction: Molecular Motors. *Chem. Rev.* **120**, 1–4 (2020).
- 13. Kolomeisky, A. B. & Fisher, M. E. Molecular motors: A theorist's perspective. *Annu. Rev. Phys. Chem.* **58**, 675–695 (2007).
- 14. Jülicher, F., Ajdari, A. & Prost, J. Modeling molecular motors. *Rev. Mod. Phys.* **69**, 1269–1281 (1997).

- 15. Hoffmann, P. M. How molecular motors extract order from chaos (a key issues review). *Reports Prog. Phys.* **79**, (2016).
- 16. Ait-Haddou, R. & Herzog, W. Brownian ratchet models of molecular motors. *Cell Biochem. Biophys.* **38**, 191–213 (2003).
- 17. Stoddart, J. F. Mechanically Interlocked Molecules (MIMs)—Molecular Shuttles, Switches, and Machines (Nobel Lecture). *Angew. Chemie Int. Ed.* **56**, 11094–11125 (2017).
- 18. Feringa, B. L. The Art of Building Small: From Molecular Switches to Motors (Nobel Lecture). *Angew. Chemie Int. Ed.* **56**, 11060–11078 (2017).
- 19. Bressloff, P. C. & Newby, J. M. Stochastic models of intracellular transport. *Rev. Mod. Phys.* **85**, 135–196 (2013).
- 20. Karnik, R., Duan, C., Castelino, K., Daiguji, H. & Majumdar, A. Rectification of ionic current in a nanofluidic diode. *Nano Lett.* **7**, 547–551 (2007).
- 21. Mahmud, G. *et al.* Directing cell motions on micropatterned ratchets. *Nat. Phys.* **5**, 606–612 (2009).
- 22. Zapata, I., Bartussek, R., Sols, F. & Hänggi, P. Voltage rectification by a squid ratchet. *Phys. Rev. Lett.* **77**, 2292–2295 (1996).
- 23. Goldobin, E., Sterck, A. & Koelle, D. Josephson vortex in a ratchet potential: Theory. *Phys. Rev. E Stat. Physics, Plasmas, Fluids, Relat. Interdiscip. Top.* **63**, 1–10 (2001).
- 24. Spiechowicz, J., Hänggi, P. & Łuczka, J. Josephson junction ratchet: The impact of finite capacitances. *Phys. Rev. B Condens. Matter Mater. Phys.* **90**, 1–11 (2014).
- Kawaguchi, M., Mino, H., Momose, K. & Durand, D. M. Stochastic resonance with a mixture of sub-and supra-threshold stimuli in a population of neuron models. *Proc. Annu. Int. Conf. IEEE Eng. Med. Biol. Soc. EMBS* 70, 7328–7331 (2011).
- 26. Metzler, R., Jeon, J. H., Cherstvy, A. G. & Barkai, E. Anomalous diffusion models and their properties: Non-stationarity, non-ergodicity, and ageing at the centenary of single particle tracking. *Phys. Chem. Chem. Phys.* **16**, 24128–24164 (2014).
- 27. Białas, K., Łuczka, J., Hänggi, P. & Spiechowicz, J. Colossal Brownian yet non-Gaussian diffusion induced by nonequilibrium noise. *Phys. Rev. E* **102**, 1–7 (2020).

- 28. Spiechowicz, J. & Łuczka, J. Subdiffusion via dynamical localization induced by thermal equilibrium fluctuations. *Sci. Rep.* **7**, 1–7 (2017).
- 29. Spiechowicz, J., Luczka, J. & Hänggi, P. Transient anomalous diffusion in periodic systems: Ergodicity, symmetry breaking and velocity relaxation. *Sci. Rep.* **6**, 1–11 (2016).
- 30. MacHura, L., Kostur, M., Talkner, P., Łuczka, J. & Hänggi, P. Absolute negative mobility induced by thermal equilibrium fluctuations. *Phys. Rev. Lett.* **98**, 1–4 (2007).
- 31. Li, J. jian, Xie, H. zhang, Li, T. C. & Ai, B. quan. Absolute negative mobility induced by fractional Gaussian noise. *Phys. A Stat. Mech. its Appl.* **560**, 125164 (2020).
- 32. Spiechowicz, J., Łuczka, J. & Hänggi, P. Absolute negative mobility induced by white Poissonian noise. *J. Stat. Mech. Theory Exp.* **2013**, (2013).
- 33. Eichhorn, R., Reimann, P. & Hänggi, P. Brownian Motion Exhibiting Absolute Negative Mobility. *Phys. Rev. Lett.* **88**, 4 (2002).
- 34. Spiechowicz, J., Hänggi, P. & Łuczka, J. Brownian motors in the microscale domain: Enhancement of efficiency by noise. *Phys. Rev. E Stat. Nonlinear, Soft Matter Phys.* **90**, 1–5 (2014).
- 35. Spiechowicz, J., Hänggi, P. & Łuczka, J. Coexistence of absolute negative mobility and anomalous diffusion. *New J. Phys.* **21**, (2019).
- 36. Eichhorn, R., Reimann, P. & Hänggi, P. Paradoxical motion of a single Brownian particle: Absolute negative mobility. *Phys. Rev. E Stat. Physics, Plasmas, Fluids, Relat. Interdiscip. Top.* **66**, 14 (2002).
- 37. Luo, Y., Zeng, C. & Ai, B. Q. Strong-chaos-caused negative mobility in a periodic substrate potential. *Phys. Rev. E* **102**, 1–14 (2020).
- 38. Alatriste, F. R. & Mateos, J. L. Anomalous mobility and current reversals in inertial deterministic ratchets. *Phys. A Stat. Mech. its Appl.* **384**, 223–229 (2007).
- 39. Mateos, J. L. Chaotic transport and current reversal in deterministic ratchets. *Phys. Rev. Lett.* **84**, 258–261 (2000).
- 40. Barbi, M. & Salerno, M. Phase locking effect and current reversals in deterministic underdamped ratchets. *Phys. Rev. E Stat. Physics, Plasmas, Fluids, Relat. Interdiscip.*

- *Top.* **62**, 1988–1994 (2000).
- 41. Hu, H. W. *et al.* Current reversal and particle separation in Brownian transport. *Phys. Rev. Res.* **3**, 1–13 (2021).
- 42. Arzola, A. V., Volke-Sepúlveda, K. & Mateos, J. L. Experimental control of transport and current reversals in a deterministic optical rocking ratchet. *Phys. Rev. Lett.* **106**, 20–23 (2011).
- 43. Schwemmer, C., Fringes, S., Duerig, U., Ryu, Y. K. & Knoll, A. W. Experimental Observation of Current Reversal in a Rocking Brownian Motor. *Phys. Rev. Lett.* **121**, 104102 (2018).
- 44. Cai, C. C., Liu, J. L., Chen, H. & Li, F. G. Current Reversals of an Underdamped Brownian Particle in an Asymmetric Deformable Potential. *Commun. Theor. Phys.* **69**, 266–270 (2018).
- 45. Chen, R., Zhang, G., Wang, C., Nie, L. & Chen, C. Current reversal in a symmetric periodic potential. *Chaos, Solitons and Fractals* **98**, 205–209 (2017).
- 46. Zeng, C., Wang, H. & Nie, L. Multiple current reversals and diffusion enhancement in a symmetrical periodic potential. *Chaos* **22**, (2012).
- 47. Yang, B., Long, F. & Mei, D. C. Negative mobility and multiple current reversals induced by colored thermal fluctuation in an asymmetric periodic potential. *Eur. Phys. J. B* **85**, 2–7 (2012).
- 48. Sintes, T. & Sumithra, K. Optimal efficiency condition and current reversals in forced underdamped ratchets. *Phys. A Stat. Mech. its Appl.* **312**, 86–98 (2002).
- 49. Speer, D., Eichhorn, R. & Reimann, P. Transient chaos induces anomalous transport properties of an underdamped Brownian particle. *Phys. Rev. E Stat. Nonlinear, Soft Matter Phys.* **76**, 1–14 (2007).
- 50. Kostur, M., Machura, L., Talkner, P., Hänggi, P. & Łuczka, J. Anomalous transport in biased ac-driven Josephson junctions: Negative conductances. *Phys. Rev. B Condens. Matter Mater. Phys.* **77**, 1–8 (2008).
- 51. Nagel, J. *et al.* Observation of negative absolute resistance in a Josephson junction. *Phys. Rev. Lett.* **100**, 1–4 (2008).

- 52. Höpfel, R. A., Shah, J., Wolff, P. A. & Gossard, A. C. Negative absolute mobility of minority electrons in GaAs quantum wells. *Phys. Rev. Lett.* **56**, 2736–2739 (1986).
- 53. Keay, B. J. *et al.* Dynamic localization, absolute negative conductance, and stimulated, multiphoton emission in sequential resonant tunneling semiconductor superlattices. *Phys. Rev. Lett.* **75**, 4102–4105 (1995).
- 54. Cannon, E. H., Kusmartsev, F. V., Alekseev, K. N. & Campbell, D. K. Absolute negative conductivity and spontaneous current generation in semiconductor superlattices with hot electrons. *Phys. Rev. Lett.* **85**, 1302–1305 (2000).
- 55. Malgaretti, P., Pagonabarraga, I. & Rubi, J. M. Entropic electrokinetics: Recirculation, particle separation, and negative mobility. *Phys. Rev. Lett.* **113**, 1–5 (2014).
- 56. Słapik, A., Łuczka, J. & Spiechowicz, J. Temperature-Induced Tunable Particle Separation. *Phys. Rev. Appl.* **12**, 1 (2019).
- 57. Słapik, A., Łuczka, J., Hänggi, P. & Spiechowicz, J. Tunable Mass Separation via Negative Mobility. *Phys. Rev. Lett.* **122**, 3–7 (2019).
- 58. Eichhorn, R., Regtmeier, J., Anselmetti, D. & Reimann, P. Negative mobility and sorting of colloidal particles. *Soft Matter* **6**, 1858–1862 (2010).
- 59. De Souza Silva, C. C., Van De Vondel, J., Morelle, M. & Moshchalkov, V. V. Controlled multiple reversals of a ratchet effect. *Nature* **440**, 651–654 (2006).
- 60. Ansari, A. *et al.* Protein states and proteinquakes. *Proc. Natl. Acad. Sci. U. S. A.* **82**, 5000–5004 (1985).
- 61. Frauenfelder, H., Sligar, S. G. & Wolynes, P. G. The energy landscapes and motions of proteins. *Science* (80-.). **254**, 1598–1603 (1991).
- 62. Charbonneau, P., Kurchan, J., Parisi, G., Urbani, P. & Zamponi, F. Fractal free energy landscapes in structural glasses. *Nat. Commun.* **5**, 1–6 (2014).
- 63. Heuer, A. Exploring the potential energy landscape of glass-forming systems: From inherent structures via metabasins to macroscopic transport. *J. Phys. Condens. Matter* **20**, (2008).
- 64. Debenedetti, P. G. & Stillinger, F. H. Review article Supercooled liquids and the glass transition. *Nature* **410**, 259 (2001).

- 65. Heuer, A., Doliwa, B. & Saksaengwijit, A. Potential-energy landscape of a supercooled liquid and its resemblance to a collection of traps. *Phys. Rev. E Stat. Nonlinear, Soft Matter Phys.* **72**, 1–13 (2005).
- 66. Delemotte, L., Kasimova, M. A., Klein, M. L., Tarek, M. & Carnevale, V. Free-energy landscape of ion-channel voltage-sensor-domain activation. *Proc. Natl. Acad. Sci. U. S. A.* 112, 124–129 (2015).
- 67. Linder, T., de Groot, B. L. & Stary-Weinzinger, A. Probing the Energy Landscape of Activation Gating of the Bacterial Potassium Channel KcsA. *PLoS Comput. Biol.* **9**, 1–9 (2013).
- 68. Archana, G. R. & Barik, D. Roughness in the periodic potential enhances transport in a driven inertial ratchet. *Phys. Rev. E* **104**, 1–8 (2021).
- 69. Archana, G. R. & Barik, D. Roughness in the periodic potential induces absolute negative mobility in a driven Brownian ratchet. *Phys. Rev. E* **106**, 1–8 (2022).
- 70. Zwanzig, R. Diffusion in a rough potential. *Proc. Natl. Acad. Sci. U. S. A.* **85**, 2029–2030 (1988).
- 71. Ou, Y. L., Hu, C. T., Wu, J. C. & Ai, B. Q. Absolute negative mobility of interacting Brownian particles. *Phys. A Stat. Mech. its Appl.* **439**, 1–6 (2015).
- 72. Speer, D., Eichhorn, R. & Reimann, P. Brownian motion: Anomalous response due to noisy chaos. *Epl* **79**, (2007).
- 73. Słapik, A., Łuczka, J. & Spiechowicz, J. Negative mobility of a Brownian particle: Strong damping regime. *Commun. Nonlinear Sci. Numer. Simul.* **55**, 316–325 (2018).
- 74. Wiśniewski, M. & Spiechowicz, J. Anomalous transport in driven periodic systems: Distribution of the absolute negative mobility effect in the parameter space. *New J. Phys.* **24**, (2022).

CHAPTER 5

Investigation of divergence of thermal conductivity in a momentumconserving one-dimensional lattice with asymmetric double-well potential

5.1 Introduction

Since decades, numerous studies have focused on the heat conduction in low-dimensional systems 1-10. Studying heat conduction in low dimensional systems, helps to understand the macroscopic law of heat conduction (Fourier's law) in its microscopic basis. Fourier law of heat conduction relates the heat flux, J, to the local temperature, ∇T , gradient as $J = -\kappa \nabla T$, where κ is the thermal conductivity, and it is considered as an intrinsic property of the material. Under a given temperature difference, the Fourier's law predicts that I scales as $I \propto N^{-1}$ with increasing system size, N,. According to Fourier's law, thermal conductivity is an intrinsic property of the system and it does not depend on the system size. In the lattice models of onedimensional chain of N particles connected through non-linear interaction potentials, the thermal conductivity κ has been numerically found to diverge with N following a power-law scaling as $\kappa \propto N^{\alpha}$. There the heat flux scales as $I \sim N^{\alpha-1}$. Divergence exponent, α , lies in the range between 0.33 and 0.5 for different forms of Fermi-Pasta-Ulam (FPU) interaction potentials. The divergent exponent values differ from system to system and with the choice of parameters. Overall, the thermal conductivity is size dependent and the heat conduction will be anomalous heat conduction 11-13. It has been a long-standing outstanding issue to find a microscopic lattice Hamiltonian that exhibits diffusive normal heat conduction which satisfies Fourier's law^{11,12}.

Experimental realisation of divergent thermal conductivity in low dimensional systems have been observed for one dimensional nanotubes 14,15 and two dimensional graphene 16 . In contrast to the momentum-conserving FPU-lattices, non-linear one-dimensional lattices without momentum-conservation such as Frenkel-Kontrova lattice and ϕ^4 lattice, show normal heat conduction $^{17-20}$. Likewise, momentum conserving lattice chains with asymmetric potential such as Lennard-Jones, Morse potential which allow bond dissociation were shown to follow convergent thermal conductivity $^{21-23}$. Moreover, finite thermal conductivity has been reported in momentum-conserving systems with an asymmetric interaction potential 24 . This finding was in contrast to established theoretical and numerical findings in one-dimensional momentum conservation systems that has been known for diverging conductivity. Das et al. 25 examined

the notion of strong low-temperature finite-size effects and challenged the prediction of normal thermal conductivity for an asymmetric lattice in 1D at low temperatures. Further, N dependence of α for single-well FPU lattices with asymmetric interparticle interactions in one-dimension was also estimated by Wang et al. using the equilibrium Green- Kubo approach of heat current autocorrelation²⁶. Here, on comparison with lattices with asymmetric interparticle interactions with the asymmetric FPU-lattice, α approaches its asymptotic thermodynamic limit at a considerably longer chain length N. Thus, α becomes a function of N at lower length scales. The dependency of chain length with the divergent exponent can also be affected with the temperature of the heat bath as well as the potential parameters. In symmetric double well potential, thermal conductivity diverged with divergence exponent $\alpha = 0.33$ at high temperature and weak divergence was observed for low temperature²⁷. In FPU- $\alpha\beta$ lattice also, two different temperature scaling observed as $\alpha = 0.4$ at higher temperature and α diverges weakly at low temperature²¹. So, additional systematic research was required to better understand the temperature-dependent divergence in an asymmetric momentum-conserving lattice.

In this chapter, we investigated the temperature dependent divergence of thermal conductivity in one-dimensional momentum conserving nonlinear lattice with an asymmetric double-well nearest-neighbour interaction potential. Using the non-equilibrium simulation method, we calculated the thermal conductivity κ for different lattice sizes N by varying heat bath temperature for different degree of asymmetry in the interaction potential. Our goal was to determine the temperature dependence of the scaling exponent for momentum conserving one-dimensional systems.

5.2 Model

The system considered is a one-dimensional lattice with a nearest-neighbour interaction potential, whose Hamiltonian can be represented as

$$H = \sum_{i=1}^{N} \frac{p_i^2}{2m} + \sum_{i=1}^{N-1} V(x_i - x_{i-1})$$
(5.1)

Where x_i is the displacement of the i^{th} particle from its equilibrium position and p_i is the momentum of the i^{th} particle. The mass m was taken as unity and total number of particles on the lattice chain is given by N. $V(x_i - x_{i-1})$ is the nearest-neighbour interaction between the two adjacent particles. Without on-site potential, the lattice becomes momentum conserving

lattice. The nearest-neighbour interaction potential chosen for the sudy belongs to the general class of the FPU- $\alpha\beta$ potential as

$$V(x) = -\frac{1}{2}k_2x^2 + \frac{1}{3}k_3x^3 + \frac{1}{4}k_4x^4$$
 (5.2)

Where k_2 , k_3 , and k_4 are three positive constants and we chose the values of $k_2 = 0.1$ and $k_4 = 0.002$. The potential becomes asymmetric $[V(x) \neq V(-x)]$ because of the cubic nonlinearity. We show the asymmetry of the double well potential in Fig.5.1 for two different values of the k_3 , which determines the asymmetry of the potential.

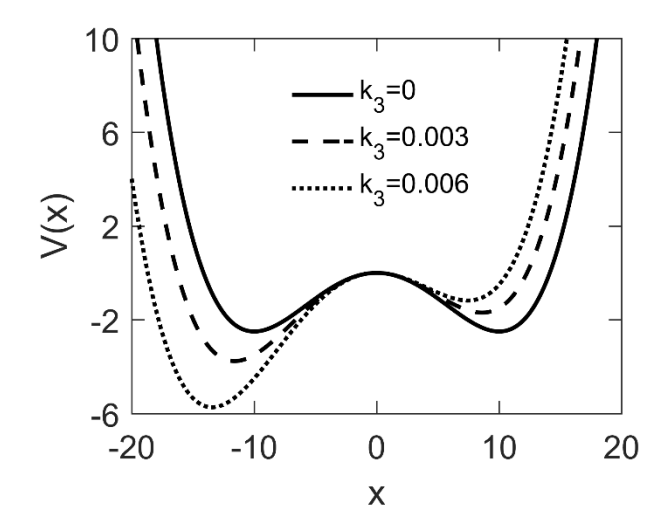


Fig. 5.1: Schematic representation of the double-well nearest-neighbour interaction potential, V(x), with different values of asymmetric parameter k_3 . The values of two other parameter were $k_2 = 0.1$ and $k_4 = 0.002$.

Both ends of the lattice chain are coupled to Langevin heat baths that have differ temperatures The equation of motion of the ith particle in the chain is given by

$$\ddot{x}_i = k_2 (2x_i - x_{i+1} - x_{i-1}) - k_3 [(x_i - x_{i-1})^2 - (x_{i+1} - x_i)^2] - k_4 [(x_i - x_{i-1})^3 - (x_{i+1} - x_i)^3] - \gamma_i \dot{x}_i + \eta_i$$
(5.3)

Where the fluctuation (η_i) and dissipation (γ_i) terms are defined as $\eta_i = \eta_L \delta_{i,1} + \eta_R \delta_{i,N}$ and $\gamma_i = \gamma \left(\delta_{i,1} + \delta_{i,N}\right)$, respectively. η_L and η_R are the thermal noise corresponding to the left and right heat baths, respectively. The heat baths are characterized by the fluctuation-dissipation relation followed by the two Markovian heat baths, $\langle \eta_L(t) \eta_L(t') \rangle = 2\gamma k_B T_L \delta(t-t')$ and $\langle \eta_R(t) \eta_R(t') \rangle = 2\gamma k_B T_R \delta(t-t')$. The k_B, γ, T_L , and T_R are the Boltzmann constant,

dissipation constant, temperature of the left and right heat bath, respectively. The value of γ and k_B were chosen as unity in the whole study. We changed the left and right bath temperatures (T_L and T_R), in order to study the effect of temperature on the divergence of thermal conductivity. Temperature difference and average temperature is defined as $\Delta T = T_L - T_R$ and $T = (T_L + T_R)/2$, respectively.

The instantaneous local heat current between i^{th} and $(i+1)^{th}$ particle is calculated as

$$j_i = \frac{1}{2} (\dot{x}_i + \dot{x}_{i+1}) \frac{\partial H}{\partial x_i}$$
 (5.4)

The time-averaged local heat current can be quantified as

$$J_i = \lim_{t \to \infty} \frac{1}{t} \int_0^t j_i(\tau) d\tau \tag{5.5}$$

At non equilibrium stationary state, global heat current is defined as

$$J = \sum_{i=1}^{N-1} \frac{J_i}{N-1} \tag{5.6}$$

The thermal conductivity with steady state global heat current is defined as

$$\kappa = \frac{JN}{\Delta T} \tag{5.7}$$

To investigate the heat conduction in one-dimensional lattice with asymmetric double-well interaction potential, we simulate the equations of motion (Eq. (5.3)) by integrating them using 4th order Runge-Kutta method with a step length of 0.01. We typically ran our simulations until the system reach the equilibrium ensuring steady heat current along the chain. We used fixed boundary condition $x_0 = x_{N+1} = 0$ in our studies. Earlier studies^{25,28} underlined the significance of boundary conditions in the heat conduction in lattice models. We use equations, Eq.(5.4) to Eq.(5.6) to calculate the local heat current and thereby thermal conductivity. We calculated thermal conductivity for various chain lengths ranging from N = 20 to N = 50000.

5.3 Results and discussions

We first examine the divergence of thermal conductivity for the asymmetric potential with various average heat bath temperatures, while keeping the temperature difference of two heat bath ΔT fixed for the asymmetric parameter $k_3 = 0.003$ as well varied ΔT for $k_3 = 0.006$ (Fig. 5.2).

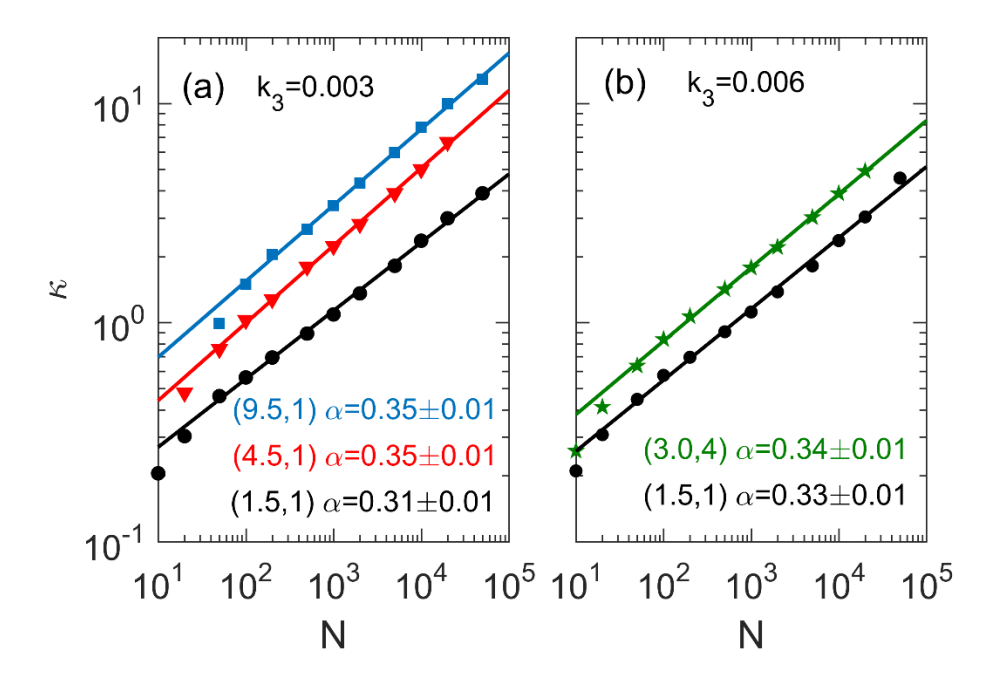


Fig. 5.2: Divergence of thermal conductivity, κ , as a function of chain length, N. Different colored symbols represent simulations with different average bath temperatures with fixed temperature difference, $(T, \Delta T)$; circle: (1.5,1), triangle: (4.5,1), square: (9.5,1), and star: (3.0,4). Solid lines are from power-law fitting $(\kappa \sim N^{\alpha})$. The values of α are indicated inside the plots for (a) $k_3 = 0.003$ and (b) $k_3 = 0.006$.

We have chosen $(T, \Delta T)$ pairs for $k_3 = 0.003$ were (9.5,1.0); (4.5,1.0); (1.5,1.0) and for $k_3 = 0.006$, $(T, \Delta T)$ were (3.0,4) and (1.5,1). In the case of $k_3 = 0.003$ (Fig. 5.2(a)), the thermal conductivity of the system displays power-law divergence, with the divergence exponent lying in the range of 0.31 - 0.35. These simulation results are consistent with the $\alpha = 1/3$ that has been suggested by renormalization group theory, mode coupling theory, and other numerical simulations^{8,27,29-31}. We observed a similar divergence of thermal conductivity for the same system with larger asymmetry ($k_3 = 0.006$) in the interaction potential [Fig. 5.2(b)]. The fact that the system's average temperature is high is a key characteristic of these divergence tendencies. Thus, the asymmetric-double well -momentum-conserving system thus exhibits behaviour that is comparable to that of the symmetric-FPU-momentum-conserving system at the high temperature limit.

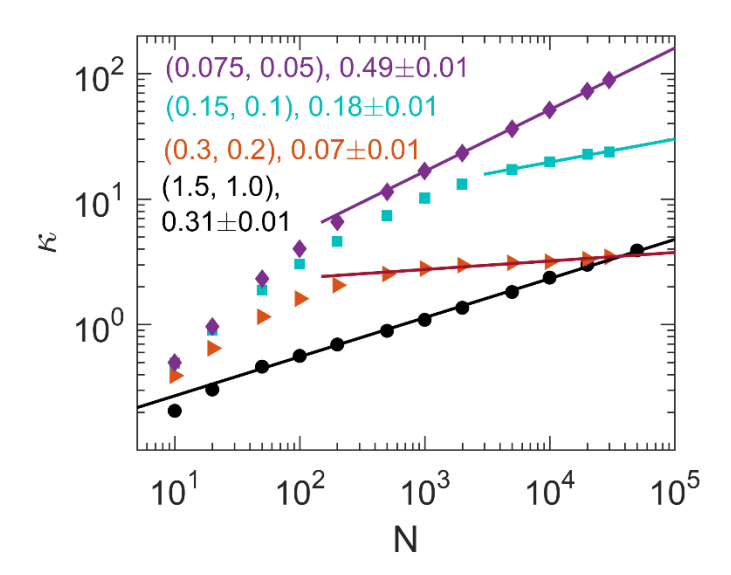


Fig. 5.3: Divergence of κ as a function of N for different average T and ΔT ; circle: (1.5,1), triangle: (0.3,0.2), square: (0.15,0.1), and diamond: (0.075,0.05). The asymmetric parameter k_3 was 0.003. The divergence exponent α values are indicated the plot.

By modifying the heat bath temperatures T_L and T_R, we next studied at the divergence of thermal conductivity for a range of average temperature values in the intermediate to low temperature range. The divergence of thermal conductivity κ at various system average temperatures T with asymmetric parameter $k_3 = 0.003$ is depicted in Fig. 5.3. From Fig. 5.3, it was observed that the divergence of thermal conductivity depends on the heat bath properties for different average temperature values. At extremely low temperature (T = 0.075), the conductivity significantly diverged with $\alpha = 0.49$. When the temperature is raised (T = 0.15), the divergence becomes small ($\alpha = 0.18$), and when temperature is raised further (T = 0.3), the thermal conductivity seems to saturate ($\alpha = 0.07$). When the temperature is high (T = 1.5), thermal conductivity κ displays its typical divergence behaviour, with = 0.31. The two distinct scaling tendencies of κ at extremely low ($\alpha = 0.49$) and very high ($\alpha = 0.31$) temperatures are the most notable aspect of the temperature-dependent thermal conductivity in this study. Additionally, the very small divergence of thermal conductivity κ (or saturation of with lattice size N) in the intermediate temperature raises the chance that Fourier's law may still be true. Additionally, in line with other findings^{21,25}, we also notice a weak divergence with fixed boundary conditions, despite the fact that fixed boundary conditions in the lattice does not facilitate thermal expansion. Usually, chains with lattices with fixed boundary conditions allows thermal expansion, and can have normal thermal conductivity due to the phonon scatterings in the lattice. Zhong et al. ²⁴ previously observed a similar saturation of thermal

conductivity κ with lattice size N in an asymmetric lattice and suggested that the system obeys Fourier's law. The question of whether the saturation in an asymmetric FPU- $\alpha\beta$ potential was actually caused by the asymmetry of the interaction potential or not was further addressed ^{25,26}.

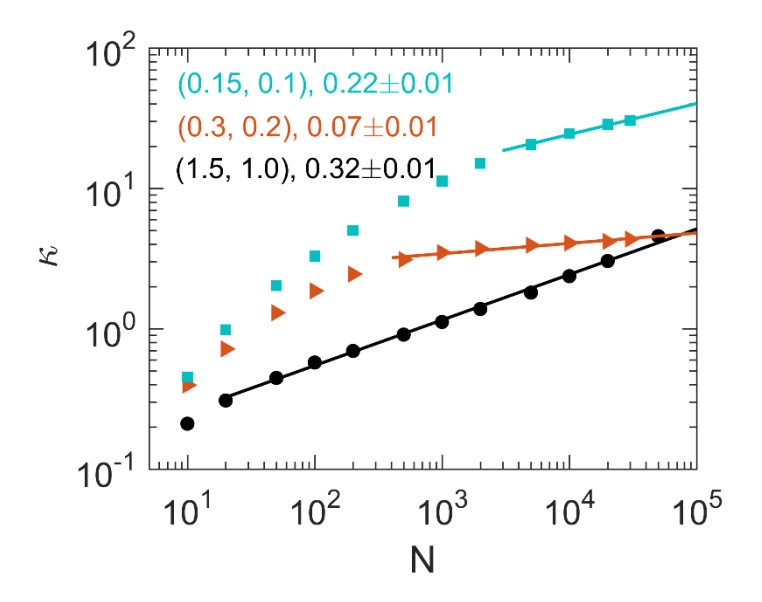


Fig. 5.4: Divergence of κ as a function of N for different average T and ΔT ; circle: (1.5,1), triangle:(0.3,0.2), square:(0.15,0.1). The asymmetric parameter k_3 was 0.006. The divergence exponent α values are indicated the plot.

Similar results were obtained by repeating the computations with a larger asymmetric parameter $k_3 = 0.0006$ (Fig. 5.4). Hence, according to the results of our simulation, divergence exponent α values in the asymmetric double-well interaction potential depend on the system's temperature.

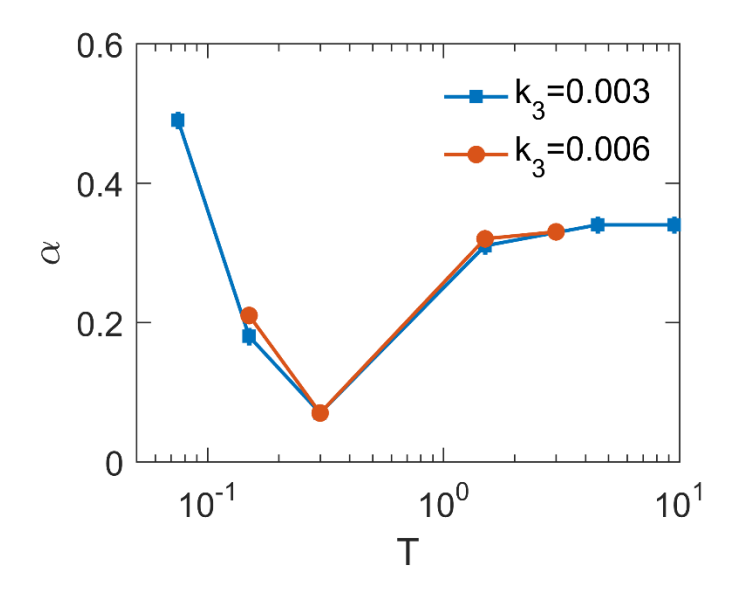


Fig. 5.5: Temperature dependence of α for two different values of asymmetric parameter k_3 . The sizes of error bars on α are nearly the same as the sizes of the markers.

We showed the divergence exponent α as a function of temperature T for two distinct values of the asymmetric parameter k_3 to establish the temperature dependence of the divergence exponent (Fig. 5.5). As the temperature T rises, α drops considerably and, after going through a minimum, it rises to saturate with $\alpha = 0.35$ at higher temperature. Both for low and high asymmetries of the potential, the intermediate temperature shows the smallest divergence of α . According to recent reports^{32,33}, the 1D anharmonic chain exhibits this kind of turnover behaviour. The divergence behaviours of thermal conductivity for two asymmetry values $(k_3=0.0003)$ and $k_3=0.0006$ are the same, as shown in Fig. 5.5. Since the two curves for different asymmetric parameter are crossing over one another, the saturation of thermal conductivity in this system is not an asymmetry induced effect. If so, higher asymmetry would have led to saturation at lower number of particles on the lattice chain N as opposed to lower asymmetry. There is no evidence of any such asymmetry-induced early saturation of thermal conductivity in the comparison of divergence of κ with N profiles for higher and lower asymmetry at different temperatures (Fig. 5.6).

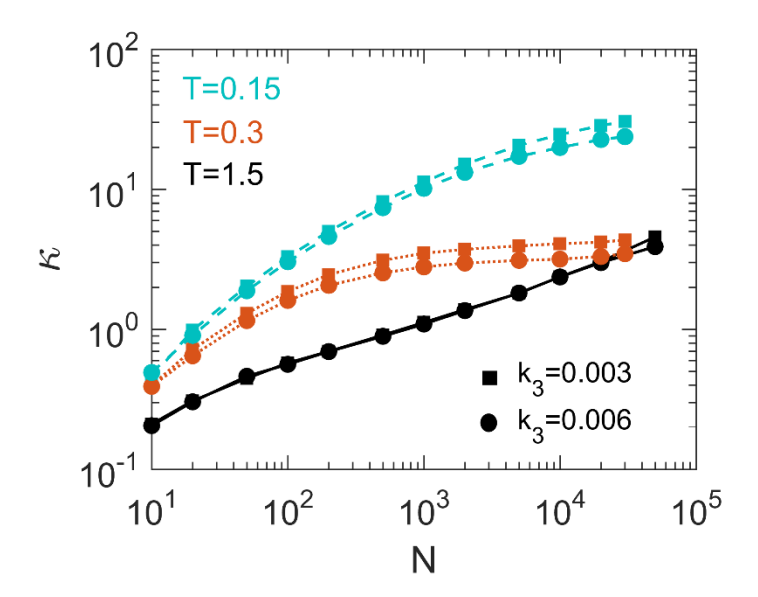


Fig 5.6: Comparison of the divergence of κ with N for different values of asymmetric parameter k_3 at various average bath temperatures, T. Solid line: T = 1.5, dotted line: T = 0.3, and dashed line: T = 0.15.

These findings suggest that the saturation of thermal conductivity κ may be a finite length effect which occurs only at intermediate temperature T. Our observations based on these studies, shows that the nature of the divergence is in fact temperature dependent.

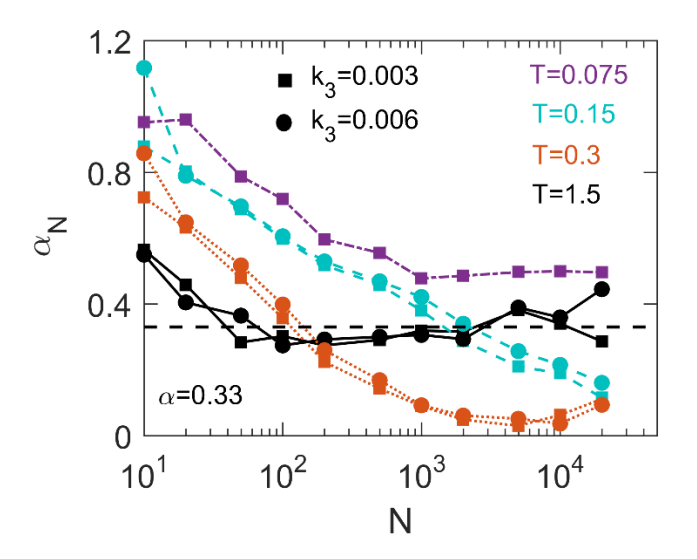


Fig. 5.7: Plot of local divergence exponent α_N with N for different values of asymmetric parameter k_3 and at different average bath temperature, T. The α_N was estimated by calculating the local slope of κ vs. N plots given in Fig. 5.3 and 5.4. Solid line: T=1.5, dotted line: T=1.5

0.3, dashed line: T = 0.15, and dashed-dot line: T = 0.075. The horizontal dashed line represents $\alpha = 0.33$.

We estimated the local divergence coefficient, α_N , by calculating out the local slope in the κ vs. N line in order to figure out the finite-size effect on. We plotted the local divergence coefficient, α_N as a function of lattice size N for different temperatures T with two asymmetric parameter k_3 . The well-known thermodynamic limit of 0.33 is reached at the shorter length of the chain for high temperature (T = 1.5), and α_N , settles closely with that value for a larger lattice chain length N. The local divergence coefficient α_N , settles to $\alpha \sim 0.5$ for very low temperature T = 0.075. This shows the two entirely different scaling nature of the system which indeed depends on the temperature of the system. In contrast, at intermediate temperature T = 0.075, as lattice size increases N, local divergence coefficient decreases below the thermodynamic limit (Fig. 5.7: dashed line $\alpha = 0.33$) and after moving through a minimum, it exhibits upward tendency for both the values of k_3 . For T = 0.15, same trend was observed, but the minimum was absent since it was likely placed at a larger chain length N. From this observations, we can conclude that at intermediate temperature, the values of divergence exponent α are not from the thermodynamic limit, since those values does not settle to a specific value.

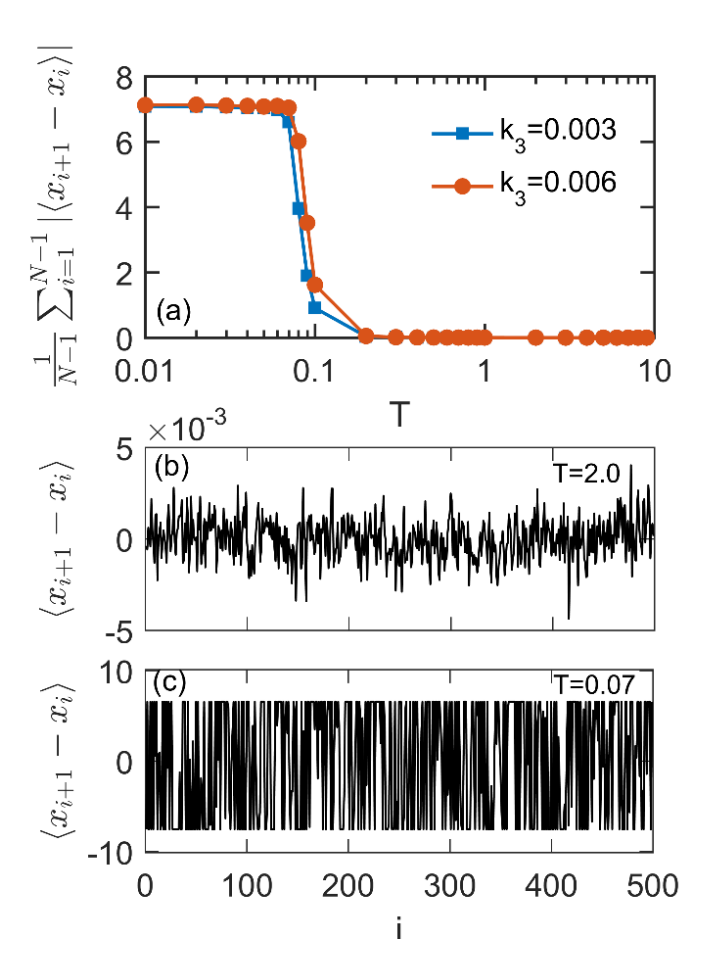


Fig. 5.8: (a) Temperature dependence of the order parameter for a chain with N = 500. The average displacement from the adjacent particle along the chain at T = 2.0 (b) and T = 0.07 (c).

Our chosen lattice system differs slightly from a typical FPU class of single-well interaction potentials due to the double well interaction potential's two wells separated by a barrier. The system will be able to hop between the two wells at the high temperature domain because of the increased thermal noise from the heat baths. But at low temperature domain, the system will be confined in one of the wells, based on the system's initial state. We computed an order parameter $\frac{1}{N-1}\sum_{i=1}^{N-1}|\langle x_{i+1}-x_i\rangle|^{33}$ for two values of the asymmetry parameter k_3 at various temperatures in order to evaluate the system's dynamic behaviour in relation to temperature [Fig. 5.8(a)]. Essentially, this order parameter is the equilibrium average of the absolute displacement from the next particle. We observe that at low and high temperatures, the value of the order parameter saturates into two separate domains, showing the system's temperature-dependent different nature. The asymmetry parameter k_3 has no impact on the order parameter's qualitative approach.

In addition, we plotted the ensemble averaged displacement $\langle x_{i+1} - x_i \rangle$ of the next particle of a lattice chain with N = 500 at high [Fig. 5. 8(b)] and low [Fig. 5.8(c)] temperatures. These two figures reflect a dichotomous dynamical nature for the lattice with double well potential as the nearest neighbouring interaction potential. At low temperature, the system is clearly contained within the two wells and at higher temperature, the fluctuations are more or less homogeneous. As a result, the qualitative differences between the system at low and high temperatures account for our observed temperature-dependent divergence features of thermal conductivity.

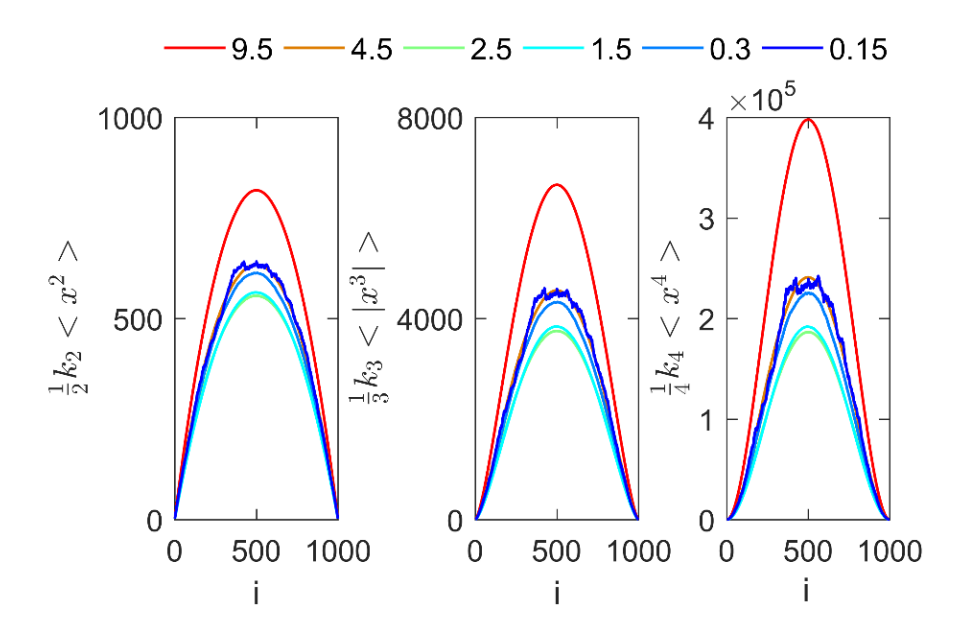


Fig. 5.9: Absolute average contributions of second, third, and fourth order terms in the potential for a chain with N = 1000 and $k_3 = 0.003$. The values of temperature are indicated at the top of the figure. The system behaves similarly with k_3 =0.006 as well.

The coefficients k_2 , k_3 , and k_4 in the potential (eq. 5.2) were chosen to have values in the range of 1-2 in earlier investigations of the thermal conductivity of nonlinear lattice with double well or FPU- interaction potential 21,26,27,33 . We used smaller set of k_2 , k_3 , and k_4 values in our computations than the previously reported ones. The values chosen are $k_2 = 0.1$, $k_3 = 0.003/0.006$ and $k_4 = 0.002$. We determined the ensemble average of the second, third, and fourth order terms in the chosen asymmetric double-well interaction potential (Fig. 5.9) at various temperatures to make sure the contributions from the cubic and quartic terms are not insignificant. According to our findings, the cubic and quartic terms' contributions are not insignificant when compared to the quadratic term. Also, the values of these coefficients exhibit

a non-monotonic temperature dependency that is in well agreement with the scaling of thermal conductivity κ that is temperature dependant. The absolute values of the coefficients in the double well potential (2) were 0.05, 0.001/0.002, and 0.0005 based on the chosen values of k_2 , k_3 , and k_4 . The Taylor expansion's truncation of the polynomial beyond fourth order is further justified by the steadily declining values of these coefficients³⁴.

5.4 Conclusion

It has been a long-standing problem to understand the diverging nature of heat conductivity in low-dimensional systems. A large number of theoretical and numerical calculations on onedimensional momentum conserving systems revealed a power-law divergence of thermal conductivity with the chain length ^{11,12}. However there have been variation in the value of the divergent exponent in the literature due to the different choice of systems and condition of study. We have shown here that from a single model system such variations can be explained. The divergent nature of in a 1D asymmetric lattice depends on the heat bath temperature, as demonstrated in this study using the nonequilibrium simulation method. The system shows exponent values 0.5 and 0.33 in the thermodynamic limit at low and high T, respectively. Consequently, based on the system's temperature, our simulations demonstrate two distinct scaling behaviour of the same system. Our calculated value of divergence exponent α (~ 0.5) equals the value previously reported by mode coupling theory at low temperature ^{30,35–37}. At high temperature, our calculation produces the exponent of 0.33 as predicted by the renormalization group analysis^{8,38}. Additionally, at the intermediate temperature, thermal conductivity κ appears to saturate against N at a relatively low value ($\alpha = 0.07$). The validity of Fourier's law was established by the asymmetric system in a previous work on a similar weak divergence of in the context of a 1D asymmetric momentum conserving lattice ²⁴. But later it was found that the saturating behaviour of thermal conductivity might not be connected to the system's actual thermodynamic limit^{21,25}. We estimated the local divergence exponent, α_N , and found that it does not saturate to a constant value in intermediate temperature in the length scale of our simulations in order to investigate the weak divergence of in the intermediate temperature. In this case, local divergence exponent, α_N declines with lattice size N and exhibits a tendency to climb once more after passing through a minimal. There should not have been any more increases in the local divergence exponent α if the system had hit its thermodynamic limit. In contrast, regardless of the degree of asymmetry in the interaction potential, α_N decreases with chain length N and saturates to its respective thermodynamic limits at low and high temperatures. Our studies show that the approach to the thermodynamic

limit of is certainly temperature dependent. These results are independent of the asymmetry in the interaction potential.

5.5 Reference

- 1. Casati, G., Ford, J., Vivaldi, F. & Visscher, W. M. One-dimensional classical many-body system having a normal thermal conductivity. *Phys. Rev. Lett.* **52**, 1861–1864 (1984).
- 2. Rieder, Z., Lebowitz, J. L. & Lieb, E. Properties of a harmonic crystal in a stationary nonequilibrium state. *J. Math. Phys.* **8**, 1073–1078 (1967).
- 3. Prosen, T. & Robnik, M. Energy transport and detailed verification of Fourier heat law in a chain of colliding harmonic oscillators. *J. Phys. A Gen. Phys.* **25**, 3449–3472 (1992).
- 4. Lepri, S., Livi, R. & Politi, A. Heat Conduction in Chains of Nonlinear Oscillators. *Phys. Rev. Lett.* **78**, 1896–1899 (1997).
- 5. Zhao, H. & Wang, W. G. Fourier heat conduction as a strong kinetic effect in one-dimensional hard-core gases. *Phys. Rev. E* **97**, 1–5 (2018).
- 6. Grassberger, P., Nadler, W. & Yang, L. Heat Conduction and Entropy Production in a One-Dimensional Hard-Particle Gas. *Phys. Rev. Lett.* **89**, 1–4 (2002).
- 7. Dhar, A. Heat conduction in a one-dimensional gas of elastically colliding particles of unequal masses. *Phys. Rev. Lett.* **86**, 3554–3557 (2001).
- 8. Narayan, O. & Ramaswamy, S. Anomalous Heat Conduction in One-Dimensional Momentum-Conserving Systems. *Phys. Rev. Lett.* **89**, 2–5 (2002).
- 9. Livi, R. Anomalous transport in low-dimensional systems: A pedagogical overview. *Phys. A Stat. Mech. its Appl.* 127779 (2022) doi:10.1016/j.physa.2022.127779.
- 10. Casati, G. & Prosen, T. Anomalous heat conduction in a one-dimensional ideal gas. *Phys. Rev. E Stat. Physics, Plasmas, Fluids, Relat. Interdiscip. Top.* **67**, 4 (2003).
- 11. Lepri, S., Livi, R. & Politi, A. Thermal conduction in classical low-dimensional lattices. *Phys. Rep.* **377**, 1–80 (2003).
- 12. Dhar, A. Heat transport in low-dimensional systems. *Adv. Phys.* **57**, 457–537 (2008).
- 13. Liu, S., Xu, X. F., Xie, R. G., Zhang, G. & Li, B. W. Anomalous heat conduction and anomalous diffusion in low dimensional nanoscale systems. *Eur. Phys. J. B* **85**, (2012).
- 14. Chang, C. W., Okawa, D., Garcia, H., Majumdar, A. & Zettl, A. Breakdown of fourier's

- law in nanotube thermal conductors. Phys. Rev. Lett. 101, 1–4 (2008).
- 15. Lee, V., Wu, C. H., Lou, Z. X., Lee, W. L. & Chang, C. W. Divergent and Ultrahigh Thermal Conductivity in Millimeter-Long Nanotubes. *Phys. Rev. Lett.* **118**, 1–5 (2017).
- 16. Xu, X. *et al.* Length-dependent thermal conductivity in suspended single-layer graphene. *Nat. Commun.* **5**, 1–6 (2014).
- 17. Hu, B., Li, B. & Zhao, H. Heat conduction in one-dimensional chains. *Phys. Rev. E Stat. Physics, Plasmas, Fluids, Relat. Interdiscip. Top.* **57**, 2992–2995 (1998).
- 18. Hu, B. & Yang, L. Heat conduction in the Frenkel-Kontorova model. *Chaos* **15**, (2005).
- 19. Hu, B., Li, B. & Zhao, H. Heat conduction in one-dimensional nonintegrable systems. *Phys. Rev. E Stat. Physics, Plasmas, Fluids, Relat. Interdiscip. Top.* **61**, 3828–3831 (2000).
- 20. Aoki, K. & Kusnezov, D. Bulk properties of anharmonic chains in strong thermal gradients: Non-equilibrium φ4 theory. *Phys. Lett. Sect. A Gen. At. Solid State Phys.* **265**, 250–256 (2000).
- 21. Savin, A. V. & Kosevich, Y. A. Thermal conductivity of molecular chains with asymmetric potentials of pair interactions. *Phys. Rev. E Stat. Nonlinear, Soft Matter Phys.* **89**, 1–12 (2014).
- 22. Gendelman, O. V. & Savin, A. V. Normal heat conductivity in chains capable of dissociation. *Epl* **106**, (2014).
- 23. Sato, D. S. K. Pressure-induced recovery of Fourier's law in one-dimensional momentum-conserving systems. *Phys. Rev. E* **94**, (2016).
- 24. Zhong, Y., Zhang, Y., Wang, J. & Zhao, H. Normal heat conduction in one-dimensional momentum conserving lattices with asymmetric interactions. *Phys. Rev. E Stat. Nonlinear, Soft Matter Phys.* **85**, 1–4 (2012).
- 25. Das, S. G., Dhar, A. & Narayan, O. Heat Conduction in the α-β Fermi-Pasta-Ulam Chain. *J. Stat. Phys.* **154**, 204–213 (2014).
- 26. Wang, L., Hu, B. & Li, B. Validity of Fourier's law in one-dimensional momentum-conserving lattices with asymmetric interparticle interactions. *Phys. Rev. E Stat. Nonlinear, Soft Matter Phys.* **88**, 1–4 (2013).

- 27. Roy, D. Crossover from Fermi-Pasta-Ulam to normal diffusive behavior in heat conduction through open anharmonic lattices. *Phys. Rev. E Stat. Nonlinear, Soft Matter Phys.* **86**, 1–5 (2012).
- 28. Cividini, J., Kundu, A., Miron, A. & Mukamel, D. Temperature profile and boundary conditions in an anomalous heat transport model. (2017) doi:10.1088/1742-5468/aa5337.
- 29. Wang, J. S. & Li, B. Intriguing Heat Conduction of a Chain with Transverse Motions. *Phys. Rev. Lett.* **92**, 5–8 (2004).
- 30. Delfini, L., Lepri, S., Livi, R. & Politi, A. Self-consistent mode-coupling approach to one-dimensional heat transport. *Phys. Rev. E Stat. Nonlinear, Soft Matter Phys.* **73**, 17–20 (2006).
- 31. Delfini, L., Lepri, S., Livi, R. & Politi, A. Comment on: Equilibration and universal heat conduction in fermi-pasta-ulam chains. *Phys. Rev. Lett.* **100**, 2–5 (2008).
- 32. Xiong, D., Zhang, Y. & Zhao, H. Temperature dependence of heat conduction in the Fermi-Pasta-Ulam- β lattice with next-nearest-neighbor coupling. *Phys. Rev. E Stat. Nonlinear, Soft Matter Phys.* **90**, 1–6 (2014).
- 33. Xiong, D. Underlying mechanisms for normal heat transport in one-dimensional anharmonic oscillator systems with a double-well interparticle interaction. *J. Stat. Mech. Theory Exp.* 43208 (2016) doi:10.1088/1742-5468/2016/4/043208.
- 34. Gendelman, O. V. & Savin, A. V. Heat conduction in a chain of colliding particles with a stiff repulsive potential. *Phys. Rev. E* **94**, 1–5 (2016).
- 35. Lee-Dadswell, G. R., Nickel, B. G. & Gray, C. G. Thermal conductivity and bulk viscosity in quartic oscillator chains. *Phys. Rev. E Stat. Nonlinear, Soft Matter Phys.* **72**, 1–8 (2005).
- 36. Van Beijeren, H. Exact results for anomalous transport in one-dimensional hamiltonian systems. *Phys. Rev. Lett.* **108**, 1–5 (2012).
- 37. Mendl, C. B. & Spohn, H. Dynamic correlators of fermi-pasta-ulam chains and nonlinear fluctuating hydrodynamics. *Phys. Rev. Lett.* **111**, 1–5 (2013).
- 38. Mai, T. & Narayan, O. Universality of one-dimensional heat conductivity. *Phys. Rev. E*

- Stat. Nonlinear, Soft Matter Phys. **73**, 1–7 (2006).

CHAPTER 6

Future Perspectives

Spatial heterogeneity, known as roughness, in the potential landscape and its impact on the transport properties of a driven inertial Brownian ratchet driven by a time-periodic force is a fascinating research area in the field of non-equilibrium statistical mechanics that has many potential future perspectives. These are some of the future directions which we can extend our idea of research in the area of role of roughness in the transport characteristics, especially in the case of a driven inertial ratchet.

- Future research could investigate the effect of rough periodic potential on the transport properties of coupled driven Brownian particles with different kind of interacting potential.
- Future research could aim to verify the theoretical predictions of constructive role of roughness in the periodic potential of a driven inertial ratchet through experimental measurements. As an example, how does we can use the effect of roughness in the transport properties in the context of mass separation of particles?

Thermal transport in low-dimensional systems has been the subject of extensive investigation during the past few decades. One of the chapter in this thesis focused on the temperature dependent divergence of thermal conductivity in momentum conserving one -dimensional lattices with asymmetric double well potential for nearest interaction. One of the potential avenues of exploration in this area of research is, we can extend the same to two-dimensional systems.

We can extend numerical investigation of heat conduction in two-dimensional systems
with various non-linear interaction potentials and their effects on the thermal transport.
Also, we can extend the study to make an understanding about the temperature
dependence of thermal conductivity with various nature of interaction potentials in twodimensional systems.

Study of mass and thermal transport in non-equilibrium environment

by Archana G R

Submission date: 09-Mar-2023 03:24PM (UTC+0530)

Submission ID: 2032888822 **File name:** Archana.pdf (3.2M)

Word count: 22488

Character count: 114258

Study of mass and thermal transport in non-equilibrium environment

ORIGINALITY REPORT

SIMILARITY INDEX

INTERNET SOURCES

PUBLICATIONS

STUDENT PAPERS

PRIMARY SOURCES

Archana G. R., Debashis Barik. "Roughness in the periodic potential induces absolute negative mobility in a driven Brownian ratchet", Physical Review E, 2022 Publication



Archana G. R., Debashis Barik. "Roughness in the periodic potential enhances transport in a driven inertial ratchet", Physical Review E, 2021



Publication

Archana G. R., Debashis Barik. "Temperaturedependent divergence of thermal conductivity in momentum-conserving one-dimensional lattices with asymmetric potential", Physical Review E, 2019



Publication

export.arxiv.org Internet Source

scholarbank.nus.edu.sg Internet Source

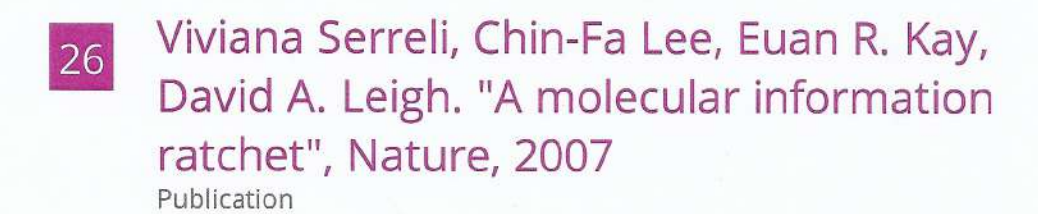
nus Associated Professes duli **Iniversity of Hyderabad** Hyderabad-500 046, India.

6	Alexander V. Savin, Yuriy A. Kosevich. "Thermal conductivity of molecular chains with asymmetric potentials of pair interactions", Physical Review E, 2014 Publication	<1%
7	S Lepri. "Thermal conduction in classical low-dimensional lattices", Physics Reports, 2003	<1%
8	Ya-li Ou, Cai-tian Hu, Jian-chun Wu, Bao-quan Ai. "Absolute negative mobility of interacting Brownian particles", Physica A: Statistical Mechanics and its Applications, 2015	<1%
9	www.researchgate.net	<1%
10	Abhishek Dhar. "Heat transport in low-dimensional systems", Advances in Physics, 2008 Publication	<1%
11	Yuhui Luo, Chunhua Zeng, Bao-Quan Ai. "Strong-chaos-caused negative mobility in a periodic substrate potential", Physical Review E, 2020 Publication	<1%
12	Wenshan Liao, Nianbei Li. "Energy and momentum diffusion in one-dimensional periodic and asymmetric nonlinear lattices	<1%

with momentum conservation", Physical Review E, 2019 Publication

13	Lecture Notes in Physics, 2016. Publication	<1%
14	www.cesec.ufpr.br Internet Source	<1%
15	Chunhua Zeng, Hua Wang, Yonggang Wei, Kongzhai Li, Jianhang Hu. "Anomalous transport controlled via potential fluctuations", Physica A: Statistical Mechanics and its Applications, 2013	<1 %
16	Jun-wen Mao, You-quan Li. "Current progress on heat conduction in one-dimensional gas channels", Frontiers of Physics in China, 2006 Publication	<1%
17	Morton H. Friedman. "Principles and Models of Biological Transport", Springer Science and Business Media LLC, 2008 Publication	<1%
18	Bao-quan Ai, Bambi Hu. "Heat conduction in deformable Frenkel-Kontorova lattices: Thermal conductivity and negative differential thermal resistance", Physical Review E, 2011 Publication	<1%

19	J Spiechowicz, J Łuczka, P Hänggi. "Absolute negative mobility induced by white Poissonian noise", Journal of Statistical Mechanics: Theory and Experiment, 2013 Publication	<1%
20	uir.unisa.ac.za Internet Source	<1%
21	Undergraduate Lecture Notes in Physics, 2013. Publication	<1%
22	www.agnld.uni-potsdam.de Internet Source	<1%
23	Spiechowicz, Jakub, Peter Hanggi, and Jerzy Luczka. "Absolute negative mobility of inertial Brownian particles induced by noise", 2013 22nd International Conference on Noise and Fluctuations (ICNF), 2013. Publication	<1%
24	Submitted to Universiti Teknologi MARA Student Paper	<1%
25	Vedanta Pradhan, O. D. Naidu, Sinisa Zubic, Patrick Cost. "Decentralized Estimation of Two-port Equivalents for Power Transmission Lines", IEEE Access, 2021 Publication	<1%



<1%

27

T. S. Chow. "Mesoscopic Physics of Complex Materials", Springer Science and Business Media LLC, 2000

<1%

Publication

Exclude quotes

On

Exclude matches

< 14 words

Exclude bibliography